**A DISSERTATION FOR THE DEGREE OF DOCTOR OF PHILOSOPHY**

# Influences of the structural characteristics of ethanol organosolv lignin on the thermal and mechanical properties of ligno-bioplastics

# 유기용매 리그닌의 구조적 특성이 리그노-바이오플라스틱의 열적 · 기계적 특성에 미치는 영향

By June-Ho Choi

PROGRAM IN ENVIRONMENTAL MATERIALS SCIENCE
DEPARTMENT OF FOREST SCIENCES
GRADUATE SCHOOL
SEOUL NATIONAL UNIVERSITY

FEBRUARY, 2021

A DISSERTATION FOR THE DEGREE OF DOCTOR OF PHILOSOPHY

# Influences of the structural characteristics of ethanol organosolv lignin on the thermal and mechanical properties of ligno-bioplastics

# 유기용매 리그닌의 구조적 특성이 리그노-바이오플라스틱의 열적·기계적 특성에 미치는 영향

Advisor Professor: In-Gyu Choi

By June-Ho Choi

PROGRAM IN ENVIRONMENTAL MATERIALS SCIENCE
DEPARTMENT OF FOREST SCIENCES
GRADUATE SCHOOL
SEOUL NATIONAL UNIVERSITY

FEBRUARY, 2021

**Influences of the structural characteristics of ethanol organosolv lignin on the thermal and mechanical properties of ligno-bioplastics**

유기용매 리그닌의 구조적 특성이 리그노-
바이오플라스틱의 열적 · 기계적 특성에 미치는 영향

지도교수 최 인 규

이 논문을 농학박사 학위논문으로 제출함
2020년 11월

서울대학교 대학원
산림과학부 환경재료과학전공
최 준 호

최준호의 농학박사 학위논문을 인준함
2021년 1월

위 원 장 곽 효 원 (인)
부위원장 최 인 규 (인)
위 원 윤 혜 정 (인)
위 원 구 본 욱 (인)
위 원 김 호 용 (인)

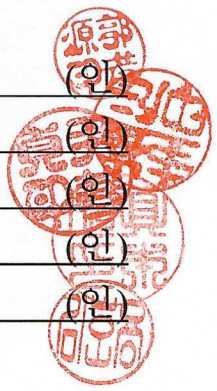

# Abstract

## Influences of the structural characteristics of ethanol organosolv lignin on the thermal and mechanical properties of ligno-bioplastics

June-Ho Choi
Program in Environmental Materials Science
Department of Forest Sciences
The Graduate School
Seoul National University

In this study, the effect of the structural characteristics of ethanol organosolv lignin (EOL) on the thermal and mechanical properties of ligno-bioplastics was investigated. A response surface methodology (RSM) based on central composite design (CCD) was adopted to investigate the influence of the extraction conditions on the structural characteristics of EOL. Via the RSM, EOL with a low molecular weight, low polydispersity index (PDI), high phenolic hydroxyl content, and condensed structure was obtained under harsh extraction conditions. The correlation between the structural characteristics of EOL and the severity of the extraction conditions was confirmed by introducing the combined severity factor (CSF), and a clear correlation consistent with the RSM results was derived. In addition, the structural characteristics of the EOL derived under different extraction conditions influenced its thermal properties. The EOL with a low molecular weight, high phenolic hydroxyl group content, and condensed structure, exhibited high thermal stability while delaying the thermal decomposition with a high glass transition temperature ($T_g$). To predict

the weight reduction rate of EOL at 300 °C, the regression model ($R^2$ = 0.837) was suggested. In accordance with the model, the lower the molecular weight of the EOL, the lower the rate of thermal degradation of EOL was expected. Meanwhile, the EOL–PLA thermo-bioplastics prepared using three types of EOL (EOL extracted under low-severity (LL), moderate-severity (ML), and high-severity (HL) conditions) exhibited improved thermal stability compared to neat PLA. According to the thermal properties of EOL, the EOL–PLA bioplastic formed with HL exhibited exceptional thermal stability. The bioplastics had different mechanical properties depending on the types of EOL. The tensile strength of the bioplastics tended to decrease as the content of lignin in the bioplastics increased. Conversely, the nominal strain at break of the bioplastics exhibited a different tendency depending on the types of EOL.

Oxypropylation of EOL was employed to improve the thermoplasticity and compatibility with PLA. Three types of EOL (LL, ML, and HL) with different structural characteristics were modified by propylene oxide (PO). During the oxypropylation, the degree of substitution (DS) and the degree of polymerization (DP) of the propyl side chain were affected by the distribution of the hydroxyl groups in the initial EOL structure. The HL with a high aromatic hydroxyl group content (4.31 mmol/g) exhibited a high DS (0.77), and the LL with a high aliphatic hydroxyl group content (2.94 mmol/g) exhibited a high DP (11.17). Moreover, the oxypropylation of EOL enhanced its thermoplasticity. In particular, a new $T_g$ (from 55 to 60 °C) and melting point were observed for the oxypropylated LL and ML. In addition, the compatibility of EOL with PLA was successfully improved by oxypropylation, which was supported by a slick and flat surface structure observed in the bioplastics with oxypropylated LL and ML. The increased compatibility of EOL with PLA induced an increase in the tensile strength of the oxypropylated EOL–PLA bioplastic to a similar level to that of the neat PLA, and the nominal strain was also increased to a higher level than that of the neat PLA. In addition, the $T_g$ of the EOL–PLA bioplastic was

increased compared to that of the neat PLA in a thermodynamic perspective, implying that the mechanical properties of the oxypropylated EOL–PLA bioplastic were improved at temperatures above the $T_g$ of the neat PLA.

Thermosetting lignopolyurethanes with different thermal and mechanical properties depending on the types of EOL were prepared. The structural characteristics and properties of lignopolyurethane highly depended on the structural characteristics of oxypropylated EOL. The oxypropylated EOL with a high hydroxyl group content showed a high reaction rate. All of the lignopolyurethanes exhibited increased thermal stability at low temperatures compared to those of the corresponding oxypropylated EOLs, whereas at high temperatures, the thermal properties of lignopolyurethane depended on the thermal properties of the corresponding initial EOLs. In addition, the structural characteristics of the EOL had a significant effect on the mechanical properties of the lignopolyurethane film. The oxypropylated EOL with a high average hydroxyl content enabled to form a lignopolyurethane film with a high crosslink density due to its high reactivity. The lignopolyurethane film with a high crosslinking density exhibited competent tensile strength.

Consequently, the thermoplastic and thermosetting properties of EOL were imparted through chemical modification methods based on the correlation between the structural characteristics and properties of the EOL. The thermal and mechanical properties of the ligno-bioplastics were found to be significantly influenced not only by the chemical modification of EOL but also by the structural characteristics of lignin, the raw material.

**Keywords: EOL, structural characteristics, thermal and mechanical properties, ligno-bioplastics, oxypropylation, lignopolyurethane**

**Student Number: 2015-21505**

# Contents

## ***Chapter 2***

**Thermal and mechanical properties of EOLs and EOL–PLA bioplastics** ..... 46

## ***Chapter 3***

**Chemical modification of EOL for improving thermoplasticity and compatibility in EOL–PLA bioplastics**.....103

## *Chapter 4*

**Preparation and characterization of lignopolyurethanes using different types of EOL** ..... 162

# List of Tables

# List of Figures

# List of Abbreviations

| | |
|---|---|
| EO | ethanol organosolv |
| EOL | ethanol organosolv lignin |
| PLA | polylactic acid PLA |
| THF | tetrahydrofuran |
| PO | propylene oxide |
| HDI | hexamethylene diisocyanate |
| PEG | polyethylene glycol |
| $M_n$ | number-average molecular weight |
| $M_w$ | weight-average molecular weight |
| PDI | polydispersity index |
| AlOH | aliphatic hydroxyl group |
| PhOH | phenolic hydroxyl group |
| $T_g$ | glass transition temperature |
| $T_m$ | melting point |
| DP | degree of polymerization |
| DS | degree of substitution |
| RSM | response surface methodology |
| CCD | central composite design |
| CSF | combined severity factor |
| OLS | ordinary least squares |
| GPC | gel permeation chromatography |
| 31P NMR | phosphorus-31 nuclear magnetic resonance |
| TGA | thermogravimetric analyzer |
| DTG | differential scanning calorimeter |
| DSC | differential scanning calorimeter |
| FE-SEM | filed-emission scanning electron microscopy |
| DMA | dynamic mechanical analysis |
| FT-IR | Fourier transform infrared spectrometric |
| E′ | storage modulus |
| E″ | loss modulus |

# *Chapter 1*

## Introduction

# 1. Background

## 1.1. Lignin as a bioplastic material

### 1.1.1. Bioplastics as alternatives to petroleum-based plastics

Plastics have contributed tremendously to affluent daily life; they have several advantages, including excellent processability, excellent mechanical properties, low specific gravity, and low price. However, in recent years, plastics have been highlighted as a cause of serious environmental pollution, such as environmental loads caused by incineration or landfills of waste generated after use, environmental hormones such as dioxin, and air pollution from the incomplete combustion of waste. According to Statista.com, the global plastic production has increased steadily for decades, reaching 359 million metric tons in 2018 (Garside, 2019). Correspondingly, the amount of plastic waste generated has steadily increased (Ren, 2003). As a countermeasure, governments, industries, and academia are constantly researching overall management systems for polymer waste, such as weight reduction, recycling, landfill, incineration, and the use of biodegradable materials in countries. Among the various strategies, bioplastic development has emerged as the most viable option for building a sustainable circulation system (Wojnowska-Baryła et al., 2020).

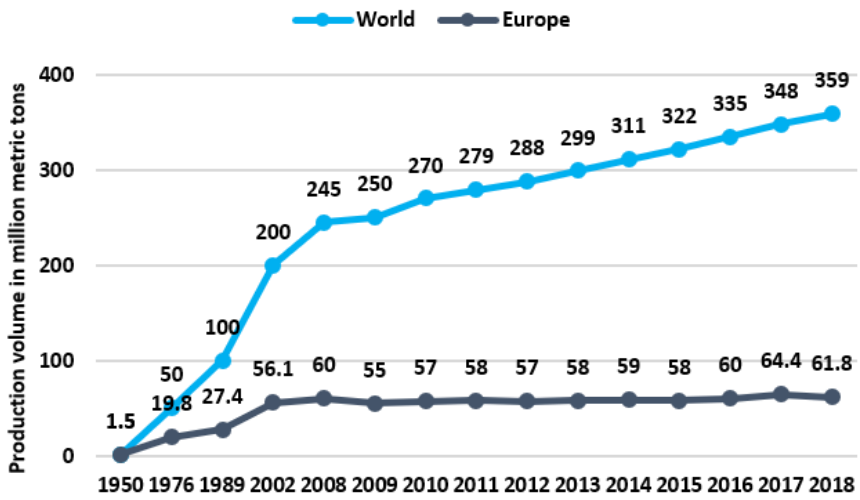


Figure 1-1. Global plastic production (Garside, 2019).

Bioplastic is a polymer plastic produced using biomass-based raw materials. Bioplastics can be classified into biodegradable plastics and bio-based plastics depending on the raw materials, decomposition mechanisms, and production methods (You et al., 2015). Biodegradable plastics are plastics that can be decomposed into water and carbon dioxide by microorganisms in soil or water. Bio-based plastics are classified based on the biomass content (in terms of the organic carbon content), regardless of the decomposition period. Conversely, similar to other plastics, bio-based plastics can be largely divided into thermoplastic plastics and thermosetting plastics, according to their characteristics. Thermoplastics are polymers that become flexible and moldable at certain temperatures and return to a solid state upon cooling. Many thermoplastics are produced using polymer compounds having weak intermolecular forces (Baeurle et al., 2006). Unlike thermosetting plastics, they can melt and return to their original state; thus, they can be recycled. The general molecular structure of thermoplastics is a linear structure that allows only weak interactions between molecules. In contrast, thermosetting plastics are polymers having a rigid structure that comprises crosslinks between polymer chains formed by heat and pressure treatment (McNaught & Wilkinson, 1997). Thermosetting plastics are heat resistant due to their rigid structure, which comprises 3D cross-linkages of polymer chains; thus, they are employed in many industries and also used as adhesives.

A typical bio-based thermoplastic is biopolyester. Biopolyester, which is biodegradable, can be obtained by biological or chemical synthesis from monomers such as lactic acid and succinic acid. Biopolyester has attracted attention as a substitute for petroleum-based thermoplastics because of its high biodegradability and biocompatibility. To date, the most studied thermoplastic biopolyesters include polylactic acid (PLA), polyhydroxyalkanoate (PHA), and polybutylene succinate (PBS) (Shen et al., 2020). Biopolyurethane is an example of bio-based thermosetting resins. Biopolyurethane can be produced

by replacing polyols derived from petrochemicals, which are the main raw materials for urethane synthesis, with polyols derived from biomass (Noreen et al., 2016). This way, the biodegradability of biopolyurethane can be improved by increasing the proportion of biodegradable raw materials.

### 1.1.2. Drawbacks of thermoplastics (biopolyester) and thermosetting (biopolyurethane) bioplastics

PLA, which is one of the environmentally friendly and biocompatible thermoplastic biopolyesters, has the advantages of fine tensile strength and small elongation at break compared to other biodegradable thermoplastic biopolyesters (Spiridon et al., 2015). PLA can be employed as a biodegradable packaging material using various manufacturing methods, such as casting, injection molding, and spinning; additionally, it can be used as a raw material for 3D printing. Moreover, attempts have been made to use PLA as a medical implant by exploiting its ability to be degraded into harmless lactic acid in the body (Auras et al., 2011).

PHA, a biodegradable polymer produced by microorganisms, can be characterized by the length of the unit chain. PHA is a thermoplastic biopolyester that can be manufactured with film, fiber, etc., and it can be used as an agricultural packaging material owing to its low intensity and highly ductile properties (Gruber & O'Brien, 2002). In particular, polyhydroxybutyrate (PHB), which is the most commonly used in the PHA family, has a high gas resistance and water resistance, making it ideal for use as a bioplastic.

PBS is a thermoplastic biopolyester that can be decomposed into water and carbon dioxide in nature by microorganisms. The range of applications for PBS continues to expand; however, commercialization has not been achieved. PBS can be processed into films, bags, and packaging/cases for food and cosmetics. In addition, it can be used as agricultural packaging and fishing nets.

However, even though most thermoplastic biopolyesters are more environmentally friendly than conventional plastics, there are some drawbacks to their mechanical (strength and elongation) and thermal properties (thermal

stability and heat resistance), which result in poor processability compared to conventional thermoplastics (Sajjan et al., 2020). Furthermore, thermoplastic biopolyesters have lower price competitiveness than conventional thermoplastics due to their unoptimized processes, the high cost of raw materials, and small-scale market size (Chanprateep, 2010; Mostafa et al., 2018).

Lactic acid, a precursor to PLA, has a chiral structure. Therefore, the copolymerization of L- and D-lactide racemic mixture forms poly-DL-lactide (PDLLA), which has an amorphous structure. In general, PDLLA and PLLA have low glass-transition temperatures ($T_g$) and low heat-distortion temperatures (HDTs), making them difficult to commercialize in the disposable plastic industry where heat-resistant materials are required. To overcome these shortcomings, the heat-deflection temperature can be increased by physically mixing PDLA having a crystalline structure. However, PDLA has a low biodegradation rate in nature, which limits its application as a biopolyester. Additionally, the inherent high brittleness of PLA limits its field of use.

PHA and PBS also have high initial investment costs, because the manufacturing process has not been fully established, and additional equipment for new processes is required. Moreover, the manufacturing cost of biopolyesters is high because the cost of raw materials is higher than that for conventional plastics. This high manufacturing cost diminishes the price competitiveness of biopolyesters, which adversely affects supply and demand, resulting in a vicious cycle.

Therefore, enhancing the mechanical properties of these thermoplastic biopolyesters and improving the price competitiveness are major prerequisites for commercialization. To satisfy both requirements, several attempts have been made to adjust the thermal and mechanical properties by manufacturing a fully biomass-based thermoplastic using components of lignocellulosic biomass, which have high price competitiveness, biodegradability, and unique properties

(Kumar & Tumu, 2019).

Meanwhile, biopolyurethane is a synthetic or biodegradable urethane produced by biomass-derived raw materials containing isocyanates or polyols. Thus far, many studies have attempted to develop biopolyurethane by synthesizing petrochemical-derived isocyanates and biomass-derived polyols. Biomass-derived polyols include biopolyether polyols and biopolyester polyols. As the polyether polyol, sucrose and sorbitol are used in the rigid polyurethane foam, and the content of these polyols is 30% or less. In addition, 1,3-propanediol, produced by the fermentation of corn sugar, is used in the manufacture of polytrimethylene ether glycol, which is used for the softening segments of elastomers and spandex fibers (Shen et al., 2009).

For biopolyester polyol, some of the polyester polyols may be biomaterials. Dibasic acid is a fermented product, e.g., succinic acid and adipic acid, and ethylene oxide and 1,2-propanediol (propylene glycol, PG), which are raw materials for polyols, can also be biosynthesized. However, biopolyether polyols and biopolyester polyols are considered not economical because they require additional processes for production and purification. Therefore, to ensure the economic feasibility of biopolyurethanes, it is necessary to use an inexpensive raw material derived from biomass that is obtained as a by-product in traditional industries.

### 1.1.3. Lignin as an additive or precursor of bioplastic materials and ligno-bioplastic

Lignin, a naturally occurring polymer, can be produced at a relatively low cost due to its simpler manufacturing process than those of other synthesized polymers; it also exhibits excellent biocompatibility and biodegradability. Accounting for approximately 20–30% of lignocellulosic biomass, lignin is the second most abundant naturally occurring polymer globally. Traditionally, lignin is produced in large quantities as a by-product of the pulp industry; recently, in biorefineries, lignin derivatives have been generated in the biofuel production process (Duval & Lawoko, 2014). Approximately 60 million metric tons of lignin is produced per year in pulp plants worldwide, most of which are used to generate the high temperature and pressure steam required for the production process (Ganewatta et al., 2019). In recent years, lignin valorization has been widely employed to create added value for economic feasibility because lignin recovery is an energy-intensive process. The global lignin market is expected to grow to $913.1 million by 2025, and many studies have attempted to use lignin in various industries (research, 2020). Lignin has the potential to be used as an additive to or a precursor of bioplastic materials (Wang et al., 2016). Lignin can be utilized in bioplastic production to provide alternatives to petroleum-based plastics.

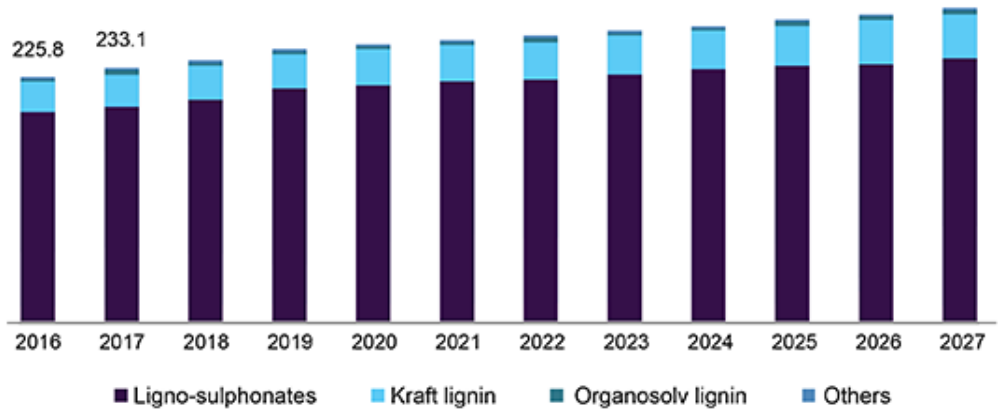


Figure 1-2. Global lignin market (research, 2020).

Interestingly, lignin has both thermoplastic and thermosetting properties due to its amorphous structure and inter- and intramolecular interactions (Jeong et al., 2013). Lignin has long been considered a phenol replacement resource in thermosetting resins, such as phenol-formaldehyde resins. In this regard, many studies have been conducted to investigate the applicability of lignin as a thermosetting resin. Contrarily, the thermoplastic properties of lignin, attributed to its amorphous structure and inter- or intramolecular hydrogen bonding, enable its use as a thermoplastic. In particular, the high thermal stability of lignin, derived from its inherent chemical structure, compensates for the thermal vulnerability of biopolyesters (Sen et al., 2015).

In this study, a bioplastic in which lignin was used as an additive or precursor was formed (denoted as ligno-bioplastic), exploiting the thermoplastic or thermosetting properties of lignin. Ligno-bioplastics include a typical thermoplastic resin (biopolyester) containing lignin and a thermosetting resin (biopolyurethane) synthesized using a lignin-derived precursor. The lignin used as an additive or precursor of ligno-bioplastic can be selectively produced and chemically modified to have a desirable structure, to achieve improved thermal and mechanical properties of the ligno-bioplastic.

## 1.2. Bottlenecks of lignin utilization for bioplastics applications derived from its structure and thermal properties

### 1.2.1. Types of lignin based on the extraction processes and organosolv lignin

The physicochemical properties of lignin are highly dependent on the extraction methods. Lignin can be obtained through chemical treatment processes that overcome the recalcitrance of biomass and facilitate the use of each component. During these processes, lignin macromolecules, which have complex inter- and intramolecular bonds in the biomass, are partially depolymerized and converted into relatively small lignin fractions (McDonough, 1992). At the same time, the converted lignin fractions can be recondensed by functional groups depending on the process conditions, forming stronger bonds (Zhao et al., 2017). Therefore, lignin isolated from various extraction processes has various structural characteristics and physicochemical properties (Figure 1-3). To use lignin as a bioplastic material, it is important to know the characteristics of the lignin obtained from the applicable process and to select the most suitable lignin for the purpose of use. In this respect, many studies have investigated the differences in the physicochemical properties of lignin obtained by various extraction methods. Well-known lignins, produced through a chemical process, include kraft lignin, sulfite lignin, soda lignin, and organosolv lignin.

Kraft lignin, produced as a by-product in the kraft pulping process, is the most abundant lignin. The kraft pulping process is conducted to cook lignocellulosic biomass using a sodium hydroxide and sodium sulfide aqueous solution at 150–180 °C. After the process, black liquor is produced together with pulp, and kraft lignin can be obtained after recovering the used chemicals

from black liquor and removing moisture (Chakar & Ragauskas, 2004). Kraft lignin has a condensed structure resulting from harsh reaction conditions, and it has a low sulfur content (1–3%) with functional groups substituted with a thiol group (–SH) (Yoon & Van Heiningen, 2008). This lignin can be dissolved in alkaline media (pH > 10); its molecular weight is in the range of 1000–3,000 Da, and its $T_g$ is in the range of 140–150 °C (Laurichesse & Avérous, 2014; Marton & Marton, 1964). Furthermore, the condensed structure of kraft lignin can adversely affect its reactivity, and the sulfur content can produce odor and result in corrosion; these limit its industrial use (Demuner et al., 2019; Yeske, 1986).

Sulfite lignin, also called lignosulfonate, is produced as a by-product in the sulfite pulping process. The sulfite pulping process is conducted at 150–180 °C using a mixed aqueous solution of sulfurous acid and sulfite (Patt et al., 2012). Lignosulfonate has a rigid structure that is condensed by C–C bonds, and it has a molecular weight ranging from 15,000 to 50,000 Da, with a $T_g$ of ~130 °C (Laurichesse & Avérous, 2014). Lignosulfonate can be dissolved in water because the functional groups are substituted with a sulfonic acid group ($–SO_3H$) during processing (Braaten et al., 2003). In addition, lignosulfonate has low purity because of its high ash content (Braaten et al., 2003).

Soda lignin can be obtained from the cooking process of soda pulp using an aqueous sodium hydroxide solution (Gosselink et al., 2004). It is recognized that soda lignin is sulfur-free and has a less condensed structure than kraft or sulfite lignin (Schorr et al., 2014). Soda lignin, dissolved in alkaline media, has a molecular weight in the range of 1000–3000 Da, an ash content range of 0.7–2.3%, and a $T_g$ value of ~140 °C (Laurichesse & Avérous, 2014).

Conversely, organosolv lignin can be obtained as a by-product during organosolv pretreatment, which is usually conducted to dissolve hemicellulose and lignin from lignocellulosic biomass to improve the cellulose accessibility of enzymes (Chum et al., 1988). Various organic solvents, such as aliphatic

alcohols, polyols, organic acids, and ketones, can be adopted for organosolv pretreatment. Among them, alcohol, which is the most widely used, has some advantages. In particular, ethanol is considered an accessible solvent because of its low cost and easy recovery (Zhao et al., 2009). Ethanol organosolv pretreatment is usually performed with or without an acid catalyst, which accelerates the cleavage of aryl-ether linkages of lignin at high temperatures using ethanol diluted with water as a solvent (Sannigrahi et al., 2010). However, organosolv pulp production has gradually diminished in the pulp industry due to its high solvent cost and explosion hazard (Zhao et al., 2009). Recently, however, organic solvent pretreatment, which is employed to easily separate the main components of biomass, has been attracting attention, with increasing interest in second-generation biomass-based biorefineries (Pan et al., 2005). Organosolv lignin has a high purity, low ash content, low polysaccharide content, and is sulfur-free, unlike other technical lignins, including kraft and soda lignins (Zhang et al., 2016a). In addition, organosolv lignin has fewer structural modifications with a low molecular weight and narrow polydispersity, because it is produced under relatively mild extraction conditions (Duval & Lawoko, 2014). It has also been reported that organosolv lignin, which can be dissolved under alkaline conditions, has a molecular weight range of 500–5000 Da and a relatively low $T_g$ (Laurichesse & Avérous, 2014). Considering the mentioned characteristics, organosolv lignin has a significant application potential in several industries.

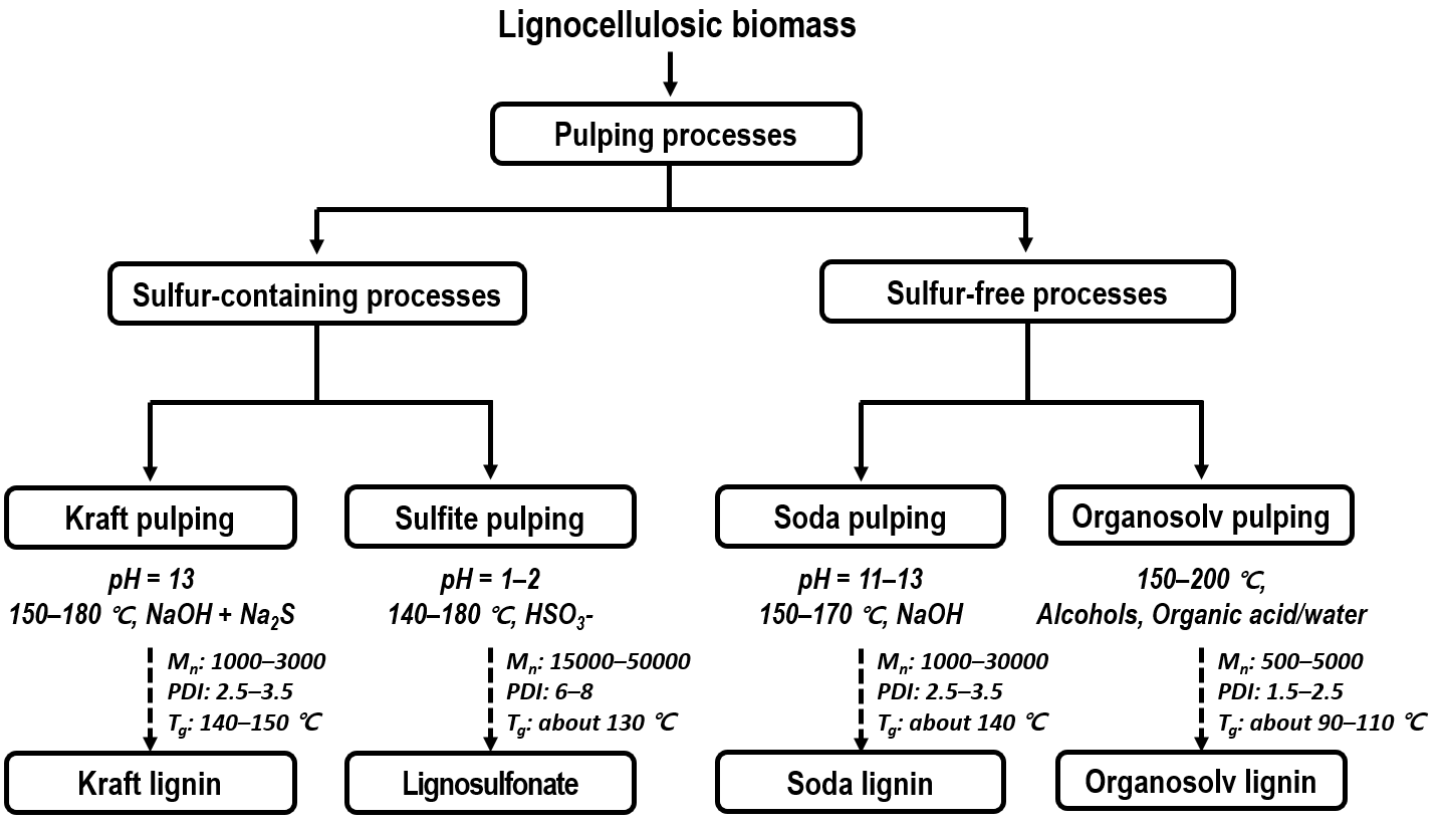


Figure 1-3. Characteristics of technical lignins based on the extraction process (Laurichesse & Avérous, 2014).

### 1.2.2. Diversity of the structural characteristics and thermal properties of lignin

Lignin is a polyphenolic macromolecule composed of phenyl propane units, including *p*-coumaryl alcohol (H unit), coniferyl alcohol (G unit), and sinapyl alcohol (S unit) (Boerjan et al., 2003). Lignin macromolecules have an amorphous 3D network structure with various intramolecular linkages formed by enzymatic radical coupling polymerization, as shown in Figure 1-4 (Boerjan et al., 2003). Lignocellulosic biomass has various lignin contents, and the proportion of monolignols and the intramolecular bond types depend on the types of lignocellulosic biomass (Calvo-Flores & Dobado, 2010). Generally, the order of the lignin content of lignocellulosic biomass based on the type is as follows: softwood > hardwood > herbaceous plant. In addition, the proportion of monolignols that constitute the lignin macromolecule and the ratio of intramolecular bond types are different (Calvo-Flores & Dobado, 2010). The lignin of gymnosperms consists of a large number of G units and a small number of H units, while the lignin of angiosperms is composed of large portions of G and S units, and a very small portion of the H unit (Boerjan et al., 2003) Contrarily, the high degree of substitution of the G unit and the S unit of lignin may cause steric hindrance and a decrease in the number of active sites, which may affect the reactivity of lignin (Duval & Lawoko, 2014).

In general, the most common intramolecular bonds of lignin are β-O-4 (aryl ether) bonds. Other main bonds include α-O-4 (aryl ether), β-5 (β-5, phenylcoumaran), 5-5 (biphenyl), 4-O-5 (diaryl ether), β-1 (1,2-diarylpropane), and β-β (resinol) bonds (Zakzeski et al., 2010). The degree of substitution and linkage type of intermolecular bonds will affect the properties and rigidity of lignin with increasing diversity. Although the diversity of the lignin structure hinders the extraction of lignin from lignocellulose in a uniform structure and

the prediction of the characteristics of the lignin produced, lignin has the potential to be used as an additive or a precursor of biodegradable plastic for imparting functionality; this is because it has several advantages, such as high thermal stability, radical-scavenging effect, and rigid structure (Yang et al., 2019). In particular, the thermal properties of lignin, such as a high $T_g$ and low mass loss at high temperatures, are important advantages that can compensate for the thermal vulnerability of biodegradable plastics (Sen et al., 2015).

Lignin macromolecules have various functional groups in their structure, including hydroxyl groups, methoxy groups, carbonyl groups, and carboxyl groups. Among these functional groups, the hydroxyl group content is predominant; the hydroxyl group can be roughly categorized into phenolic hydroxyl groups and aliphatic hydroxyl groups. The phenolic and aliphatic hydroxyl group contents are strongly influenced by the extraction conditions. The hydroxyl groups of lignin undergo inter- and intramolecular hydrogen bonding, resulting in the various physicochemical properties of lignin. Hydrogen bonds can cause steric hindrance by reducing the accessibility of the functional groups in lignin (Duval & Lawoko, 2014). Furthermore, the high hydroxyl group content of the lignin macromolecule results in a hydrophilic surface (Kai et al., 2016).

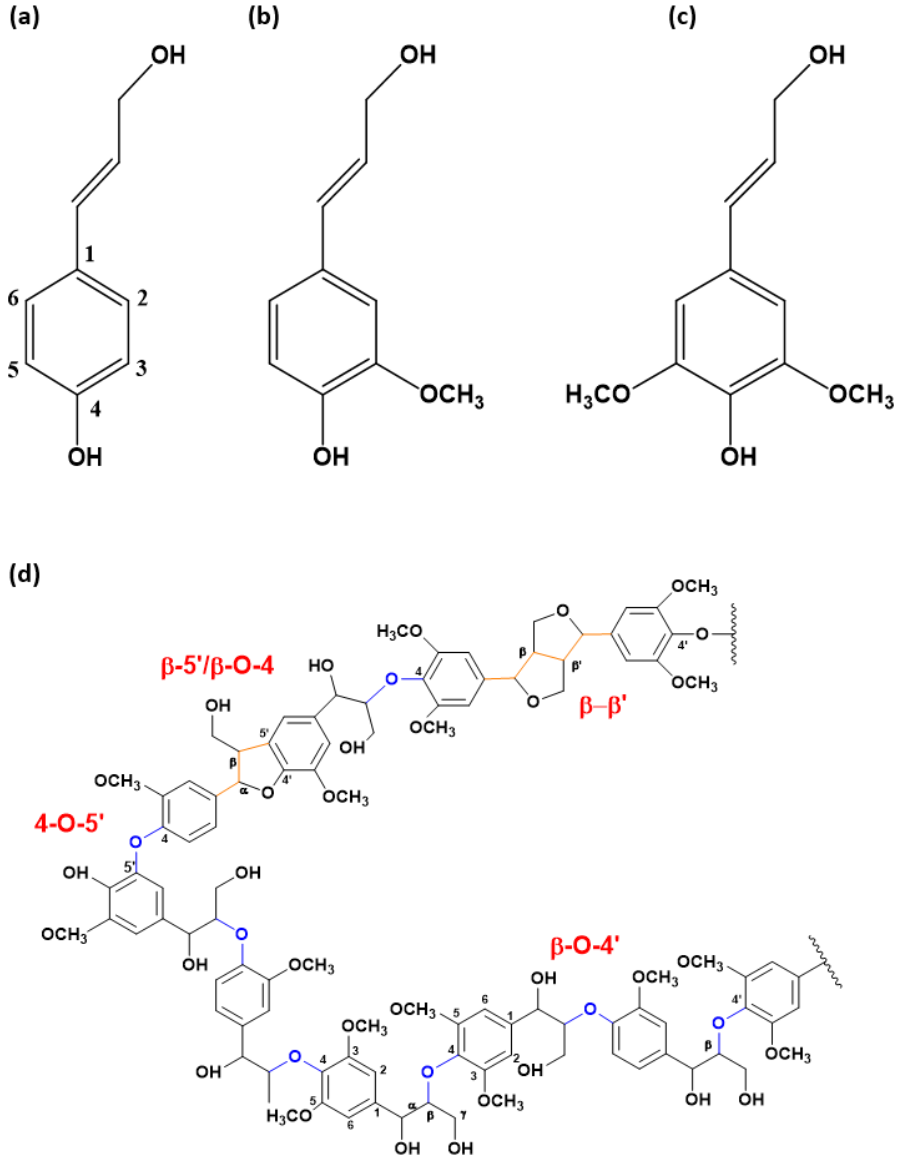


Figure 1-4. Chemical structures of lignin monomeric precursors and the macromolecular structure: (a) ρ-coumaryl alcohol, (b) coniferyl alcohol, (c) sinapyl alcohol, and (d) Lignin macromolecular structure (Amiri et al., 2019).

The phenolic structure in lignin provides thermal stability at high temperatures (Brodin et al., 2010). Lignin macromolecules cross-linked in three dimensions have the characteristics of thermoset materials (Cui et al., 2013). Studies have shown that lignin does not exhibit significant weight loss at temperatures below 300 °C and tends to form a crosslinked structure at high temperatures, enhancing its thermosetting properties (Brodin et al., 2010). However, these thermoset properties and low fluidity, attributed to the crosslinked structure in a network, limit the use of lignin in thermoplastics. On the other hand, lignin has a higher $T_g$ than those of most synthetic materials, which is one of the most significant factors that determine its thermal properties (Irvine, 1985). Lignin has condensed rigid phenolic moieties and a high frequency of intermolecular hydrogen bonding interactions, which limit the thermal mobility. The thermal properties of lignin vary depending on the types of lignin. Lignin derived from softwood shows a relatively high $T_g$ (138–160 °C), while lignin derived from hardwood has a relatively low $T_g$ (110–130 °C) (Thakur et al., 2014). Therefore, the properties of lignin are significantly influenced by its structural characteristics. Thus, understanding the relationship between the structure and the physicochemical properties of lignin is important in improving the commercial utilization of lignin in bioplastic production.

### 1.2.3. Bottlenecks of lignin utilization in bioplastic production

The following challenges are associated with the utilization of lignin in the bioplastic industry. 1) Lignin has a diverse structure, which hinders the prediction of its physicochemical properties (Baumberger et al., 2007). 2) Conventionally, lignin is incompatible with many kinds of hydrophobic thermoplastic matrix polymers, depending on the surface characteristics derived from numerous functional groups (Collins et al., 2019b). Lignin macromolecules have various functional groups in their structure, including hydroxyl groups, methoxyl groups, carbonyl groups, and carboxyl groups. Among them, the hydroxyl groups cause inter- and intramolecular hydrogen bonding, resulting in a hydrophilic surface. 3) Lignin has a low reactivity, which is attributed to the lack of active sites, due to the substitution of the methoxyl group. This hinders the chemical modification of lignin into thermosetting plastic materials (Laurichesse & Avérous, 2014). In addition, the high degree of substitution of the G unit and the S unit of lignin inhibits reactivity. This is attributed to the steric hindrance caused by the high degree of substitution by the methoxyl group in the phenyl propane unit and the abundant inter- and intramolecular hydrogen bonds (Duval & Lawoko, 2014). 4) Lignin has a rigid structure and non-uniform thermal properties, which reduce its processability (Hatakeyama & Hatakeyama, 2006). Many researchers have been working on the homogenization and chemical modification of lignin. However, the utilization of lignin as a functional additive and matrix in the bioplastic industry is still limited. Therefore, chemical modification of lignin with an understanding of the relationship between structure and properties of lignin is required to overcome these obstacles.

## 1.3. Strategies for improving the commercial utilization of lignin in bioplastic production

### 1.3.1. Selective production of lignin with desirable structure

As mentioned above, there are obstacles to the utilization of lignin in bioplastic production, attributed to its inherent properties. Nevertheless, many researchers have attempted to devise methods to apply lignin as a raw material in bioplastic production by exploiting its properties as a naturally occurring polymer. One of the concepts that increase the potential of lignin utilization is lignin structure selection. The following strategies for selecting the lignin structure are suggested. 1) By solvent fractionation. The lignin solvent fractionation method involves the sequential separation of lignin fractions with different solubilities, based on the structure, using several organic solvents. The lignin separated through solvent fractionation has a lower polydispersity index than that of the non-fractionated lignin, and it also exhibits different structural characteristics, including the molecular weight and functional group contents; consequently, it has different physicochemical properties (Duval et al., 2016; Park et al., 2018). However, the solvent fractionation method does not confer the desirable properties of lignin or lignin-containing bioplastic since the lignin whose structure has already been determined is extracted within a limited range. In addition, the use of a large amount of solvent for fractionation leads to an increase in the production cost, and the solvent recovery process through distillation also results in additional facility cost and energy consumption. Therefore , the solvent fractionation of lignin is not sufficient to enhance its applicability in bioplastic production. 2) By extraction condition control. During the delignification process, lignin macromolecules, which have complex inter- and intramolecular bonds within the biomass, are partially

depolymerized and converted into relatively small lignin fractions (McDonough, 1992). In addition, the converted lignin fractions can be recondensed by functional groups, depending on the process conditions, forming stronger bonds (Zhao et al., 2017). Thus, the characteristics of lignin significantly depend on the extraction conditions. Therefore, it is necessary to investigate the characteristics of organosolv lignin in relation to the extraction conditions.

### 1.3.2. Compatibilization of lignin and thermoplastic resins by functionalization

Depending on the compatibility with the matrix polymer used with lignin, the lignin–polymer bioplastic may be an unstable blend or a phase-separated blend (Collins et al., 2019b). Lignin generally exhibits high compatibility with polar matrix polymers due to the relatively high content of hydroxyl groups on its surface (Pouteau et al., 2004). Although lignin exhibits thermoplastic behavior, applying it as a matrix of thermo-bioplastics is difficult because it is susceptible to crosslinking at high temperatures and exhibits brittleness due to the formation of high-density crosslinks (Sakakibara, 1980). In addition, the surface properties of lignin containing a high hydroxyl group content aggravate the thermal stability at low temperatures and disrupt compatibility with hydrophobic plastic matrices. To compensate for these limitations of lignin as a thermoplastic material, many chemical modification methods have been devised. As part of the chemical modification method, the functionalization of the hydroxyl group of lignin has been attempted to improve the compatibility of lignin with a polymer matrix.

The functionalization of lignin to improve compatibility with the thermoplastic matrix can be achieved by the reaction of heterogeneous comonomers via the functional groups present in aliphatic chains and aromatic rings. The most common reactions can be broadly divided into esterification and grafting. Through functionalization, the thermoplasticity and compatibility of lignin with biopolyesters can be enhanced with the formation of a homogeneous thermo-bioplastic (Li & Sarkanen, 2005; Sadeghifar et al., 2012).

Lignin is often modified through esterification to increase the functional group reactivity or improve compatibility with thermoplastic biopolyesters. Lignin-based polyesters, which are polymers containing the ester functional

group in repeat units, are synthesized by the reaction of a hydroxyl group of lignin with a carboxylic acid, an acyl chloride, and an anhydride, yielding water, hydrochloric acid, and carboxylic acid, respectively (Evtugin & Gandini, 1996). Lignin-based polyesters are known to be thermally stable compared to raw lignin, and they can impart the intended characteristics depending on the comonomers (Guo & Gandini, 1991; Guo et al., 1992; Saito et al., 2012). However, with esterification, chemical equilibrium is attained in the reaction system; thus, it is difficult to elicit a complete reaction, and specific conditions are required to favor the ester formation. Moreover, in the production of lignin-based polyesters, the inhibition of the reactivity by the steric hindrance of lignin remains an obstacle (Guo & Gandini, 1991; Saito et al., 2012).

Grafting of lignin is achieved through radical polymerization and ring-opening polymerization (ROP) of matrix monomers, which are initiated by the hydroxyl groups of lignin (Sadeghifar et al., 2012). The lignin graft copolymer is generally synthesized by radical polymerization, where vinyl-based monomers are chain-polymerized to lignin macromolecules (Sadeghifar et al., 2012). Many studies have been conducted to form a lignin graft copolymer by introducing a chain reaction of vinyl monomers. In the reaction, the chain reaction of comonomers with the functional groups of lignin, as well as the homopolymerization of comonomers occurs together. To solve this problem, atom transfer radical polymerization (ATRP), which can improve the selectivity of the reaction, was developed (Wang et al., 2011). In addition, the presence of the radicals created by the initiator not only induces grafting of vinylic monomers to lignin, but may also cause polymerization of the vinyl monomers to each other, which deteriorates the production efficiency. Further, the grafting site of lignin macromolecules is unknown, since lignin has several radical resonance structures. Therefore, ATRP was proposed to solve the problem of low selectivity of the lignin graft copolymer. ATRP is achieved by two steps. The first step involves the preparation of a lignin macroinitiator by grafting a

radical-generating initiator on the phenolic hydroxyl groups of lignin. The second step involves grafting the heterogeneous monomers on the initiating site of the lignin macroinitiator. Thus, the chemical modification of lignin via ATRP is cumbersome as it involves two steps. Further, it involves many chemicals other than lignin, resulting in the diminished economic feasibility of lignin commercial utilization.

Conversely, the lignin graft copolymer can also be obtained by the ring-opening polymerization of compounds, such as cyclic ethers, lactone, and lactide, initiated by the hydroxyl group of lignin macromolecules. The most generally used cyclic ether for producing the lignin graft copolymer is propylene oxide (PO), and many studies have been attempted to confer compatibility and functionality on lignin through grafting with PO. The fully oxypropylated lignin only has an aliphatic hydroxyl group in its structure, and the aromatic hydroxyl group is substituted with a secondary aliphatic hydroxyl group. In addition, aliphatic hydroxyl groups are converted into branched forms with extended side chains. The substituted aliphatic hydroxyl group is relatively free from steric hindrance and hydrogen bonds, thereby improving accessibility, which can lead to increased reactivity for chemical modification (Cateto et al., 2009; Kelley et al., 1988a).

### 1.3.3. Macromoleculization of lignin with bifunctional monomers

For a macromoleculization complex synthesized using a bifunctional crosslinking agent, lignin can be employed as macromonomers for lignin-based copolymers. Lignin, a macromolecule having a high number of reactive sites per molecule, generally has a molecular weight in the range of hundreds to thousands g/mol; consequently, it is suitable for utilization as a “macro”-monomer of lignin-based copolymers (Duval & Lawoko, 2014). However, the high degree of substitution of the G unit and S unit of lignin not only reduces the number of reactive sites, but also induces steric hindrance, which has an adverse effect on the reactivity with the crosslinking agent (Duval & Lawoko, 2014; Hu et al., 2011). To increase the reactivity of lignin, several methods of preparing a prepolymer have been proposed, including removing methoxy groups from the lignin aromatic ring or sequentially derivatizing lignin with formaldehyde and phenol (Alonso et al., 2004; Hu et al., 2011).

Lignin macromolecules can react with a diisocyanate to form a thermosetting polyurethane resin. During the reaction, the aliphatic hydroxyl groups of lignin mainly react with a diisocyanate to form urethane resin, whereas the aromatic hydroxyl groups are known to have very poor reactivity (Evtuguin et al., 1998). To increase the reactivity of lignin with a diisocyanate, the modification of the aromatic hydroxyl group to an aliphatic hydroxyl group has been proposed. The mechanical properties of the lignin macromolecular complex are significantly influenced by the network crosslinking density, which depends on the molecular weight and hydroxyl group content of the lignin macromolecule participating in the crosslinking. Therefore, it is considered that the crosslink density and properties of the lignin macromolecular complex can be regulated by controlling the properties of the lignin macromolecule.

# 2. Objectives

Lignin, a naturally occurring polymer, has a high potential to be used as an additive to or a matrix of a bioplastic, to overcome the drawbacks of thermoplastics (biopolyester) and thermosetting plastics (biopolyurethane), such as poor thermal or mechanical properties and low price-competitiveness. However, there are several obstacles to the utilization of lignin in bioplastic production. First, lignin has unpredictable and non-uniform properties, attributed to its structural diversity. Second, it has low compatibility with most thermoplastic biopolyesters due to its relatively polar surface characteristics, derived from the numerous hydroxyl groups in its molecular structure. Third, lignin has a low reactivity, which is attributed to the lack of active sites and steric hindrance, caused by a high degree of substitution; this limits its application as a thermosetting plastic resin. Forth, lignin has a rigid structure and undesirable properties, which reduces its processability.

To improve the potential of lignin utilization, several phased strategies have been devised. Lignin with a desirable structure can be selectively extracted. The characteristics of lignin significantly depend on the extraction conditions, and the desired lignin structure can be obtained by controlling the extraction conditions. The compatibility with biopolyester and thermoplasticity of lignin can be improved by the functionalization of its constituent hydroxyl groups. In addition, macromoleculization of lignin can be employed to develop the thermosetting plastic resin.

Therefore, the investigation of the relationship between the lignin structure and the properties is important to prepare suitable lignin with the desired properties. Moreover, appropriate chemical modification strategies that strengthen the intended structure are necessary to enhance the desired properties. It is also necessary to understand the effect of the structural characteristics of lignin on

the chemical modification processes and the properties of the end-product.

In this study, the thermoplastic or thermosetting properties of lignin were enhanced by chemical modification, and it was utilized as an additive or a precursor of bioplastics. Using the modified lignin, thermoplastic and thermosetting bioplastics were developed, and the bioplastics containing lignin were designated as ligno-bioplastics. For this purpose, the response surface methodology (RSM) based on the central composite design (CCD) was adopted to investigate the effect of the extraction conditions (reaction temperature, sulfuric acid concentration, and ethanol concentration) on the structural characteristics (molecular weight, hydroxyl content, and intramolecular coupling structure) of ethanol organosolv lignin (EOL). Subsequently, the oxypropylation of three types of EOLs with different structures was carried out to improve the compatibility with biopolyesters, as well as the thermoplasticity to achieve a homogeneous thermo-bioplastic. Afterward, polyurethane synthesis was performed to develop a thermosetting lignopolyurethane. Eventually, the effect of the structural characteristics of lignin on the physicochemical properties of ligno-bioplastics was evaluated.

Therefore, the aims of this study are as follows:

1. Understanding the effects of extraction conditions on the structure of EOL for application as a bioplastic material.
2. Evaluating the correlation between the structure and thermal properties of EOL.
3. Improving the thermoplasticity of EOL and compatibility with biopolyester to achieve a miscible thermo-bioplastic
4. Preparing lignopolyurethanes with different thermal and mechanical properties depending on the types of EOL

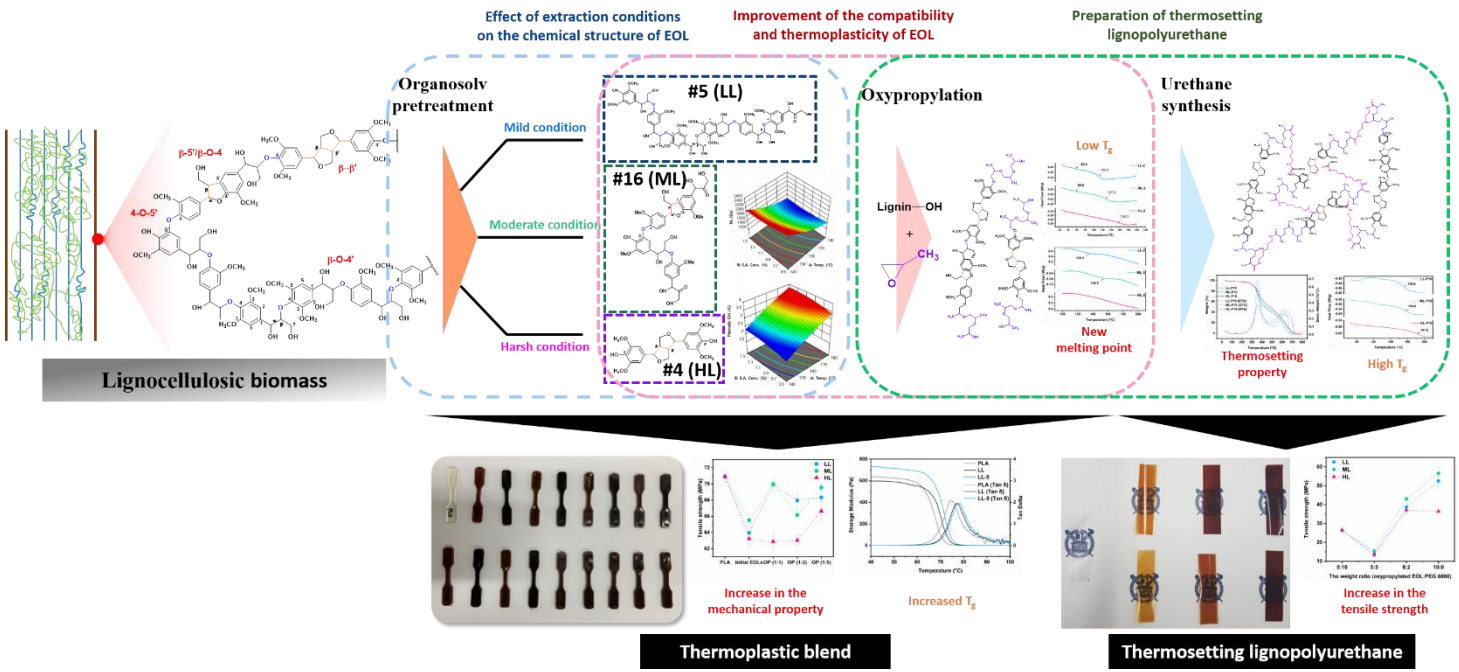


Figure 1-5. Scheme for ligno-bioplastic production.

# 3. Literature review

## 3.1. Investigation of the correlation between the structure and properties of lignin for its application in bioplastic production

### 3.1.1. Control of the lignin structure by adjusting the extraction conditions

For the effective application of lignin to bioplastics, the properties of bioplastics containing lignin must be predicted. In the same context, it is important to predict the properties of lignin, i.e., the feedstock, to select and prepare suitable lignin that exhibits the desired properties. The physicochemical properties of the lignin macromolecule are influenced by its structural characteristics, including its intramolecular bonds, functional groups, and molecular weight. Although the structure of the lignin macromolecule is mostly affected by the extraction method, it can be partially adjusted by modulating the reaction conditions even in the same extraction method. Therefore, it is necessary to specifically investigate the change in the structure of lignin in response to controlled reaction conditions. Several researches have been conducted to determine the effect of the extraction conditions on the structure of lignin.

During organosolv pretreatment, the decomposition and recondensation of organosolv lignin occur simultaneously, and this reaction behavior is significantly affected by the reaction conditions (reaction temperature = T, reaction time = m, catalyst concentration = c, alcohol concentration = C). In the study of pretreatment with methanol as an organic solvent using Eucalyptus

globulus, the molecular weight of lignin decreased with an increase in the reaction temperature and reaction time, as well as a decrease in the methanol concentration. The weight-average molecular weights ranged from 112 (T = 194 °C, t = 104 m, C = 38%) to 3615 Da (T = 176 °C, t = 56 m, C = 62%) (Gilarranz et al., 2000). In addition, in the previous paper on the production of EOL using eucalyptus, the severity factor was introduced to investigate the effects of the reaction conditions on the molecular structure of lignin. As the severity of the reaction increased, the weight-average molecular weight of the EOL decreased to 3490 Da and subsequently increased with further increase in the severity (Yáñez-S et al., 2014). In the study comparing the structural differences between EOL and milled wood lignin extracted from Miscanthus, the molecular weight decreased as the severity of the reaction increased (El Hage et al., 2010).

The contents of phenolic and aliphatic functional groups of the organosolv lignin are also dependent on the organosolv pretreatment conditions. The aromatic hydroxyl group content of the organosolv lignin tends to increase with an increase in the reaction temperature, reaction time, and concentration of the acid catalyst. In a study where methanol organosolv pretreatment was performed using Eucalyptus globulus, the highest phenolic hydroxyl content determined ranged from 1.42 (T = 194 °C, t = 104 m, C = 62%) to 2.96 mmol/g (T = 194 °C, t = 104 m, C = 38%) (Gilarranz et al., 2000). The Yáñez-S research team also reported that as the pretreatment severity increased, the content of aromatic hydroxyl groups increased with the introduction of a condensation phenol structure, which resulted in a significant decrease in the content of aliphatic hydroxyl groups (Yáñez-S et al., 2014). In the study on the extraction of EOL from bamboo by controlling the reaction conditions of ethanol organosolv pretreatment, the introduction of phenolic hydroxyl and carboxyl groups was promoted with the elimination of the methoxy group as the reaction temperature and reaction time increased (Fan et al., 2015).

Conversely, the intramolecular coupling structure of organosolv lignin also varies depending on the extraction conditions. In the coupling structure of the lignin macromolecule, aryl ether bonds account for the largest proportion. It is known that aryl ether bonds can be easily cleaved under alkaline or acid conditions (Ghozatloo et al., 2006). In a previous study characterizing EOL using Eucalyptus globulus, the effect of the extraction condition on the molecular structure was investigated. The content of β-O-4 bonds decreased as the severity of the extraction conditions increased, while the content of condensed phenolics increased (Yáñez-S et al., 2014). Another paper on EOL treatment with Miscanthus reported that as the severity of the treatment increased, the dehydration reaction of the lignin side chain occurred and the β-aryl ether cleavage progressed (El Hage et al., 2010).

Briefly, as shown in previous studies, the structural characteristics of lignin, such as the molecular weight, phenolic hydroxyl groups, and intramolecular coupling structure, can be partially regulated by controlling the extraction conditions. In addition, the properties of lignin to be displayed in bioplastics mainly depend on the structure of the lignin. Therefore, it is essential to investigate the conditions under which lignin, having a desirable structure, can be produced from the raw materials used in lignin extraction.

### 3.1.2. Thermal properties of lignin based on its structure

Lignin is a natural polymer that has a 3D network structure composed of a phenyl propane unit. It has various functions, such as thermal stability, antioxidant activity, and ultraviolet (UV) shielding properties derived from its structure. Recently, many studies have been actively conducted to impart functionality on bioplastics by blending of lignin; however, the irregular and unpredictable properties of lignin are considered as barriers to its application in the bioplastic industry. Therefore, to strengthen the required functions of lignin and predict its properties, the correlation between the structure and properties of lignin must be elucidated.

Lignin is known to be relatively stable at high temperatures because it has a backbone structure with aromatic rings. In addition, it has a $T_g$ range of 100–170 °C, which is higher than those of most synthetic polymers (Irvine, 1985). The high $T_g$ of lignin is attributed to the strong hydrogen bonding interactions of the phenolic hydroxyl group and the condensed rigid structure of the aromatic moieties, which limit transcalency (Laurichesse & Avérous, 2014; Yoshida et al., 1987). The structural characteristics of lignin and the inter- and intramolecular hydrogen bonds contribute to its thermoplasticity; however, the poor fluidity of lignin hinders its use as a thermoplastic resin. In addition, lignin is considered to have thermosetting properties since it forms a crosslink at high temperatures. Although many attempts have been made to industrially exploit the properties of lignin, including its relatively stable structure at high temperatures and its high natural abundance, the unpredictable thermal properties still limit its utilization.

In a previous study on the correlation between the structure and thermal properties of lignin isolated from a genetically modified poplar, the $T_g$ of lignin was clearly correlated with the degree of condensation of the structure. In other

words, it was found that the higher the proportion of C–C bonds in the molecule, the higher the $T_g$ (Baumberger et al., 2002). A study was conducted to reveal the correlation between the structural characteristics and thermal properties of three types of lignin produced sequentially during pretreatment with an ionic liquid. Thermogravimetric analysis (TGA) results revealed that the higher the molecular weight and the content of the β-O-4 linkage, the higher the maximum decomposition temperature of the lignin decomposition step (Wen et al., 2013a). A research team at Seoul National University investigated the thermal properties of structurally modified milled wood lignin, which were treated at various temperatures. The heat-treated lignin introduced C–C bonds with the decomposition of intramolecular β-O-4 bonds, which increased the maximum decomposition temperature in the thermal decomposition step of lignin (Kim et al., 2014). In a previous study, the structural analysis of sequentially collected lignin fractions using ionic-liquid pretreatment with ethanolamine acetate was performed. The ionic-liquid-treated lignin had a more condensed structure and fewer β-O-4 bonds than the enzymatically hydrolyzed lignin, resulting in improved thermal stability (Zhou et al., 2020). In a previous study on the induction of the esterification of kraft lignin (KL) using maleic anhydride (MA), succinic anhydride (SA), and phthalic anhydride (PA), the thermal properties of chemically modified KL were confirmed. Each modified lignin had a reduced hydroxyl group content and an increased carbonyl group content. PA-modified lignin showed a separated decomposition step and exhibited a sharp decrease in mass at low temperatures. The $T_g$ increased for MA- and SA-modified lignin but decreased for PA-modified lignin (Ibrahim et al., 2011). In a paper on the sequential solvent fractionation of lignin, it was reported that lignin fractions with a high molecular weight and phenolic OH group content had a high $T_g$ and char yield (Sadeghifar et al., 2017).

Studies have shown that factors such as the intramolecular bond structure, molecular weight, and aromatic hydroxyl content have a complex effect on the

thermal behavior, including the maximum decomposition temperature and $T_g$. It is considered that the lignin that has a condensed structure, in which C–C bonds are introduced instead of ether bonds in the intramolecular structure, exhibits the maximum decomposition rate and $T_g$ at high temperatures. A high $T_g$ of lignin may indicate the occurrence of thermal deformation at high temperatures, which contributes to the thermal stability as a thermosetting plastic resin. However, the high $T_g$ of lignin also reduces the processability of lignin as a thermoplastic resin. Therefore, it is important to impart desirable thermal properties, which cannot be achieved without understanding the relationship between the structure and the properties of lignin.

## 3.2. Unmodified lignin–PLA bioplastics

### 3.2.1. Mechanical properties of lignin–PLA bioplastics

In many studies on the formation of thermo-bioplastics using lignin and PLA, the tensile strength of the bioplastics tended to decrease. A study was conducted to investigate the properties of melt blended lignin–PLA bioplastics. In the lignin–PLA bioplastic containing a lignin content of 5–15%, the tensile strength was lower than that of neat PLA (Anwer et al., 2015). In another study, the tensile strength was reduced in the lignin–PLA bioplastics with a lignin content of 7%, while Young's modulus increased (Spiridon & Tanase, 2018). Another study was conducted to prepare a lignin–PLA film using lignin nanoparticles. The lignin nanoparticles were non-uniformly distributed due to the aggregation in the lignin–PLA film, resulting in a decrease in tensile strength (Yang et al., 2015). According to the results of previous studies, the lignin–PLA bioplastic exhibits low tensile strength.

The reasons for the poor mechanical properties of the lignin–PLA bioplastics can be summarized as follows. (1) Since lignin is poorly compatible with PLA in terms of miscibility, the interfacial bonding strength is weak, resulting in a decrease in the tensile strength. PLA exhibits higher hydrophobicity than lignin, which weakens the bonding strength between the interfaces, resulting in poor mechanical properties. In addition, the strong hydrogen bonding in lignin causes aggregation in the thermo-bioplastic. (2) The presence of lignin interferes with the continuous arrangement of PLA, which may reduce the tensile strength. The mechanical strength of the lignin–PLA bioplastics is not only significantly influenced by the interaction of the mixed interfaces, but also by the unique properties of the components. Therefore, it is important to identify the structural factors of lignin affecting the mechanical properties in

thermo-bioplastics and to select and modify the optimal lignin structure. Moreover, to enhance the compatibility of lignin, suitable chemical modification is required to prevent aggregation of lignin and enhance interfacial affinity.

### 3.2.2. Thermal properties of lignin–PLA bioplastics

For the thermal properties of the lignin–PLA bioplastic, according to studies, the thermal stability of the bioplastic tends to vary. With the evaluation of the availability of the lignin–PLA bioplastic as a biodegradable packaging material, the $T_g$ of the bioplastics decreased due to the low molecular weight and plasticity of lignin (Domenek et al., 2013). In a study in which lignin–PLA bioplastics were prepared using commercial alkali lignin and organosolv lignin extracted from almond shells, the thermal stability of the bioplastic increased with the addition of 5% lignin, although there was no change in the $T_g$ (Gordobil et al., 2014). In a study evaluating the thermal, dynamic mechanical, and morphological properties of a PLA-based bioplastic with lignin as a filler, TGA revealed that the lignin–PLA bioplastic began to decompose at a lower temperature than that for neat PLA (Anwer et al., 2015). In contrast, in another study using the lignin–PLA bioplastic, the $T_g$ tended to decrease continuously, although the decomposition initiating temperature increased with increasing the lignin content of the bioplastic (Li et al., 2003). In a previous study using triallyl isocyanurate as a crosslinking agent to increase the compatibility of the lignin–PLA bioplastic, the $T_g$ and melting point of the bioplastic decreased (Kumar et al., 2019).

Studies evaluating the thermal properties of lignin–PLA bioplastics have revealed conflicting thermal decomposition properties, depending on the types of lignin used. The lignin structure varies widely depending on the raw material and the extraction method, and consequently, lignin exhibits non-uniform thermal properties. Therefore, it is necessary to determine the lignin structure that can exhibit high thermal stability in a thermo-bioplastic while investigating the chemical modification methods that can improve the thermal stability.

## 3.3. Chemical modification of lignin for lignin–PLA bioplastics

### 3.3.1. Lignin graft copolymer

As mentioned above, the utilization of natural lignin as a bioplastic material is limited due to the difficulty in predicting the physicochemical properties. This is attributed to the complexity of the inter- and intramolecular bonding structure and the many hydroxyl groups contained on the surface. Moreover, the thermoplasticity of lignin and its low compatibility with biopolyesters impede its utilization as a thermoplastic material. To overcome these limitations and ensure the utilization of lignin in the thermoplastic field, many research groups have devised various strategies. These research groups focused on the chemical modification of lignin macromolecules by reacting chemicals that impart different functionalities on the functional groups of lignin. The modification not only increases the compatibility of lignin with the matrix polymer but also promotes the intended functionality.

The lignin graft copolymer can be prepared by the radical polymerization of the vinyl monomers on the hydroxyl group of lignin. Many studies have been conducted to produce a lignin graft copolymer by generating a radical on a functional group of a lignin macromolecule and inducing a chain reaction of vinylic monomers initiated by the generated radical. Each grafted lignin copolymer exhibits the desired functionalities, such as water solubility (lignin/polyacrylic acid copolymer) and hydrophobicity (lignin/polystyrene copolymer), depending on the properties of the grafted side-chain polymer (Chen et al., 1996; Ibrahim et al., 2010). However, the presence of the radicals created by the initiator not only induces grafting of vinylic monomers to lignin but may also induce the polymerization of the vinyl monomers to each other,

which decreases the production efficiency. Further, the grafting site of lignin macromolecules is unknown, since lignin has several radical resonance structures. Therefore, ATRP was proposed to solve the problem of low selectivity of the lignin graft copolymer. ATRP is achieved by two steps. The first step involves the preparation of a lignin macroinitiator by grafting a radical-generating initiator on the phenolic hydroxyl groups of lignin. The second step involves grafting heterogeneous monomers on the initiating site of the lignin macroinitiator. The lignin macroinitiator can be obtained by reaction with 2-bromoisobutyryl bromide, and grafting monomers such as N-isopropyl acrylamide and styrene can be used for ATRP (Gao et al., 2012; Hilburg et al., 2014). The lignin graft copolymer produced via ATRP has a high selectivity and can exhibit the intended properties depending on the characteristics of the monomers used for the grafting reaction (Wang et al., 2011). However, the lignin graft copolymer produced via this method has low price competitiveness in the bioplastic market, because an indispensable initiator must be used in the manufacturing stage. Moreover, the copolymer has a low molar fraction of lignin in its chemical structure; thus, it cannot be recognized as a copolymer based only on the properties of lignin. Therefore, it is necessary to compensate for the disadvantages of lignin and increase compatibility with polymer resins while maintaining the characteristics of lignin with a high proportion in the copolymer structure.

The hydroxyl groups of lignin macromolecules are often etherified to impart functionality or increase compatibility with matrices of thermo-bioplastics. The etherification of lignin can be performed through the ring-opening polymerization of compounds, such as cyclic ethers, lactone, and lactide, initiated by the attack of the hydroxyl group of the lignin macromolecule. The most generally used cyclic ether for producing the lignin graft copolymer is propylene oxide (PO), and many studies have attempted to confer compatibility and functionality on lignin through grafting with PO. Usually, in the lignin/PO

copolymer, PO is grafted to the lignin side chain with a degree of polymerization of 1–7, and the degree of polymerization depends on the stoichiometry of the lignin and PO monomers participating in the polymerization, as well as the amount of the catalyst used (Duval & Lawoko, 2014; Nadji et al., 2005).

The oxypropylated lignin retains a large proportion of the aliphatic hydroxyl groups, and the aromatic hydroxyl groups are replaced by secondary aliphatic hydroxyl groups. The substituted aliphatic hydroxyl group is free from steric hindrance in the chemical modification processes, resulting in a more homogeneous reactivity. In this respect, oxypropylated lignin has been widely used as a lignin macromonomer in several processes. The $T_g$ and viscosity of the lignin graft copolymer tend to decrease as the length of the grafted chain increases (Cateto et al., 2009; Kelley et al., 1988a). This phenomenon is also observed in lignin/polycaprolactone copolymers prepared using ε-caprolactone. As the length of the polycaprolactone side chain increases, the $T_g$ tends to decrease due to the weakened intermolecular hydrogen bonds (Hatakeyama et al., 2002).

Therefore, it is considered that the oxypropylation patterns differ based on the structural characteristics (molecular weight and hydroxyl group content) of lignin, and the oxypropylated lignin, whose structural characteristics and properties are properly controlled, can display improved compatibility with biopolyester, forming a homogeneous thermo-bioplastic with improved thermoplasticity and reactivity (Li & Sarkanen, 2005; Sadeghifar et al., 2012). However, thus far, studies on oxypropylated lignin have focused on increasing the functionality for use as a precursor of lignin macromoleculization (polyurethane synthesis), and few studies have attempted to improve the mechanical properties by the direct formation of a thermo-bioplastic with biopolyester, despite its high potential for use as a thermoplastic material. In addition, many studies have simply focused on the change in the properties

according to the stoichiometry of the lignin hydroxyl group and PO, while the change in reactivity or properties, attributed to the difference in the structural characteristics of the raw lignin, has not been investigated in detail.

### 3.3.2. Macromoleculization

Lignin, which has a molecular weight in the range of several thousand daltons and multiple functional groups per molecule, is suitable for use as a macromonomer for lignin macromolecular complex. This can be achieved by inducing cross-linked bonds between the lignin macromolecules using a bifunctional crosslinking agent. The lignin macromolecular complex may have a linear or branched copolymer structure depending on the ratio of the functional group of lignin and the dose of a bifunctional crosslinking agent.

Lignin macromolecules can react with a diisocyanate to form thermosetting biopolyurethane. During the reaction, the aliphatic hydroxyl groups of lignin mainly react with the diisocyanate to form urethane resin, while the aromatic hydroxyl groups are known to have very poor reactivity (Evtuguin et al., 1998). To increase the reactivity of lignin with a diisocyanate, a modification of the aromatic hydroxyl group to an aliphatic hydroxyl group has been proposed. Contrarily, it is known that the properties of a polyurethane are significantly affected by the crosslink density. One of the main parameters for determining the crosslink density in lignopolyurethanes, synthesized using lignin-derived polyol, is the molar ratio of the functional groups of isocyanates (NCO) and hydroxyl groups of lignin (OH). According to studies on lignopolyurethane synthesis, the higher the lignin content, the higher the density of crosslink, due to the increase in the molar ratio of hydroxyl groups; this leads to an increase in the tensile strength and a decrease in elongation (Das et al., 2015; Tavares et al., 2016). The thermal properties of polyurethane also depend considerably on the crosslink density. An increase in the crosslink density results in a decrease in the molecular mobility, increasing $T_g$ (Gouveia et al., 2019). In a study in which lignopolyurethane was synthesized using EOL, the $T_g$ increased as the lignin content increased, and this phenomenon was attributed to an increase in

the crosslinking density and rigidity of lignin (Avelino et al., 2018).

The thermal and mechanical properties of the lignin macromolecular complex largely depend on the network crosslinking density; the molecular weight of the lignin macromolecule between crosslinking agents and the number of functional groups contained in its structure are known as general factors influencing the crosslinking density. The crosslink density tends to be inversely proportional to the molecular weight between crosslinks and directly proportional to the number of lignin functional groups (Flory & Rehner Jr, 1943). A high crosslink density corresponds to a high stiffness and glassiness of the lignin macromolecular complex (Rials & Glasser, 1984; Yoshida et al., 1990). Furthermore, the crosslink density directly affects $T_g$. An increase in the crosslinking density increases $T_g$ by reducing the molecular mobility (Reimann et al., 1990; Saraf et al., 1985). In contrast, oxypropylated lignin can be used as a precursor for polyurethane synthesis by exploiting the high content of highly reactive aliphatic hydroxyl groups in its structure. Oxypropylated lignin increases the average molecular weight between crosslinks as the side-chain length increases, which can lead to a decrease in the crosslink density. It has been reported that oxypropylated lignin increases processability during the lignopolyurethane synthesis process and reduces brittleness (Upton & Kasko, 2016). In a previous study in which lignopolyurethane was prepared by varying the ratio of lignin/PO/catalyst, the density of the foam was reduced by up to 30% when formulated using oxypropylated lignin, resulting in increased processability in the blending process (Cateto et al., 2014). In a study in which lignopolyurethane was prepared by reacting oxypropylated lignin with methylene diphenyl diisocyanate (MDI), the tensile strength was improved by 135% due to the high accessibility of the hydroxyl group and rigid structure of oxypropylated lignin (Li & Ragauskas, 2012). In another research in which lignopolyurethane was synthesized using oxypropylated lignin having different side-chain lengths, the lignopolyurethanes prepared using oxypropylated lignin

with increased chain length tended to have a relatively low $T_g$ (Kelley et al., 1988b). Therefore, a lignopolyurethane properly synthesized using oxypropylated lignin displays improved tensile strength and processability without an additional increase in brittleness, which is due to the reduced $T_g$. The crosslink density of lignopolyurethane can be adjusted depending on the lignin structure.

Lignopolyurethane can be developed with appropriately controlled properties, depending on the lignin structure. However, most researches related to lignopolyurethane have focused on controlling the physicochemical properties by simply changing the amount of lignin added or modifying the synthesis method. In addition, lignin exhibits various physicochemical properties due to its complex bonding structures and functional groups, which makes it difficult to predict reactivity and final properties in bioplastic applications. Therefore, it is necessary to predict the crosslinking density of lignopolyurethane according to reactivity derived from lignin structures and to evaluate the thermal and mechanical properties of the final product.

# *Chapter 2*

## Thermal and mechanical properties of EOLs and EOL–PLA bioplastics

# 1. Introduction

Recently, fine plastic issues have emerged as a significant environmental problem, and it is expected to become increasingly serious as the amount of plastics production increases. According to Statista.com, global plastic production has increased steadily for decades, reaching 359 million metric tons in 2018 (Garside, 2019). Correspondingly, the amount of plastic waste generation has steadily increased, and only part of this waste is recycled, with the rest incinerated or delivered to landfills. Plastic incineration can lead to air pollution from the harmful gases generated during the process. In addition, petrochemical-based plastics take a long time to decompose and can cause soil contamination when deposited in landfills (Verma et al., 2016).

Biodegradable plastics, which are defined as plastics that can be decomposed into water and carbon dioxide by microorganisms in soil or water, have attracted much attention as alternative materials and solutions to ameliorate the environmental pollution caused by petroleum-based plastics in response to the depletion of petroleum resources and environmental pollution. In particular, biopolyesters such as include polylactic acid (PLA), polyhydroxyalkanoate (PHA), and polybutylene succinate (PBS) are considered to have a high potential to replace petroleum-based thermoplastics. However, even though most biopolyesters have the advantage of being biodegradable, there are some drawbacks to their mechanical properties, such as strength and elongation. Their thermal properties, including thermal stability and heat resistance, are weaker compared to conventional petrochemical-based plastics, resulting in poor processability (Sajjan et al., 2020). Furthermore, biopolyesters have lower price competitiveness than conventional plastics due to their uncommon processes, the high price of raw materials, and the small-scale market size (Chanprateep, 2010; Mostafa et al., 2018). Therefore, enhancing the

mechanical properties of biopolyesters and improving their price competitiveness are emerging as major issues for commercialization. To satisfy both goals, several efforts have been attempted to adjust the mechanical and thermal properties by manufacturing a fully biomass-based thermoplastic using components of lignocellulosic biomass that have high price competitiveness, biodegradability, and unique properties (Kumar & Tumu, 2019).

Lignin, a naturally occurring polymer, can be produced at a relatively low cost due to its simple manufacturing process compared to that of other synthesized polymers and has the advantages of excellent biocompatibility and biodegradability (Yang et al., 2019). Accounting for approximately 20-30% of lignocellulosic biomass, lignin is the second most abundant naturally occurring polymer in the world. Lignin has unique properties, such as thermal stability and antioxidant, antifungal and antibacterial activities, and a rigid structure (Ganewatta et al., 2019). In particular, the thermal properties of lignin, which are derived from its inherent structure, can be remarkable advantages for the thermal vulnerability of biopolyesters (Sen et al., 2015). In this respect, lignin has the potential to be used as an additive or a precursor of bioplastics material.

On the other hand, lignin macromolecules have complex bonding structures and functional groups, and these structures lead to unique properties. Lignin macromolecules have various functional groups in their structure, including hydroxyl groups, methoxy groups, carbonyl groups, and carboxyl groups. Among these functional groups, the hydroxyl group content is predominant, and hydroxyl groups can be roughly categorized into phenolic hydroxyl groups and aliphatic hydroxyl groups. Phenolic hydroxyl group and aliphatic hydroxyl group contents are strongly influenced by the extraction conditions. The hydroxyl groups of lignin cause inter- and intramolecular hydrogen bonding, resulting in the various physicochemical properties of lignin. Hydrogen bonds can cause steric hindrance by reducing the accessibility of the functional groups in lignin (Duval & Lawoko, 2014). The phenolic structure in lignin provides

thermal stability at high temperatures (Brodin et al., 2010). Interestingly, lignin has both thermoplastic and thermosetting properties due to its amorphous structure and inter- and intramolecular interactions (Jeong et al., 2013). Lignin macromolecules cross-linked in three dimensions have the characteristics of thermoset materials (Cui et al., 2013). In this way, the properties of lignin are greatly influenced by its structural characteristics.

However, lignin produced by a delignification process has diverse structure, making it difficult to predict its physicochemical properties (Baumberger et al., 2007). The lignin structure greatly depends on the extraction conditions. During processing, lignin macromolecules, which have complex inter- and intramolecular bonds within the biomass, are partially depolymerized and converted into smaller lignin fractions (McDonough, 1992). In addition, the converted lignin fractions can be recondensed by functional groups, depending on the process conditions, forming stronger bonds (Zhao et al., 2017). Therefore, it is necessary to investigate the structural characteristics of organosolv lignin according to the extraction conditions. Furthermore, the correlation between the structural characteristics and the thermal properties of lignin needs to be evaluated to enhance the potential for commercial utilization of lignin as bioplastic material.

# 2. Materials and methods

## 2.1. Ethanol organosolv lignin (EOL) preparation

### 2.1.1. Raw materials

A debarked jolcham oak (*Quercus serrata*) was supplied by the Taehwasan Academic Forest. The logs were milled by a sawdust producer (UR-300B, Yulim Machinery, Gyeongsan, Republic of Korea), and then, the sawdust was finely ground into particles of approximately 0.5 mm by the Pulverisette 15 cutting mill (FRITSCH GmbH, Idar-Oberstein, Germany). The fine powders were air-dried to a moisture content of less than 5% and stored at 4 °C until used.

### 2.1.2. Conditions for EOL extraction

Response surface methodology (RSM) based on the central composite design (CCD) was adopted to investigate the effect of the extraction conditions on the structural characteristics of EOL. Table 2-1 shows the reaction conditions composed of 23 factorial points and 3 central points selected based on the results of previous studies conducted in our laboratory: reaction temperature: 160 °C; sulfuric acid concentration: 1%; and ethanol concentration: 60%. The independent variables were set as the reaction temperature (X1, °C), sulfuric acid concentration (X2, %), and ethanol concentration (X3, %). The coded level of each run corresponded to the actual independent variable as follows (variable = value of the center point/variation of the coded level per point): reaction temperature = 160/20, sulfuric acid concentration = 1/0.5, ethanol concentration = 60/20. The dependent variables were set as the number-average

molecular weight (Y1, Da), weight-average molecular weight (Y2, Da), polydispersity index (Y3), phenolic hydroxyl group content (Y4, mmol/g), and aliphatic hydroxyl group content (Y5, mmol/g). The reaction time was fixed to 5 min as a control variable. The combined severity factors (CSF) of ethanol organosolv (EO) extraction conditions performed according to the experimental matrices was calculated as follows (Jang et al., 2016):

$$\text{Combined severity factor (CSF)} = log\{t \times exp\left[\frac{T_H - 100}{14.75}\right]\} - pH$$

Table 2-1. The central composite design (Center points: 160, 1, 60) for the RSM with CSF

| Std | Run | Coded level | | | Variables | | | CSF |
|---|---|---|---|---|---|---|---|---|
| | | Reaction Temp. $X_1$ | $H_2SO_4$ Conc. $X_2$ | EtOH Conc. $X_3$ | Reaction Temp. (℃) | $H_2SO_4$ Conc. (%. (w/v)) | EtOH Conc. (%, (v/v)) | |
| 3 | 1 | -1 | 1 | -1 | 140.0 | 1.50 | 40.0 | 1.14 |
| 7 | 2 | -1 | 1 | 1 | 140.0 | 1.50 | 80.0 | 1.08 |
| 1 | 3 | -1 | -1 | -1 | 140.0 | 0.50 | 40.0 | 0.65 |
| 5 | 4 | -1 | -1 | 1 | 140.0 | 0.50 | 80.0 | 0.46 |
| 16 | 5 | 0 | 0 | 0 | 160.0 | 1.00 | 60.0 | 1.42 |
| 17 | 6 | 0 | 0 | 0 | 160.0 | 1.00 | 60.0 | 1.42 |
| 2 | 7 | 1 | -1 | -1 | 180.0 | 0.50 | 40.0 | 1.82 |
| 10 | 8 | 1.68 | 0 | 0 | 193.6 | 1.00 | 60.0 | 2.41 |
| 13 | 9 | 0 | 0 | -1.68 | 160.0 | 1.00 | 26.4 | 1.63 |
| 9 | 10 | -1.68 | 0 | 0 | 126.4 | 1.00 | 60.0 | 0.43 |
| 14 | 11 | 0 | 0 | 1.68 | 160.0 | 1.00 | 93.6 | 1.60 |
| 12 | 12 | 0 | 1.68 | 0 | 160.0 | 1.84 | 60.0 | 1.73 |
| 4 | 13 | 1 | 1 | -1 | 180.0 | 1.50 | 40.0 | 2.31 |
| 11 | 14 | 0 | -1.68 | 0 | 160.0 | 0.16 | 60.0 | 0.62 |
| 8 | 15 | 1 | 1 | 1 | 180.0 | 1.50 | 80.0 | 2.25 |
| 15 | 16 | 0 | 0 | 0 | 160.0 | 1.00 | 60.0 | 1.42 |
| 6 | 17 | 1 | -1 | 1 | 180.0 | 0.50 | 80.0 | 1.63 |

### 2.1.3. EOL extraction process

Ethanol organosolv (EO) extraction was conducted to dissolve lignin from the complex cell wall structure of the biomass according to an experimental matrix of 17 runs extracted from the CCD. 50 g of wood powder was loaded with 400 mL of solvent prepared to depend on each run's reaction conditions. The EO extraction was carried out using a 1,000 mL-capacity batch type reactor. The reactor was heated to the target temperature for 40 min and then maintained for 5 min. After the reaction was completed, the reactor was quenched to 60 °C using an ice chamber. The liquid fraction was collected by solid-liquid separation with filter paper (No. 52, Hyundai Micro Co., Seoul, Republic of Korea).

An 8-fold dilution of the liquid fraction was prepared with deionized water to precipitate the EOL, and the suspension was allowed to stabilize for 24 h. The precipitated lignin was separated from the liquid fraction using the same filter paper as was used for the solid-liquid separation and lyophilized for 72 h. The EOL yield was calculated as follows: EOL yield (%) = EOL obtained (g) in the filtrate/lignin content (g) in the oven-dried raw material × 100

## 2.2. Structural characteristics of the EOL

### 2.2.1. Molecular weight

The acetylation of the EOL was determined to analyze the molecular weight. 50 mg of EOL was reacted with an acetic anhydride-pyridine (1:1, v/v) mixture at 105 °C for 2 h. After the reaction was complete, the acetylated EOL was collected by dropping in deionized water. 5 mg of acetylated EOL was dissolved in 1 mL of tetrahydrofuran (THF). The sample was filtered by a 0.45 μm polytetrafluoroethylene (PTFE) filter (Advantec Co., Japan). After preparation of the sample, the number-average molecular weight ($M_n$), weight-average molecular weight (Mw), and polydispersity index (PDI) were analyzed by gel permeation chromatography (GPC) with Nexera LC-40 (Shimadzu, Japan) equipped with an SDV 1000A 5 μm 8 × 300 mm S/N 91112605 column. The mobile phase flow rate was 1 mL/min. The calibration curves were set using 12 polystyrene standards with a range of molecular weights from 266 to 62,500 Da.

### 2.2.2. Hydroxyl group content

The hydroxyl group content of the EOL was determined by phosphorus-31 nuclear magnetic resonance (31P NMR) spectroscopy, as described in previous studies. Pyridine and deuterated chloroform were mixed to prepare a solvent solution (1.6:1(v/v)). A mixture solution was prepared by adding 100 mg of cyclohexanol (internal standard) and 90 mg of chromium acetylacetonate (relaxation reagent) to 25 mL of the solvent solution. Approximately 20 mg of lignin was accurately weighed and placed in a 4-mL vial. A total of 400 μL of the solvent solution and 150 μL of the mixture solution were used to dissolve

the EOL. The mixture was stirred for 5 min. After mixing, 70 μL of 2-chloro-4,4,5,5-tetramethyl-1,2,3-dioxaphospholane was introduced into the mixture as a phosphorylating reagent. The mixture was blended with a vortex mixer for a few seconds. The completely prepared samples were transferred to a 5-mm NMR tube for analysis by 31P NMR spectroscopy. The 31P NMR spectra of the EOL from 17 runs were obtained using a 600 MHz NMR spectrometer (ADVANCE 600, Bruker, Germany) equipped with a 14.095 Tesla superconducting 51-mm bore magnet and 5 mm BBO BB-H&F-D CryoProbe Prodigy.

### 2.2.3. Intramolecular coupling structure of EOL

The intramolecular coupling structure of EOL was investigated using quantitative 2D-heteronuclear single quantum coherence (HSQC) NMR spectroscopy. Quantitative 2D-HSQC NMR spectroscopy was performed using a 600 MHz NMR spectrometer (ADVANCE 600, Bruker, Germany). 50 mg of EOL was prepared by dissolving it in dimethylsulfoxide (DMSO)-d6 for analysis. Each HSQC experiment was performed using Bruker's 'hsqcetgpsisp2.2' pulse program with the following parameters: a 90° pulse, 0.08 s acquisition time, 2.0 s pulse delay, 1JC-H at 150 Hz, 48 scans, and acquisition of 1024 data points (for 1H) over 512 increments (for 13C). Data processing and analysis were performed using MestReNova v6.0 software. The coupling structure of the EOL sample according to HSQC spectroscopy was determined by correlating the data from databases cited in the literature (Constant et al., 2016; Wen et al., 2013b). The C9 unit (S unit and G unit) in aromatic/unsaturated (δC/δH 100–125/6.5–7.5) regions and the coupling structure (β-O-4, β-β, and β-5) in the oxygenated aliphatic side chain (δC/δH 50–90/2.5–6.0) regions were determined by a quantitative method based on the

2D-HSQC spectra using aromatic units as internal standards (Wen et al., 2013b). The internal standard (C9) and coupling structure ($I_x$%) are calculated as follows:

$$C9 = 0.5(S + S') + G$$

$$I_x\% = \frac{I_x}{I_{C9}} \times 100$$

$I_x$ is obtained as the integral of the α-position of β-O-4, β-β and β-5.

## 2.3. Thermal properties of EOL

### 2.3.1. Thermal decomposition characteristics of EOL

The thermal decomposition characteristics of EOL obtained from 17 runs were analyzed by a thermogravimetric analyzer (Discovery TGA, TA Instruments, USA). Approximately 10 mg of sample was scanned from 25 to 800 °C at a constant heating rate of 10 °C/min. After reaching the target temperature, the furnace was cooled in a high-quality nitrogen inert atmosphere with a 50 mL/min $N_2$ flow.

### 2.3.2. Glass transition temperature of EOL

The glass transition temperatures of EOLs were investigated using a differential scanning calorimeter (Discovery DSC, TA instruments, USA). DSC analysis was conducted in the temperature range from -25 to 250 °C under high-quality nitrogen flow. The first heating scan was conducted in the temperature range from 25 to 180 °C at a heating rate of 10 °C/min, and the target temperature was held for 2 min to exclude the thermal history of the EOLs. Then, the temperature of the furnace was decreased to -25 °C and held for 10 min. For the second heating scan, the temperature was heated from -25 to 250 °C at the same heating rate as used in the 1$^{st}$ scan. The glass transition temperatures of the EOLs were determined by the second heating scan data.

### 2.3.3. Statistical analysis

Linear least squares analysis of the dataset, which contained the correlation between the thermal decomposition behaviors and the structural characteristics

of lignin, was performed by a routine implemented in Python (version 3.9). Multiple linear regression was used to quantify the effect of the molecular weight ($M_w$/1000), phenolic hydroxyl group content (PhOH), and aliphatic hydroxyl group content (AlOH) on the weight loss of EOL at 300 °C. The regression model was derived as follows:

$y_j = \beta_0 + \beta_1 x_{1j} + \beta_2 x_{2j} + \beta_3 x_{3j} + \varepsilon_j$

$y_j$ = dependent variable (weight loss of EOL at 300 °C)

$x_{1j},\ x_{2j},\ x_{3j}$= independent variable ($M_w$/1000, PhOH, and AlOH)

$\beta_1, \beta_2,\ \beta_3$= regression coefficients

$\beta_0$= intercept

$\varepsilon_j$ = residual

In this study, the ordinary least squares (OLS) method was applied to fit the sample data. The least squares method substitutes the regression coefficients that minimize the sum of the residual squares with their estimated values. In this case, the sum of squares of the residuals can be obtained as follows:

$$SSE = \sum_{i=1}^{n} \varepsilon_i^2 = \sum_{i=1}^{n} \{ y_i - (\beta_0 + \beta_1 x_{1j} + \beta_2 x_{2j} + \beta_3 x_{3j}) \}^2$$

$SSE =$ sum of squares of residuals

A regular equation is used to find the factor that minimizes the sum of squares of the residuals. The $SSE$ is organized by substituting $b_0,\ b_1, b_2,\ b_3$ for the $\beta_0,\ \beta_1, \beta_2,\ \beta_3$ that makes the value 0 by partial differentiation. Calculate the regression coefficient of each independent variable by combining the applied regular equations and arranging about $b_0,\ b_1, b_2,\ b_3$.

## 2.4. EOL–PLA bioplastic

### 2.4.1. Preparation of EOL–PLA bioplastics

For preparation of EOL–PLA bioplastics, three types of EOL (#5, #16, and #4) with different structural characteristics were selected. Selected three types of EOL extracted in low-severity condition (#5), moderate-severity condition (#16), and high-severity condition (#4) EOLs were named LL, ML, and HL, respectively. EOL and PLA (2003D, NatureWorks, USA) were mechanically mixed and melted at various mixing ratios (0, 1, 5, 10% (w/w) of EOL in the EOL–PLA bioplastic) using a specimen molding machine (KP-M2100H, Kipae, Republic of Korea). The operating conditions were the same for all samples: 200 °C operating temperature, 5 min operation time, and 100 rpm. Then, the bioplastics were injected to mold a specimen for the tensile strength test.

### 2.4.2. Thermal properties of EOL–PLA bioplastics

The TGA and DSC analysis were adopted for the investigation of thermal properties of EOL–PLA bioplastics. The TGA analysis was performed as described in section 2.2.4 of Chapter 2. The DSC analysis was performed as described in section 2.2.5 of Chapter 2.

### 2.4.3. Mechanical properties of EOL–PLA bioplastics

To obtaining the tensile strength and elongation of oxypropylated EOL–PLA bioplastics, the tensile tests were carried out according to ASTM D638 with a tensile testing machine (Low Force Universal Testing Systems, Instron, USA). The test was performed with a gap between the grips of 25.4 mm and a constant strain rate of 10 mm/min.

# 3. Results and Discussion

## 3.1. Structural characteristics of EOL based on the extraction conditions

For the effective utilization of lignin in bioplastics applications, the properties of bioplastics containing lignin have to be predicted. In the same context, it is important to determine the properties of the lignin feedstock to select and prepare suitable lignin that exhibits the desired properties. The physicochemical properties of lignin macromolecules are influenced by their structural characteristics, such as intramolecular bonds, functional groups, and molecular weight. The structural characteristics of the lignin macromolecules are most affected by the extraction method. However, the lignin structure can be partially adjusted depending on the extraction conditions even when the same extraction methods are used. Therefore, it is necessary to specifically investigate how the lignin structure changes as the extraction conditions are controlled. During organosolv pretreatment, the decomposition and recondensation of organosolv lignin occur simultaneously, and this reaction behavior is greatly affected by the reaction conditions.

### 3.1.1. Molecular weight and PDI

In general, EOL has a molecular weight in the range of 500-5,000 Da, and the molecular weight of EOL is affected by the organosolv pretreatment reaction conditions (Laurichesse & Avérous, 2014). The results of the RSM analysis used to investigate the effect of the extraction conditions on the molecular weight of EOL are shown in Table 2-2 and Figure 2-1. The F-value of the molecular weight model ($M_n$= 33.04, $M_w$= 82.8) implies that the model is significant (Table 2-2). P-values less than 0.0500 indicate that the model terms are significant. In this case, A (reaction temperature) and B (sulfuric acid concentration) are significant model terms. Within the range covered by this model, the number-average molecular weight of lignin tended to decrease with increasing reaction temperature and sulfuric acid concentration (Figure 2-1(b)). During the process of EO extraction, an increase in the reaction temperature and sulfuric acid concentration stimulated the extensive decomposition of aryl-ether bonds, which are easily cleaved under acidic conditions. The decomposition of aryl-ether bonds converts lignin macromolecules into smaller fractions of the same molecular weight (Sannigrahi et al., 2010). The excessive severity of the extraction conditions may decompose lignin into small fractions that cannot be recovered. In addition, recondensation between phenolic compounds derived from lignin macromolecules, including a benzyl carbocation reaction and an α-position condensation, can occur simultaneously, resulting in a rigid structure of lignin and an increase in the polydispersity (McDonough, 1992; Zhao et al., 2017). However, as the maximum point was not observed in the extraction condition range adopted in this study, excessive decomposition or condensation was assumed to have not been induced. Interestingly, even for the same extraction method, the molecular weight of lignin was distributed over a wide range depending on the extraction conditions.

In the case of the $M_w$, the lignin extracted under harsh conditions (X1: 180 °C, X2: 1.5%, X3: 40%) was approximately 2200 Da, while the lignin extracted under mild conditions was approximately 6200 Da.

Table 2-2. Statistical analysis of variance (ANOVA) for the EOL molecular weight models

| Source | Sum of squares | DF | Mean square | F-value | P-value |
|---|---|---|---|---|---|
| Model ($M_n$) | 2.E+06 | 9 | 3.E+05 | 33.04 | < 0.0001 |
| A-Temp. | 2.E+06 | 1 | 2.E+06 | 245.88 | < 0.0001 |
| B-S.A. Conc. | 1.E+05 | 1 | 1.E+05 | 13.54 | 0.0079 |
| C-EtOH Conc. | 6.E+03 | 1 | 6.E+03 | 0.70 | 0.4308 |
| Model ($M_w$) | 4.E+07 | 9 | 5.E+06 | 82.80 | < 0.0001 |
| A-Temp. | 3.E+07 | 1 | 3.E+07 | 539.81 | < 0.0001 |
| B-S.A. Conc. | 3.E+06 | 1 | 3.E+06 | 58.55 | 0.0001 |
| C-EtOH Conc. | 6.E+04 | 1 | 6.E+04 | 1.15 | 0.3184 |

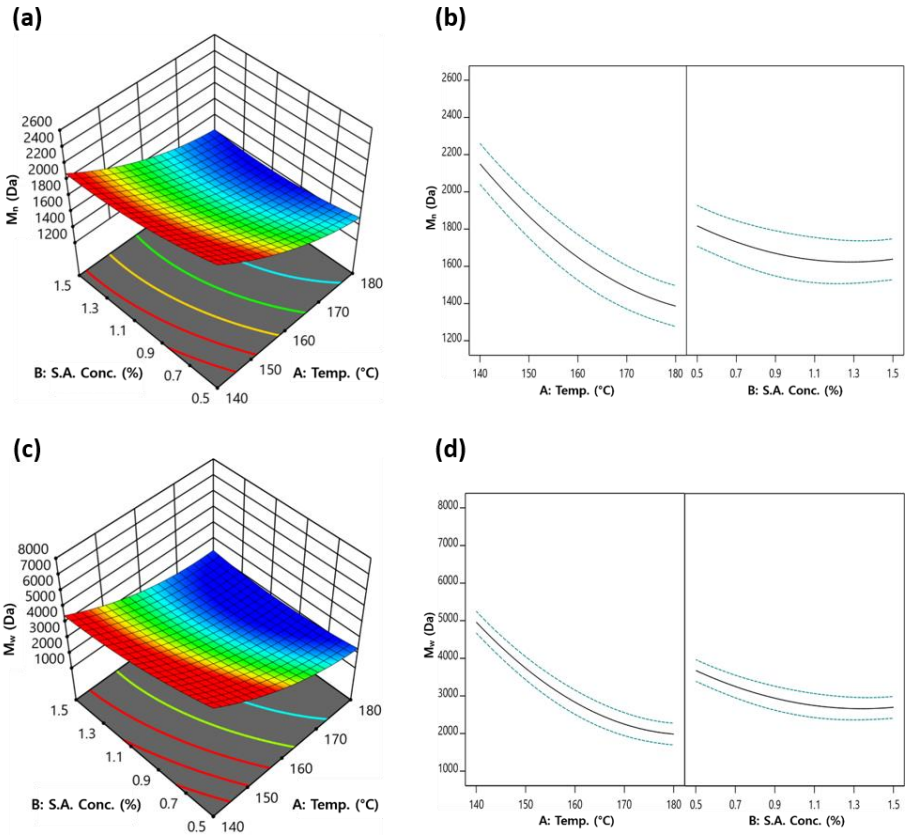


Figure 2-1. The effect of the extraction conditions on the EOL molecular weight. (a) The contour plot of the RSM for the number-average molecular weight ($M_n$) model. (b) The one-factor plots of $M_n$ versus significant variables. (c) The contour plot of the RSM for the weight-average molecular weight ($M_w$) model. (d) The one-factor plots of $M_w$ versus significant variables.

Furthermore, Table 2-3 and Figure 2-2 show the effect of the extraction conditions on the polydispersity index of the EOL. As shown in Table 2-3, the polydispersity index model was found to be significant according to the statistics, and the reaction temperature and sulfuric acid concentration were significant model terms. The PDI of the EOL tended to decrease with increasing reaction temperature and sulfuric acid concentration (Figure 2-2). As the severity of the extraction conditions increased, lignin macromolecules with higher molecular weights containing a large number of aryl-ether bonds in the structure depolymerized more often than lignin molecules with smaller molecular weights (Gilarranz et al., 2000; Tirtowidjojo et al., 1988). For this reason, $M_w$ decreased more significantly than $M_n$, leading to a decrease in the PDI. In this model, the PDI was approximately 2.5 under mild extraction conditions and decreased to approximately 1.5 as the extraction conditions became severe. The EOL obtained by adjusting the extraction conditions had a narrow PDI value compared to other technical lignin, which guarantees high potential for industrial application (Pan et al., 2005).

Table 2-3. Statistical analysis of variance (ANOVA) for the EOL polydispersity index model

| Source | Sum of squares | DF | Mean square | F-value | P-value |
|---|---|---|---|---|---|
| Model (PDI) | 2.87 | 9.00 | 0.32 | 45.06 | < 0.0001 |
| A-Temp. | 1.89 | 1.00 | 1.89 | 267.05 | < 0.0001 |
| B-S.A. Conc. | 0.30 | 1.00 | 0.30 | 42.68 | 0.0003 |
| C-EtOH Conc. | 0.00 | 1.00 | 0.00 | 0.10 | 0.7559 |

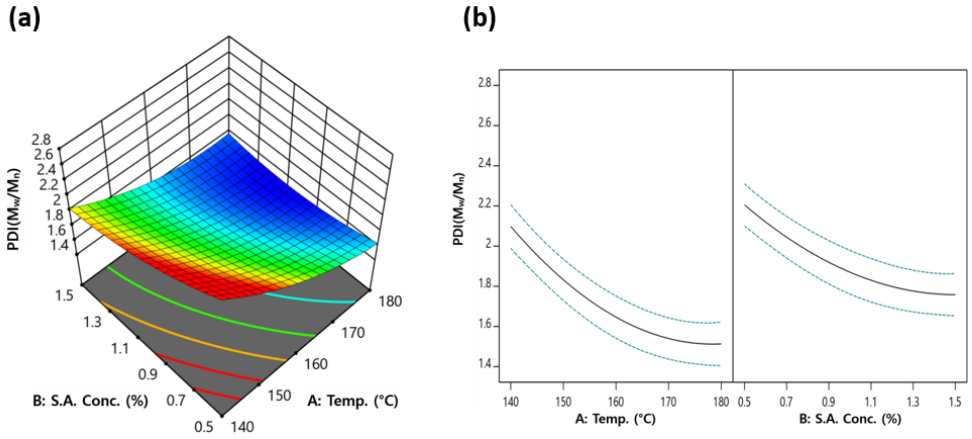


Figure 2-2. The effect of the extraction conditions on the EOL polydispersity index (PDI). (a) The contour plot of the RSM for the PDI model. (b) The one-factor plots of PDI versus significant variables.

### 3.1.2. Hydroxyl group content

Lignin macromolecules have various functional groups in their structure, including hydroxyl groups, methoxy groups, carbonyl groups, and carboxyl groups. Among these groups, the hydroxyl group content is predominant, and hydroxyl groups can be roughly categorized into phenolic hydroxyl groups and aliphatic hydroxyl groups. The phenolic hydroxyl group and aliphatic hydroxyl group content levels are strongly influenced by the extraction conditions. These lignin hydroxyl groups cause inter- and intramolecular hydrogen bonding, resulting in different physicochemical properties of the lignin. (Duval & Lawoko, 2014). Table 2-4 and Figure 2-3 describe the effect of the extraction conditions on the phenolic and aliphatic hydroxyl contents of the EOL.

The F-values of the phenolic hydroxyl group and the aliphatic hydroxyl group model were 18.10 and 13.09, respectively. The P-values were 0.0005 and 0.0013, respectively, which indicates that these models are significant within the set range. As shown in Table 2-4, the extraction temperature and sulfuric acid concentration had a low P-value (< 0.5), which indicates these two independent variables are powerful model terms. In the contour plot results, the phenolic hydroxyl group content increased with increasing reaction temperature and sulfuric acid concentration. Under the extraction process with high temperature and acidic conditions, β-O-4 bonds, which are the dominant chemical coupling structure of EOL, are actively cleaved by nucleophilic substitution reaction, resulting in an increase in the phenolic hydroxyl groups content (Goyal et al., 1992; McDonough, 1992).

On the other hand, the content of the aliphatic hydroxyl group decreased as the temperature of the extraction increased, showing an opposite tendency to that of the phenolic hydroxyl group. In general, a solvent molecule including methoxy group or ethoxy group is introduced as a nucleophile instead of a

hydroxyl group at the electrophilic site of the lignin side chain produced by the decomposition of aryl-ether bonds during the organosolv extraction process (El Hage et al., 2010). Moreover, as the severity of the extraction condition increased, dehydration and demethoxylation reactions were accelerated in the lignin side chain along with cleavage of side chains, including the Cα-Cβ and Cβ-Cγ linkages (Du et al., 2013; Liu et al., 2015). Therefore, the cleavage of ether bonds in the process of organic solvent extraction is accompanied by the inactivation of side chain functional groups.

Table 2-4. Statistical analysis of variance (ANOVA) for the EOL hydroxyl content models

| Source | Sum of squares | DF | Mean square | F-value | P-value |
|---|---|---|---|---|---|
| Model (PhOH) | 6.51 | 9.00 | 0.72 | 18.10 | 0.0005 |
| A-Temp. | 5.54 | 1.00 | 5.54 | 138.74 | < 0.0001 |
| B-S.A. Conc. | 0.48 | 1.00 | 0.48 | 12.14 | 0.0102 |
| C-EtOH Conc. | 0.05 | 1.00 | 0.05 | 1.33 | 0.2868 |
| Model (AlOH) | 16.01 | 9.00 | 1.78 | 13.09 | 0.0013 |
| A-Temp. | 10.77 | 1.00 | 10.77 | 79.29 | < 0.0001 |
| B-S.A. Conc. | 2.56 | 1.00 | 2.56 | 18.83 | 0.0034 |
| C-EtOH Conc. | 0.12 | 1.00 | 0.12 | 0.89 | 0.3771 |

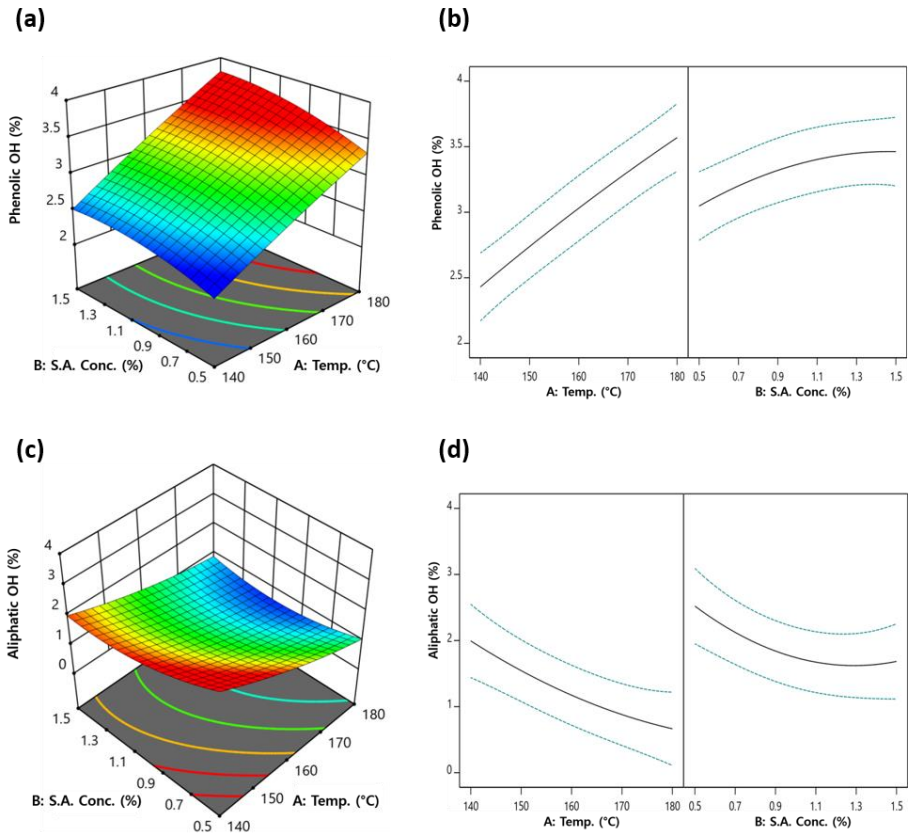


Figure 2-3. The effect of the extraction conditions on the EOL hydroxyl group content. (a) The contour plot of the RSM for the phenolic hydroxyl group (PhOH) model. (b) The one-factor plots of Phenolic OH versus significant variables. (c) The contour plot of the RSM for the aliphatic hydroxyl group (AlOH) model. (d) The one-factor plots of Aliphatic OH versus significant variables.

Figure 2-4 illustrates the 31P NMR spectroscopy of three types of EOL (LL: #5, EOL extracted under mild condition, ML: #16, EOL extracted under moderate condition, and HL: #4, EOL extracted under harsh condition). The intensity of peaks corresponding to the aliphatic hydroxyl groups showed a tendency to decrease as the severity of extraction conditions increased. On the contrary, the peak intensity of phenolic hydroxyl groups including C5 substituted OH and guaiacyl OH tended to increase as the severity of extraction conditions increased. In particular, as shown in the quantification table of the phenolic hydroxyl group region, the peak intensity of the condensed OH region, which is a C5 substituted-OH region excluding syringyl OH, increased remarkably as the severity of the extraction conditions increased (Table 2-5). In the EO extraction process, aryl-ether decomposition of the lignin and recondensation of the produced lignin fragments are achieved simultaneously, and recondensation is promoted under harsh conditions, resulting in strengthened peaks of C5 substituted-OH.

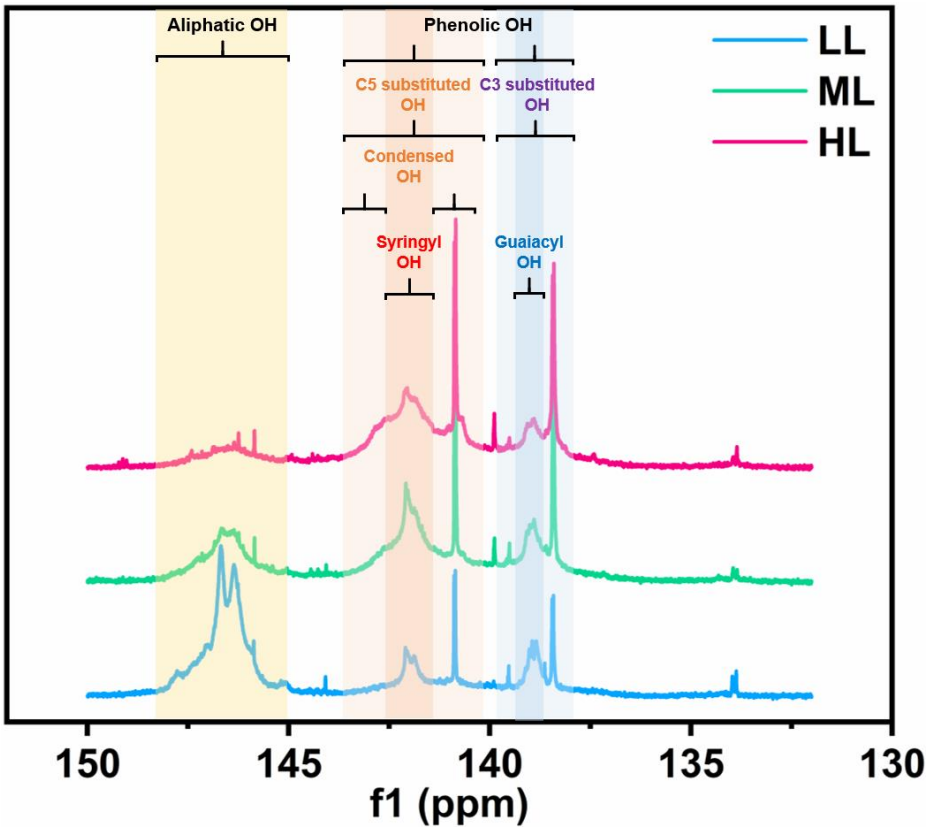


Figure 2-4. The representative 31P NMR spectrum of three types of EOL (LL, ML, and HL).

Table 2-5. Quantification of aliphatic and phenolic hydroxyl groups of three types of EOL

| | LL (#5, mild condition) | ML (#16, moderate condition) | HL (#4, harsh condition) |
|---|---|---|---|
| Aliphatic OH | 2.94 | 1.40 | 0.88 |
| C5 substituted OH | 1.17 | 2.16 | 2.79 |
| Syringyl OH | 0.54 | 1.06 | 1.20 |
| Condensed OH | 0.63 | 1.10 | 1.59 |
| C3 substituted OH | 0.96 | 1.25 | 1.52 |
| Guaiacyl OH | 0.46 | 0.53 | 0.50 |
| Total | 5.07 | 4.81 | 5.19 |

### 3.1.3. Intramolecular coupling structure

Lignin has diverse intramolecular bonds in its chemical structure, including β-O-4 (aryl ether), α-O-4 (aryl ether), β-5 (β-5, phenylcoumaran), 5-5 (biphenyl), 4-O-5 (diaryl ether), β-1 (1,2-diarylpropane), and β-β (resinol) bonds (Zakzeski et al., 2010). The linkage type of the intermolecular bonds affects the properties of the lignin. In addition, the diversity of the intermolecular bonds in lignin makes it difficult to extract lignin from lignocellulose as a uniform structure. These intramolecular coupling structures of the organosolv lignin also vary depending on the extraction conditions. In this study, to investigate the effect of extraction conditions on the intramolecular coupling structure, 2D-HSQC NMR analysis of three types of EOL obtained from different extraction conditions of different severities, was performed. In addition, the 31P NMR spectroscopy was referred for determination of syringyl (S)/guaiacyl (G) ratio. Figure 2-5 describes the results of the 2D-HSQC NMR analysis of three types of EOL produced by different extraction conditions of different severities. Table 2-6 summarizes the quantification of the side chain units connected by ether linkages and the S/G unit ratio in the EOL structure.

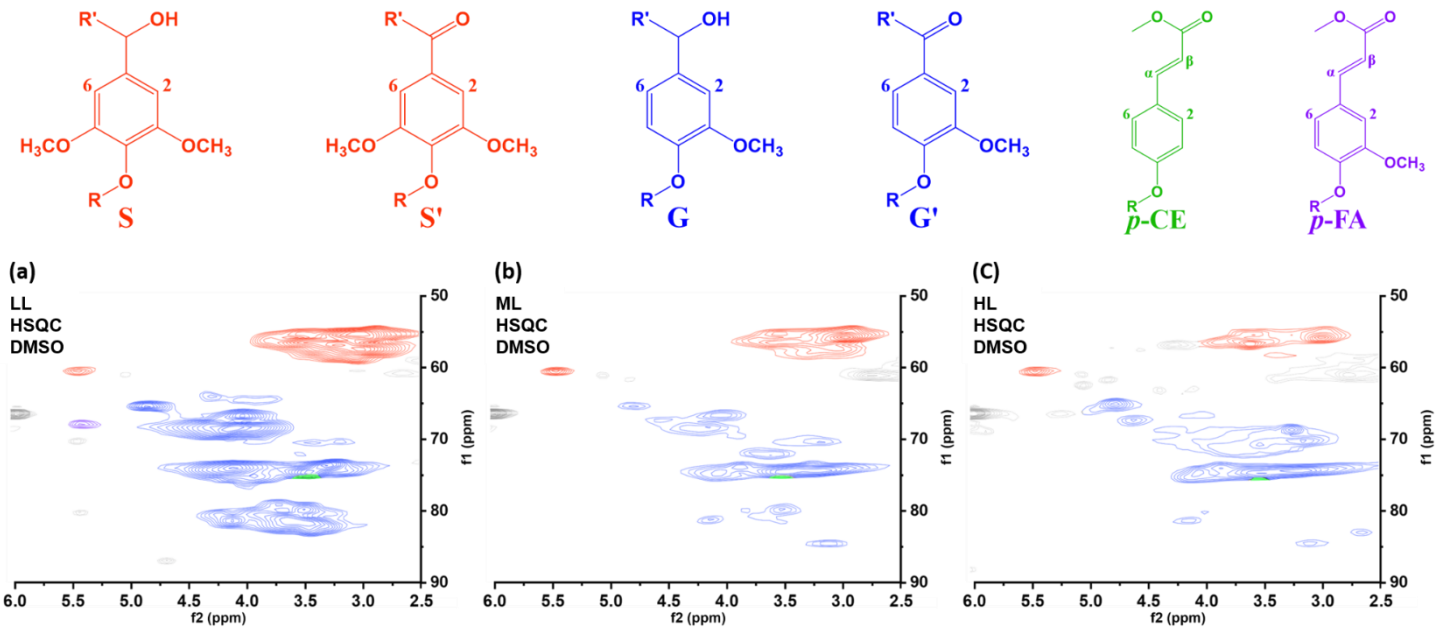


Figure 2-5. Aromatic/unsaturated (δC/δH 100–125/6.5–7.5) regions in the representative 2D-HSQC NMR spectra of the EOL with the main lignin aromatic structures identified. (a) LL (#5) extracted under mild conditions. (b) ML (#16) extracted under moderate conditions. (c) HL (#4) extracted under harsh conditions.

Table 2-6. Quantification of oxygenated aliphatic side chain units connected by ether linkages and the S/G unit ratio of three types of EOL

| | LL (#5, mild condition) | ML (#16, moderate condition) | HL (#4, harsh condition) |
|---|---|---|---|
| β-O-4 | 21.90 | 9.03 | 2.98 |
| β-β | 9.29 | 7.98 | 4.99 |
| β-5 | 5.28 | 2.71 | 0.39 |
| Total ether linkages | 41.47 | 35.72 | 16.37 |
| S/G unit ratio | 1.22 | 1.73 | 1.83 |

As shown in Figure 2-5, guaiacyl (G) and syringyl (S) units with substructures were observed in the EOL aromatic regions. As the severity of the extraction conditions increased, the intensity of the spectrum of the G unit region of the EOL was reduced compared to that of the S unit region, which resulted in a higher S/G unit ratio (Table 2-6). The G unit has a chemical structure in which one ortho position is substituted with a methoxy group, while the S unit has a chemical structure in which both ortho positions are substituted with a methoxy group. The high degree of substitution of S units means that all of the two active sites are coupling with another aromatic moiety (Duval & Lawoko, 2014). In this respect, the S unit moiety has a relatively less condensed structure and contains a structure composed of aryl-ether bonds that are more easily decomposed under acidic conditions, than the G unit moiety with C-C bond introduced at C5 position (Li et al., 2012). Meanwhile, in the EO extraction process, the G unit moiety in which the C5 site of the aromatic ring was not connected as C-C bond at C5 position could be extracted under relatively mild conditions, and the amount of the extracted S unit moiety increased as the severity of the extraction increased, resulting in high S/G ratio. Moreover, as shown in Table 2-5, as the extraction conditions were severely increased, not only the concentration of syringyl OH increased but also the concentration of C5 substituted OH increased. As mentioned in section 3.1.2 of chapter 2, the recondensation of small lignin fractions liberated from the lignin macromolecules could be stimulated under severe extraction conditions, resulting in a more condensed structure.

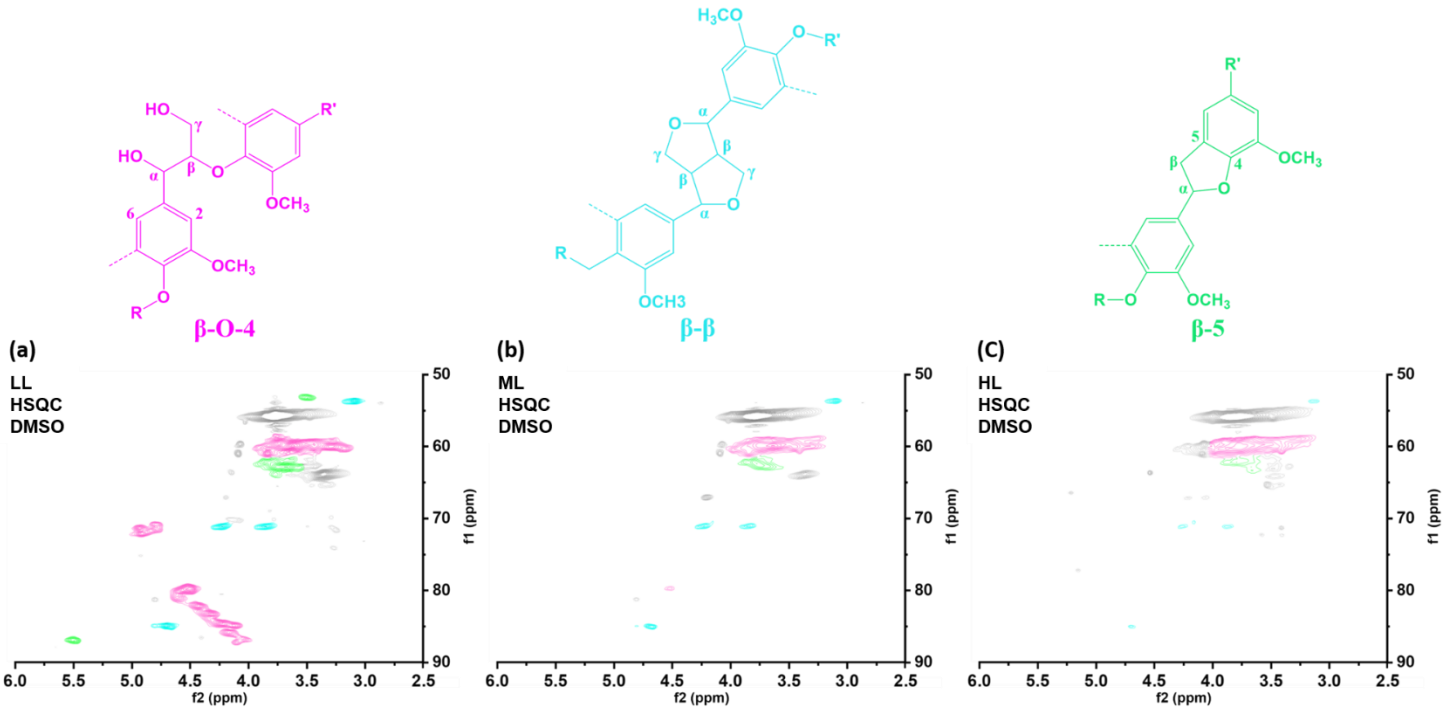


Figure 2-6. Oxygenated aliphatic side chain (δC/δH 50–90/2.5–6.0) regions in the representative 2D-HSQC NMR spectra of EOL with the main lignin side chain structures identified. (a) LL (#5) extracted under mild conditions. (b) ML (#16) extracted under moderate conditions. (c) HL (#4) extracted under harsh conditions.

Figure 2-6 shows the lignin side chain region, and various side chain coupling structures, such as β-O-4, β-β, and β-5, were observed. The β-O-4 linkage, which is known to be the dominant linkage, was observed at the highest concentration in all three types of EOL, followed by the β-β and β-5 linkages. In the organosolv pretreatment, the decomposition and recondensation of organosolv lignin occur simultaneously, and these reactions are greatly affected by the reaction conditions (Zhao et al., 2017). The aryl-ether linkages of lignin, which are easily decomposed under acidic conditions, are cleaved in the organosolv extraction process. Some of the lignin-derived and intermediate products produced during the decomposition of lignin form a more rigid structure through recondensation including an α-position condensation in the side chain and a benzyl carbocation reaction in the aromatic ring (Wayman & Lora, 1980). Therefore, the concentrations of three main coupling structures of the aryl-ether bond decreased with increasingly severe extraction conditions, and this was accompanied by a decrease in the molecular weight of the extracted EOL and the formation of a condensed structure.

### 3.1.4. Correlation between CSF of extraction condition and the structural characteristics of EOL

The structural characteristics of EOL obtained through ethanol organic solvent pretreatment is highly dependent on extraction conditions. However, there are various extraction factors that affect the structure of EOL, which makes it difficult to compare the importance of each factor and evaluate the correlation between each factor (Pedersen & Meyer, 2010). Therefore, a combined severity factor (CSF) was proposed to express the complex effects of the factors of the extraction conditions as a single numerical value. Figure 2-7 shows the correlation between CSF values and structural characteristics ($M_n$, $M_w$, phenolic hydroxyl group content, and aliphatic hydroxyl group content) of EOL for 17 extraction conditions based on the results of RSM analysis.

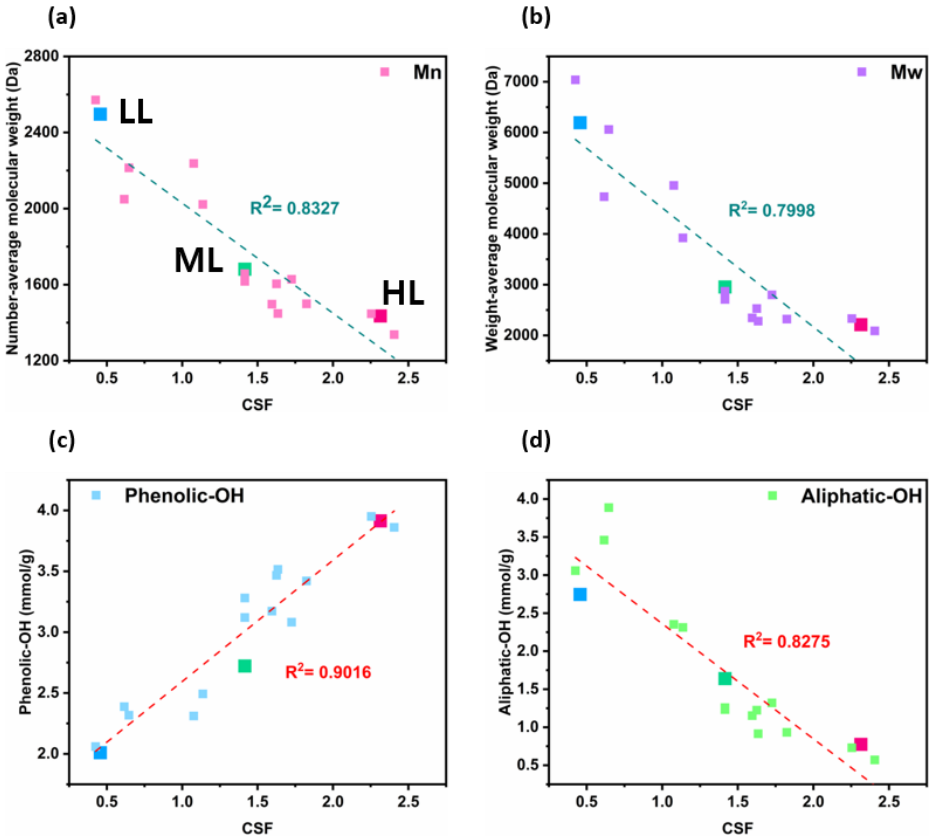


Figure 2-7. Correlation plot for structural characteristics of EOL versus CSF. (a) $M_n$. (b) $M_w$. (c) Phenolic-OH. (d) Aliphatic-OH.

The molecular weight and the distribution of hydroxyl groups of EOL showed a high correlation with the CSF of the extraction conditions. In particular, the models in which phenolic hydroxyl group content (Phenolic OH) of EOL was plotted against the CSF of extraction condition has a high R-squared value (0.9016) indicating a high correlation. These results are consistent with the RSM analysis results. In the molecular weight model of RSM analysis, the reaction temperature and sulfuric acid catalyst concentration are significant model terms. As these two factors increase, the molecular weight of EOL decreases (section 3.2.1 of chapter 2). Accordingly, the CSF value exhibited a high value as the reaction temperature and the sulfuric acid catalyst concentration increased, and the EOL obtained under the extraction condition with a high CSF value exhibited a small molecular weight.

In addition, in the hydroxyl distribution model of RSM analysis, as the reaction temperature and sulfuric acid concentration increased, the aromatic hydroxyl group content increased and the aliphatic hydroxyl group content decreased. A similar trend was also shown in the plot for the correlation of the hydroxyl group distribution with CSF, which supports the inference that EOLs with lower molecular weights and higher aromatic hydroxyl content can be obtained under higher severity extraction conditions.

## 3.2. The thermal properties of EOL depending on its structural characteristics

### 3.2.1. Statistical analysis of the correlation between weight loss at 300 °C and the structural characteristics of EOL

Lignin is known to be relatively stable at high temperatures because it has a backbone structure with aromatic rings (Brodin et al., 2010; Irvine, 1985). These thermal properties of lignin are among its attractive functions in the field of bioplastics. Lignin has both thermoplastic and thermosetting properties due to its amorphous structure and inter- and intramolecular interactions (Jeong et al., 2013). The structure of the lignin and the inter- and intramolecular hydrogen bonds contribute to the thermoplasticity of lignin, but the poor fluidity of lignin hinders its use as a thermoplastic resin in the bioplastic field. In addition, lignin is also considered to have thermosetting properties since it forms a cross-link at high temperatures. In this way, the thermal properties of lignin macromolecules are influenced by its structural characteristics, including intramolecular bonds, functional groups, and molecular weight. Although many attempts have been made to industrially utilize the properties of lignin, which includes the relatively stable structure of lignin at high temperature and abundance as a natural polymer, the unpredictable thermal properties still limit its utilization. Therefore, it is important to determine which lignin structure affects the thermal properties of EOL. Figure 2-8 shows the correlation between the thermal decomposition behaviors and the structural characteristics of the EOLs.

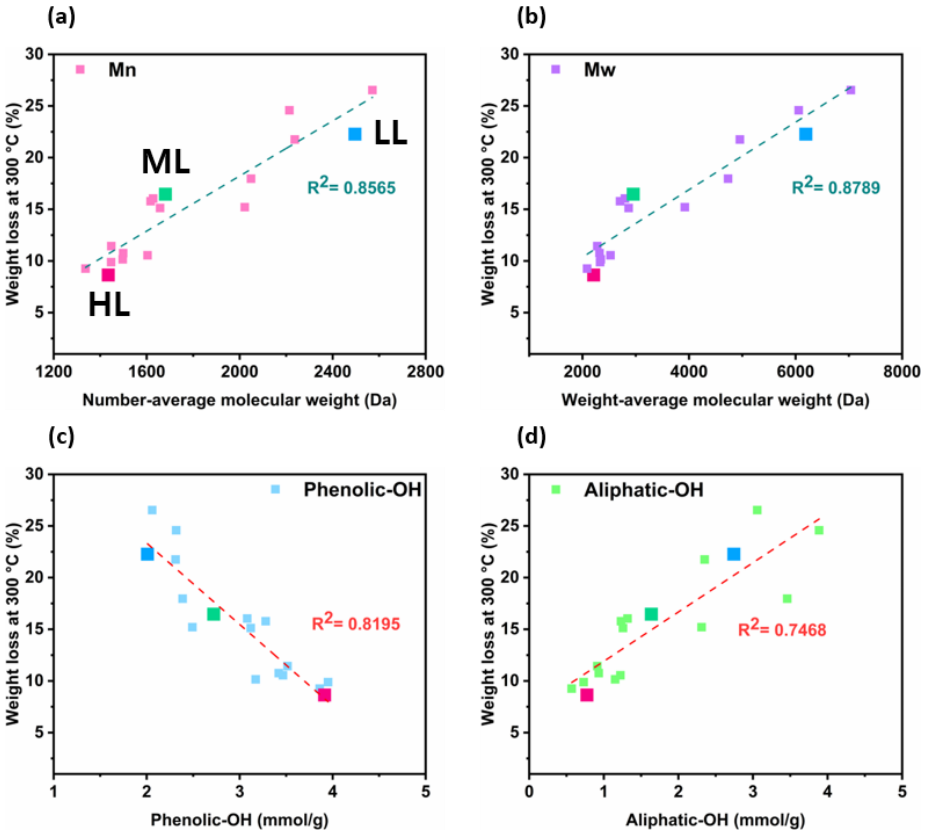


Figure 2-8. Correlation plot for weight loss at 300 °C versus the structural characteristics of EOL. (a) $M_n$. (b) $M_w$. (c) Phenolic-OH. (d) Aliphatic-OH.

As shown in Figure 2-8, the lignin structure influenced the thermal degradation behavior of the EOLs. In particular, the models in which the weight loss rate at 300 °C was plotted against the number-average molecular weight ($M_n$), weight-average molecular weight ($M_w$), and phenolic hydroxyl group content (Phenolic OH) of the EOL have a high R-squared value indicating a significant correlation. In general, it is known that polymers, including starch and polylactic acid, exhibit higher thermal stability because they have a higher molecular weight, that is, a higher degree of polymerization (Ahmed et al., 2009). However, in this study, EOL, which has a higher molecular weight, tended to exhibit greater weight loss at 300 °C. Lignin, which is a polyphenolic macromolecule, usually has various intramolecular linkages (Vanholme et al., 2010). In general, oxygen-containing functional groups including aryl-ether bonds are known to be chemically degradable as well as thermally unstable than saturated hydrocarbon (Li et al., 2014). Several studies also have reported that lignin with a condensed structure has better thermal stability (Kim et al., 2014). Therefore, the EOL with a condensed structure, in which C-C bonds are introduced instead of ether bonds, exhibited a lower weight loss rate at 300 °C.

On the other hand, as shown in the results of the correlation between the aromatic hydroxyl group and the weight loss rate at 300 °C, it was shown that the higher content of phenolic hydroxyl groups in the lignin macromolecule contributes to the thermal stability. The hydroxyl group has a relatively low thermal stability compared to other oxygen-containing functional groups, and it promotes the thermal degradation at relatively low temperature (Li et al., 2014). However, the condensed rigid structure of the aromatic moieties and high frequency of intermolecular hydrogen bond interactions of phenolic hydroxyl groups contribute to the thermal stability of lignin (Brodin et al., 2010; Yoshida et al., 1987). Therefore, the EOL with a low aliphatic hydroxyl content and a high phenolic hydroxyl content, which was extracted under severe conditions, showed a low weight loss rate at 300 °C.

Based on the analysis results, a multiple linear regression analysis was conducted to predict the weight loss rate of EOL at 300 °C. According to the p-values of each independent variable, the $M_w$/1000 (0.009) was the most important variable, and the aliphatic hydroxyl content (0.676) was found to be the least important variable for the weight loss rate at 300 °C (Table 2-7). This is a result that is consistent with the correlation plot between structural characteristics and weight loss rate at 300 °C.

Table 2-7. Regression analysis results of OLS method for weight loss rate of EOL at 300 °C corresponded its structural characteristics (R-Square= 0.911, Adjust R-Square=0.837)

| Analysis of Variance | | | |
|---|---|---|---|
| Source | Degree of freedom | F-value | Pr > F |
| Regression | 3 | 44.51 | <.0001 |
| Residual | 13 | - | - |
| Total | 17 | - | - |

| Parameter Estimates | | | | |
|---|---|---|---|---|
| Variable | Regression Coefficients | Standard Error | t-value | Pr > \|t\| |
| Intercept | 17.51 | 7.385 | 2.371 | 0.034 |
| $M_w$/1000 | 2.399 | 0.776 | 3.092 | 0.009 |
| PhOH | -3.217 | 1.736 | -1.853 | 0.087 |
| AlOH | -0.515 | 1.205 | -0.428 | 0.676 |

On the other hand, the intercept of the model was 17.51, and the regression coefficients of the independent variables ($M_w$/1000, PhOH, and AlOH) were 0.002, -3.217, and -0.515, respectively. The regression equation of this model for predicting the weight loss obtained through this is as follows:

$$Weight\ loss\ rate\ of\ EOL\ at\ 300\ °C = 2.399(M_w/1000) - 3.217(PhOH) - 0.515(AlOH) + 17.51$$

The R-squared value of validation of this model was 0.837, showing high significance (Figure 2-9). It means that the residuals between the predicted value and the measured value of weight loss rate of EOL at 300 °C considering molecular weight and hydroxyl group distribution is small, and that each variable has a significant correlation with the weight loss rate at 300 °C. Therefore, the weight loss rate of EOL at 300 °C can be predicted through the molecular weight and hydroxyl distribution. In particular, the lower molecular weight of EOL extracted from same biomass by EO extraction, the slower rate of thermal degradation of EOL was expected.

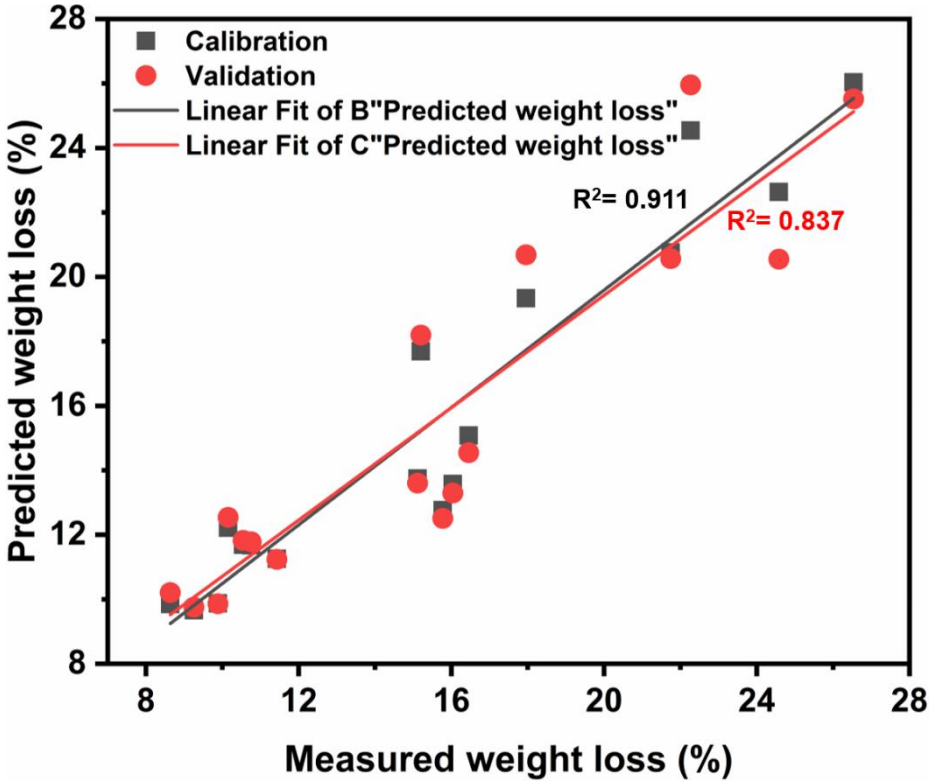


Figure 2-9. The regression plot for validation and calibration results of the OLS model.

### 3.2.2. Thermal decomposition characteristics and glass transition temperature of three types of EOL

These results can be supplemented by the TGA thermal curve and DSC curve of three types of EOL (Figure 2-10). Three types of EOL with different structural characteristics also displayed different thermal decomposition patterns. LL, which had the largest molecular weight and the highest aliphatic hydroxyl group content because of the mildest extraction conditions, showed the lowest decomposition starting temperature derived from the low thermal stability of aliphatic hydroxyl groups. In the first derivative thermogravimetry (DTG), the initial decomposition rate was found to decrease as the extracted lignin had a smaller molecular weight and a higher phenolic hydroxyl group content. Furthermore, the char yield at 800 °C was highest for HL. The condensed chemical structure, in which C-C bonds are introduced instead of ether bonds, could be involved in the high char yield of EOL.

As a result of the DSC analysis, the glass transition temperature of three types of EOL showed a high value, from 138.7 (LL) to 174.1 (HL). It is known that lignin has a higher glass transition temperature ($T_g$), which is one of the most significant factors that determine its thermal properties, than most synthetic materials (Irvine, 1985). It is originated that they have condensed rigid phenolic moieties and a high frequency of intermolecular hydrogen bond interactions. In this respect, low molecular weight lignin, which is extracted under harsh conditions, has a high $T_g$ due to the introduction of many phenolic hydroxyl groups and the formation of a rigid phenolic structure (Thakur et al., 2014). In this way, lignin has different structural characteristics depending on the extraction conditions, and the inherent characteristics have a complex effect on the thermal properties of lignin. Therefore, it is necessary to understand the

relationship between the structural characteristics and properties of lignin for the effective application of EOL.

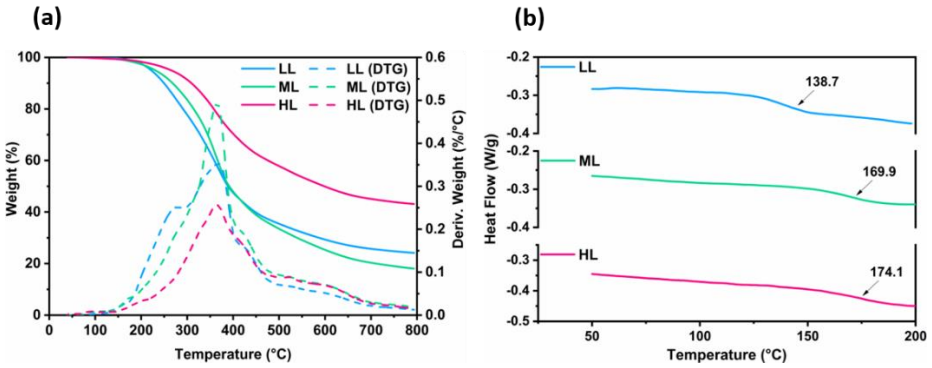


Figure 2-10. The representative TGA thermal curve and DSC curve of three types of EOL. (a) TGA thermal curve. (b) DSC curve.

## 3.3. The properties of the EOL–PLA bioplastics depending on the structural characteristics of EOLs

### 3.3.1. Thermal properties of the EOL–PLA bioplastics depending on types of EOL

The addition of lignin can significantly change the properties of PLA, such as its thermal properties, mechanical strength, and biodegradation behavior. Figure 2-11 shows the thermal decomposition behavior of EOL–PLA bioplastics based on three types of EOL with neat PLA. The neat PLA exhibited a very narrow decomposition temperature range between 300 °C and 350 °C. The EOL–PLA bioplastics showed improved thermal stability compared to neat PLA. Previous studies evaluating the thermal properties using lignin-PLA bioplastics revealed conflicting thermal decomposition properties depending on the types of lignin used (Anwer et al., 2015; Domenek et al., 2013; Gordobil et al., 2014; Li et al., 2003). In general, organosolv lignin has high purity, is sulfur-free, and has low ash and polysaccharide contents compared to other technical lignins, including kraft and soda lignin. In particular, organosolv lignin is thermally stable at relatively high temperatures because it contains few thiols (-SH) and sulfonic acid (-$SO_3H$) groups, which can be easily decomposed during pyrolysis (Han et al., 2018; Lin et al., 2015). In addition, the narrow polydispersity of EOL contributes to an even distribution within the thermo-bioplastic.

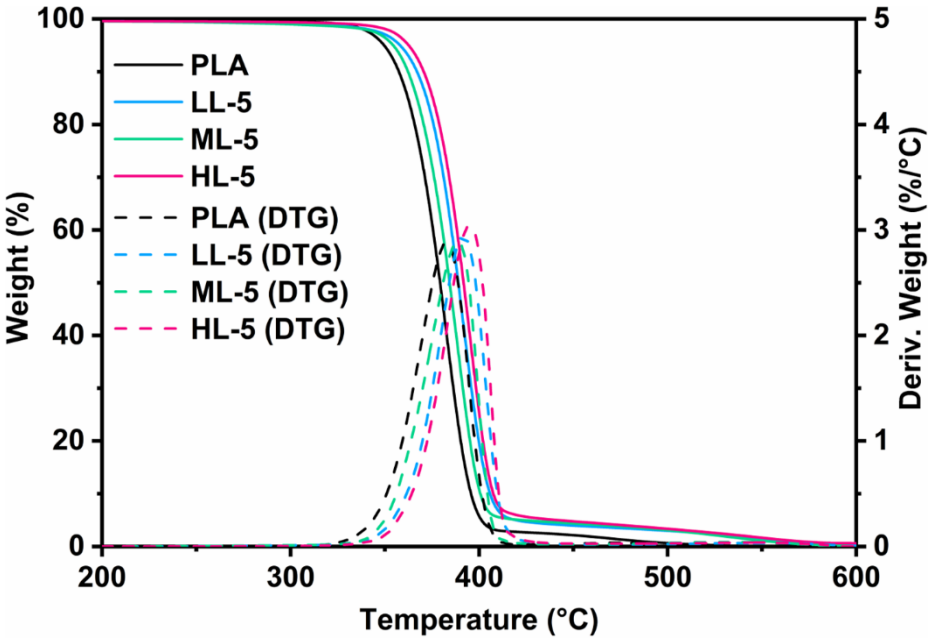


Figure 2-11. The representative TGA thermal curve of EOL–PLA bioplastics based on three types of EOL (LL-5: EOL–PLA bioplastic with 5% (w/w) of LL, ML-5: EOL–PLA bioplastic with 5% (w/w) of ML, HL-5: EOL–PLA bioplastic with 5% (w/w) of HL).

In this study, all EOL–PLA bioplastics with 5% (w/w) EOL had an increased starting point of thermal decomposition and increased the maximum decomposition temperature. The three EOL–PLA bioplastics exhibited similar thermal decomposition temperature ranges (from 350 to 400 °C) and behaviors. Among them, the bioplastic using HL extracted under severe conditions had a starting point of thermal decomposition that was higher than that of the other bioplastics and neat PLA, and it had the highest maximum decomposition temperature. By the blending of HL with PLA, the starting point of thermal decomposition of PLA was delayed from 339 °C to 351 °C, and the maximum decomposition temperature was increased from 383 °C to 395 °C. Although the addition of EOL did not significantly change the thermal properties of PLA, it was possible to slightly improve the thermal stability by substituting 5% of PLA with a biomass-derived component with a low raw material cost. This result corresponds to the thermal properties of EOL, which depend on its structural characteristics (section 3.2 of chapter 2). The results of the thermal analysis of the EOLs showed that HL had a higher starting temperature for thermal decomposition and a slower initial decomposition rate than the other two EOL types. In this respect, the bioplastic with evenly distributed HL was considered to exhibit high heat resistance compared to the bioplastics containing the other EOLs. Consequently, the EOL–PLA bioplastics had improved thermal properties compared to those of neat PLA. Moreover, the EOL–PLA bioplastics exhibited slightly different thermal properties depending on the types of lignin, and this difference became apparent as the lignin content in the bioplastic increased. Therefore, it is important to impart desirable thermal properties within a thermo-bioplastic by understanding the relationship between the structural characteristics and the properties of lignin.

### 3.3.2. Mechanical properties of the EOL–PLA bioplastics depending on types of EOL

The properties of the lignin-biopolyester bioplastics are largely affected by the compatibility between both polymers mixed. Due to a large number of hydroxyl groups in the molecular structure, the surface of lignin is relatively polar compared to most of the biopolyesters (Pouteau et al., 2004). Moreover, strong interaction between the molecules of lignin tends to cause aggregation of lignin each other in thermo-bioplastics, resulting in non-uniform mechanical properties of them. Figure 2-12 shows the tensile strength and nominal strain at break of EOL–PLA bioplastics based on three types of EOL with different lignin content.

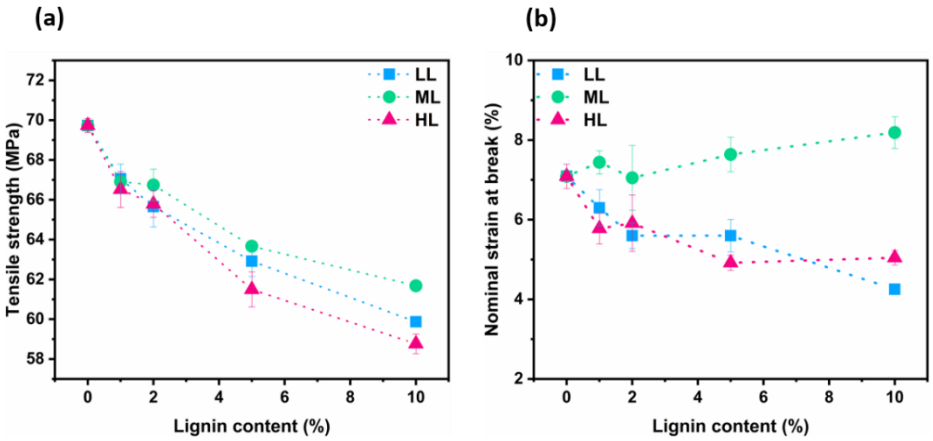


Figure 2-12. Tensile strength and nominal strain at break of EOL–PLA bioplastic based on three types of EOL with diverse EOL content. (a) Tensile strength of EOL–PLA bioplastics based on three types of EOL. (b) Nominal strain at break of EOL–PLA bioplastics based on three types of EOL.

The tensile strength of EOL–PLA bioplastics showed a tendency to decrease as the content of lignin in the bioplastics increased. Due to the large number of hydroxyl groups in the molecular structure, the surface of lignin is relatively polar compared to PLA (Pouteau et al., 2004). The different surface properties of these two polymers act as a factor to lower the bonding force between the interfaces and cause a decrease in the tensile strength of the EOL–PLA bioplastics. In addition, it is considered that lignin does not dissolve at a thermo-bioplastic molding temperature of 200 °C, making it difficult to form a uniform thermo-bioplastic. In the graph of the tensile strength of EOL–PLA bioplastics based on three types of EOL with diverse lignin content (Figure 2-12(a)), the tensile strength of the bioplastic with HL decreased most dramatically. HL has the highest total hydroxyl content and has the highest glass transition temperature among three types of EOL derived from condensed structure. These properties acted as an obstacle that hindered the compatibility with PLA in the bioplastic and resulted in a greater reduction in tensile strength. In addition, the large molecular weight of LL contributed to the decrease in tensile strength. LL has the highest molecular weight among three types of EOL, which means that the macromolecular structure of LL has a long chain length. In general, the lignin macromolecules have a higher molecular weight and a longer chain length, the greater the attractive force between molecules, and such an increase in the attractive force between molecules may cause aggregation in a thermo-bioplastic formed with a polymer matrix having poor compatibility (Norgren et al., 2001).

On the other hand, the nominal strain at break of the EOL–PLA bioplastic showed significantly different tendencies depending on the types of EOL. Several studies have reported that the addition of lignin increases the elongation of lignin–PLA bioplastic (Ren et al., 2016). However, it was found that not all lignin increased the elongation of the lignin–PLA bioplastic as shown in the results of nominal strain at break of EOL–PLA bioplastics based on three types

of EOL (Figure 2-12(b)). In the case of the elongation of the thermo-bioplastic, as well as the tensile strength, the compatibility between heterogeneous polymers is greatly affected. The highly compatible heterogeneous polymers form a structure that facilitates energy dispersion by forming a strong entanglement between chains. Therefore, the obtained lignin structure has different effects on the mechanical properties of the thermo-bioplastic, and it means that out of three types of EOL, ML has the best compatibility with PLA for mechanical properties.

# 4. Summary

In conclusion, the extraction conditions (extraction temperature, sulfuric acid concentration, and ethanol concentration) have a significant effect on the structural characteristics (molecular weight, phenolic and aliphatic hydroxyl group content) of EOL within RSM analysis. The EOL with low molecular weight, low PDI, and high phenolic hydroxyl content was obtained under harsh extraction conditions. In addition, the EOL with a more condensed structure, which was due to the decomposition of aryl-ether linkages in the macromolecular structure, was extracted as the severity of the extraction conditions increased. The correlation between the structural characteristics of EOL and the severity of the extraction conditions was confirmed by introducing the CSF value, and a clear correlation was derived.

The structural characteristics of EOL derived from different extraction conditions influenced its thermal properties. In particular, the molecular weight and phenolic hydroxyl group showed a distinct correlation. As a result of the multiple linear regression analysis performed to predict the mass reduction rate at 300 °C, the highest regression coefficient with high molecular weight was shown, which was found to be the most important variable. Meanwhile, the regression model with R-Square value (0.837) was suggested. In accordance with the model, the lower molecular weight of EOL extracted from same biomass by EO extraction, the slower rate of thermal degradation of EOL was expected. In addition, three types of EOL with different structural characteristics also displayed different thermal properties. The EOL that had low molecular weight, high phenolic hydroxyl content, and low aryl ether linkage content, had a low starting temperature of thermal decomposition and a low initial decomposition rate with high $T_g$.

In a manner corresponding with the thermal properties of the EOL, the EOL–PLA bioplastics prepared using three different EOL types exhibited improved thermal stability compared to neat PLA with slightly different thermal decomposition behaviors depending on the EOL type used. Especially, the PLA bioplastic with HL, which had a low molecular weight and phenolic hydroxyl group content due to the harsh extraction condition, impeded the starting point of thermal decomposition of PLA from 339 °C to 351 °C, and increased the maximum decomposition temperature from 383 °C to 395 °C. On the other hand, EOL–PLA bioplastics had a different tendency on mechanical properties depending on the types of EOL. The tensile strength of EOL–PLA bioplastics showed a tendency to decrease as the content of lignin in the bioplastics increased. Whereas, the nominal strain at break of EOL–PLA bioplastics has a different tendency depending on the types of EOL. Therefore, the different properties can be imparted within the thermo-bioplastic by control of structural characteristics of lignin.

# *Chapter 3*

## Chemical modification of EOL for improving thermoplasticity and compatibility in EOL–PLA bioplastics

# 1. Introduction

Traditionally, lignin is incompatible with many kinds of thermoplastic biopolyesters depending on the surface characteristics. This is attributed to the numerous functional groups, which hinder lignin utilization in the thermoplastic industry (Collins et al., 2019b). Lignin macromolecules have various functional groups in their structures, including hydroxyl groups, methoxyl groups, carbonyl groups, and carboxyl groups. Among them, the hydroxyl groups of lignin undergo inter- and intramolecular hydrogen bonding, resulting in a hydrophilic surface (Kai et al., 2016). In addition, lignin has anisotropic thermal properties, including thermoplastic and thermosetting properties, attributed to its amorphous chemical structure and inter- and intramolecular interactions (Jeong et al., 2013). However, the thermoset properties and low fluidity, attributed to the crosslinked structure in a network, limit the use of lignin in thermoplastics. Furthermore, lignin has a higher $T_g$ than those of most synthetic materials, which is one of the most significant factors determining its thermal properties (Irvine, 1985). Lignin has condensed rigid phenolic moieties and a high frequency of intermolecular hydrogen bond interactions, which limit the thermal mobility.

To ensure the commercial utilization of lignin in the thermoplastic field, many research teams have devised various strategies. These studies focused on the chemical modification of lignin macromolecules by reacting chemicals that impart different functionalities on the lignin. This modification not only increases the compatibility of lignin with the matrix polymer but also promotes the intended functionality.

In particular, lignin is often modified through etherification to increase the reactivity of its functional groups or improve its compatibility with biopolyesters. The etherification of lignin can be achieved through the ring-

opening polymerization of compounds, such as cyclic ethers, lactone, and lactide, which are initiated by the hydroxyl group of lignin macromolecules (Sadeghifar et al., 2012). The most generally used cyclic ether for producing the lignin graft copolymer is propylene oxide (PO), and many studies have attempted to confer compatibility and functionality on lignin through grafting with PO. Usually, in the lignin/PO copolymer, PO is grafted to the lignin side chain with a degree of polymerization of 1–7 (Duval & Lawoko, 2014; Nadji et al., 2005). The oxypropylated lignin retains a large proportion of the aliphatic hydroxyl groups, and the aromatic hydroxyl groups are replaced by secondary aliphatic hydroxyl groups. The substituted aliphatic hydroxyl groups are free from steric hindrance, resulting in improved compatibility and thermoplasticity of lignin. The degree of polymerization depends on the stoichiometry of the functional groups of lignin and the PO monomers participating in the polymerization. In particular, the hydroxyl content of the lignin participating in the reaction has a significant influence on the degree of polymerization, and the hydroxyl group content of the lignin can be varied by controlling the extraction conditions. Oxypropylated lignin exhibits different physicochemical properties depending on the chain length. The $T_g$ and viscosity of the lignin graft copolymer tend to decrease as the length of the grafted chain increases (Cateto et al., 2009; Kelley et al., 1988a). Therefore, it is considered that the oxypropylation patterns depend on structural characteristics (molecular weight and hydroxyl group content) of lignin, and the oxypropylated lignin, whose structure and properties are properly controlled, can display improved compatibility with biopolyester, forming a homogeneous thermo-bioplastic with enhanced thermoplasticity (Li & Sarkanen, 2005; Sadeghifar et al., 2012).

Here, the oxypropylation of three types of ethanol organosolv lignin (EOL) with different structural characteristics was conducted to improve the thermoplasticity and compatibility with biopolyesters. Further, the effect of the structural characteristics of EOL on oxypropylation was investigated. Three

types of EOL having different structural characteristics were obtained by controlling the severity of the extraction condition. The EOLs were oxypropylated using PO with diverse molar ratios. Subsequently, the thermal and mechanical properties of the oxypropylated EOL and PLA-based bioplastics were evaluated.

# 2. Materials and methods

## 2.1. EOL preparation

### 2.1.1. Raw materials

A Jolcham oak (*Quercus serrata*), which was supplied by the Taehwasan Academic Forest of Seoul National University, was used for the EOL. The raw material was milled to a particle size of approximately 0.5 mm by a twin-screw extruder, and it was stored at 4 °C until use.

### 2.1.2. EOL extraction

Ethanol organosolv (EO) pretreatment was conducted to extract the lignin from biomass under three extraction conditions with different combined severity factors (CSFs). The CSFs were calculated as follows:

$$\text{Combined severity factor (CSF)} = log\{t \times exp\left[\frac{T_H - 100}{14.75}\right]\} - pH$$

$T_H$ = extraction temperature (°C)

Table 3-1 summarizes the extraction conditions of three types of EOLs (EOL extracted under the low-severity (LL), moderate-severity (ML), and high-severity conditions (HL)). Fifty grams of wood powder was loaded with 400 mL of a solvent prepared according to each extraction condition. The EO pretreatment was carried out using a high-temperature and high-pressure reactor. After the reaction, the reactor was quenched to under 60 °C using an ice chamber, and the liquid fraction containing the dissolved lignin was separated from the solid fraction for recovery. The EOL was precipitated by 8-fold dilution of filtrates with distilled water, and the suspension was stabilized

for 24 h. The precipitated lignin was separated from the liquid fraction using a filter paper (No. 52, Hyundai Micro Co., Seoul, Republic of Korea) and lyophilized for 72 h.

Table 3-1. Extraction conditions of three types of EOL

| | LL (#5) | ML (#16) | HL (#4) |
|---|---|---|---|
| Reaction temp. (°C) | 140 | 160 | 180 |
| Reaction time (min) | 5 | 5 | 5 |
| Sulfuric acid conc. (%) | 0.5 | 1 | 1.5 |
| Ethanol conc. (%) | 80 | 60 | 40 |
| CSF | 0.46 | 1.42 | 2.31 |

### 2.1.2. Properties of EOL based on the extraction condition

The structural characteristics of EOL (molecular weight, hydroxyl content, and coupling structure) were investigated in relation to the extraction conditions (temperature, sulfuric acid concentration, and ethanol concentration). The number-average molecular weight ($M_n$), weight-average molecular weight ($M_w$), and polydispersity index (PDI) were determined by gel permeation chromatography (1260 Infinity II LC system, Agilent, USA) using the same procedure described in Section 2.2.1 of Chapter 2. The hydroxyl group contents were analyzed by phosphorus-31 nuclear magnetic resonance (31P NMR) spectroscopy (JEOL JNM-LA400 with LFG, JEOL, Japan) using the same procedure described in Section 2.2.2 of Chapter 2. The coupling structure of each EOL was investigated by quantitative 2D-HSQC NMR spectroscopy (600 MHz, ADVANCE 600, Bruker, Germany) using the same procedure described in Section 2.2.3 of Chapter 2. The $T_g$ of each EOL was determined by differential scanning calorimetry (DSC) (Discovery DSC, TA instruments, USA) using the same procedure described in Section 2.2.5 of Chapter 2. The characteristics of three types of EOL are shown in Table 3-2.

Table 3-2. Characteristics of three types of EOL

| | LL | ML | HL |
|---|---|---|---|
| Molecular weight ($M_n$, Da) | 1549 | 956 | 805 |
| Molecular weight ($M_w$, Da) | 6466 | 2132 | 1321 |
| PDI | 4.17 | 2.23 | 1.64 |
| Aliphatic OH (mmol/g) | 2.94 | 1.4 | 0.88 |
| Phenolic OH (mmol/g) | 2.13 | 3.41 | 4.31 |
| Total OH (mmol/g) | 5.07 | 4.81 | 5.19 |
| Total ether linkages (%) | 41.47 | 35.72 | 16.37 |
| S/G unit ratio | 1.22 | 1.73 | 1.83 |
| $T_g$ (°C) | 138.7 | 169.9 | 174.1 |

## 2.2. Oxypropylated lignin preparation

### 2.2.1. Oxypropylation of three types of EOL

Oxypropylation was applied to improve the compatibility of lignin with biopolyesters and its functional group reactivity (Sadeghifar et al., 2012). Three types of EOL having different structures were reacted with PO. The EOL was dissolved in an aqueous NaOH solution (0.5 M). Thereafter, PO was added to the solution at diverse molar ratios with hydroxyl groups of EOL (hydroxyl group of ML:PO = 1:1, 1:2, and 1:5). The mixture was reacted at 40 °C for 18 h. After the reaction, the oxypropylated lignin was recovered by acidifying with 2 M HCl. The obtained oxypropylated EOLs were washed with deionized water until pH 6 was achieved, followed by freeze-drying. The oxypropylated EOLs were named as follows, according to the molar ratio of the lignin hydroxyl group and PO. Three types of EOL oxypropylated in a 1:1 molar ratio were denoted as LL-1, ML-1, and HL-1. Three types of EOL oxypropylated in a 1:2 molar ratio were denoted as LL-2, ML-2, and HL-2. Three types of EOL oxypropylated in a 1:5 molar ratio were denoted as LL-5, ML-5, and HL-5.

### 2.2.2. Properties of the oxypropylated EOLs in relation to their structural characteristics

#### 2.2.2.1. Molecular weight of the oxypropylated EOLs

10 mg of the oxypropylated EOL was dissolved in 1 mL of tetrahydrofuran (THF). The sample was filtered using a 0.45 μm polytetrafluoroethylene (PTFE) filter (Advantec Co., Japan). Subsequently, $M_n$, $M_w$, and PDI were analyzed using a gel-permeation chromatograph (Nexera LC-40, Shimadzu, Japan), equipped with an SDV 1000A 5 μm 8 × 300 mm S/N 91112605 column. The mobile phase flow rate was 1 mL/min. The calibration curves were set using 12 polystyrene standards with a range of molecular weight of 266–62,500 Da.

#### 2.2.2.2. Hydroxyl group content of the oxypropylated EOLs

The phenolic and aliphatic hydroxyl group contents of the oxypropylated EOLs were determined by 31P NMR spectroscopy, with reference to previous researches. A solvent solution was prepared by mixing pyridine and deuterated chloroform (1.6:1 (v/v)). For preparing the mixture solution, 100 mg of cyclohexanol (internal standard) and 90 mg of chromium acetylacetonate (relaxation reagent) were added to a 25 mL solvent solution. Thereafter, 20 mg of the oxypropylated EOL was dissolved in 400 μL of the solvent solution and 150 μL of the mixed solution. After the mixture was stirred for 5 min, 70 μL of 2-chloro-4,4,5,5-tetramethyl-1,2,3-dioxaphospholane was added to the mixture as a phosphorylating reagent. Afterward, the prepared samples were transferred to a 5 mm NMR tube for 31P NMR spectroscopy analysis. The 31P NMR spectra of the oxypropylated EOLs were obtained using a 600 MHz NMR spectrometer (ADVANCE 600, Bruker, Germany), equipped with a 14.095

Tesla superconducting 51 mm bore magnet and a 5 mm BBO BB-H&F-D CryoProbe Prodigy.

### 2.2.2.3. Methyl proton content of the oxypropylated EOLs

The content of the new methyl proton, which was introduced by oxypropylation, was monitored using 1H NMR spectroscopy. The sample (60 mg) was dissolved in 600 μL of dimethyl sulfoxide (DMSO)-$d_6$ with tetramethylsilane (TMS), and 2,3,4,5,6-pentafluorobenzaldehyde was used as an internal standard. The phenolic and aliphatic hydroxyl group contents of the oxypropylated EOLs were determined by 31P NMR spectroscopy, with reference to previous researches. Thereafter, the prepared samples were transferred to a 5 mm NMR tube for 1H NMR spectroscopy analysis. The 1H NMR spectra of the oxypropylated EOLs were obtained using a 600 MHz NMR spectrometer (ADVANCE 600, Bruker, Germany), equipped with a 14.095 Tesla superconducting 51 mm bore magnet and a 5 mm BBO BB-H&F-D CryoProbe Prodigy.

### 2.2.2.4. Determination of the degree of substitution (DS) and degree of polymerization (DP)

The DS of the oxypropylated EOLs was determined by quantitative 31P NMR spectroscopy. The DS value is the ratio of the modified hydroxyl group content to the total hydroxyl group content obtained through quantitative 31P NMR, which can be calculated as follows:

$$\text{Degree of substitution (DS)} = \frac{\int OH_{modified}}{\int OH_{total}}$$

The DP was determined using quantitative 31P NMR and 1H NMR spectroscopies. The attached propyl unit per modified OH group was calculated

by the ratio of $CH_3$ content derived from oxypropylation to the modified OH content, as follow:

$$\text{Degree of polymerization (DP)} = \frac{\int CH_{3\,modified}}{\int OH_{modified}}$$

### 2.2.2.5. Thermal properties of oxypropylated EOLs

The thermal decomposition characteristics of the oxypropylated EOLs derived from three types of EOLs were analyzed using a thermogravimetric analyzer (Discovery TGA, TA Instruments, USA). Approximately 10 mg of the samples were scanned from 25 to 800 °C at a constant heating rate of 10 °C/min. After the sample was heated to the target temperature, the furnace was quenched with a high-quality $N_2$ inert atmosphere at a flow rate of 50 mL/min.

The $T_g$ of the oxypropylated EOLs was determined by DSC (Discovery DSC, TA instruments, USA). The DSC analysis conditions were set by referring to the thermal decomposition behavior of each sample, and all the DSC analyses were performed under high-quality $N_2$ flow. The first heating scan was performed in a temperature range where the thermal decomposition of the sample did not occur, at a heating rate of 10 °C/min, and this temperature was maintained for 2 min to exclude the thermal history. Subsequently, the temperature of the furnace was decreased to −25 °C and held for 10 min. For the second heating scan, the process was conducted at temperatures ranging from −25 to 250 °C, at the same heating rate as that of the first scan. The $T_g$ of the oxypropylated EOLs was determined using the second heating scan data.

The melting point ($T_m$) of the oxypropylated EOLs was investigated by simultaneous DTA/TGA (SDT) (SDT, TA instruments, USA). SDT analysis was carried from 25 to 600 °C at a constant heating rate of 10 °C/min, under air conditions. After the sample was heated to the target temperature, the furnace was quenched with air at a flow rate of 50 mL/min.

## 2.3. Oxypropylated EOL–PLA bioplastics

### 2.3.1. Preparation of the EOL–PLA bioplastics

The oxypropylated EOL–PLA bioplastics with various types of oxypropylated EOLs were manufactured. The oxypropylated EOLs and PLA were mechanically melted and mixed at 5% (w/w) of the mixing ratio using a specimen molding machine (KP-M2100H, Kipae, Republic of Korea). The same operation conditions were set for all samples, as follows: operating temperature, 200 °C; operating time, 5 min; and speed, 100 rpm. Thereafter, the blends were injected to mold a specimen for the tensile strength test.

### 2.3.2. Morphologies of the EOL–PLA bioplastics

The morphologies of the PLA-based bioplastics with the initial EOLs and oxypropylated EOLs were observed by filed-emission scanning electron microscopy (FE-SEM, SUPRA 55VP, Carl Zeiss, Germany). The bioplastic was broken using an impact tester for morphological analysis. The sides of the sample, except the fracture side, were wrapped with copper tape to prevent charging and fixed on an aluminum stub. Next, the samples were sputter-coated with 8 nm thick Pt–Pd. The surface of the bioplastics was imaged with beams at a voltage of 2 kV.

### 2.3.3. Properties of oxypropylated EOL–PLA bioplastics based on its structural characteristics

#### 2.3.3.1. Thermal properties of the oxypropylated EOL–PLA bioplastics

The TGA and DSC analysis were adopted for investigation of thermal properties of oxypropylated EOL–PLA bioplastics. The TGA and DSC analysis was performed as described in section 2.3.2 of Chapter 2.

### 2.3.3.2. Mechanical properties of the oxypropylated EOL–PLA bioplastics

The tensile strength and elongation of the oxypropylated EOL–PLA bioplastics were determined as described in Section 2.3.3 of Chapter 2.

### 2.3.3.3. Thermodynamic properties of the oxypropylated EOL–PLA bioplastics

The thermodynamic properties of the oxypropylated EOL–PLA bioplastics were estimated using a dynamic mechanical thermal analyzer (DMA/SDTA861e, Mettler Toledo, Switzerland) in dual cantilever mode. The storage modulus (E′), loss modulus (E″), and loss factor (tan delta) were measured as a function of the temperature in the range of 25–135 °C, at a heating rate of 3 °C/min and a frequency of 1 Hz. The test specimen dimensions were approximately 12.5 × 65.0 × 3.0 mm (width × length × thickness).

# 3. Results and Discussion

## 3.1. Structural characteristics of the oxypropylated EOL

### 3.1.1. Molecular weight of the oxypropylated EOLs

The structural characteristics of a polymer, including its molecular weight, molecular weight distribution, and side-chain structure, significantly affect its physicochemical properties. In particular, it is known that the branched structure of polymers has a significant correlation with its viscosity, strength, toughness, and thermal properties (Lutz & Peruch, 2012). The structure of the side-chain can be modified by controlling the DP of PO, and its reaction patterns and properties are largely dependent on the structural characteristics of lignin. Figure 3-1 shows the GPC results of the oxypropylated EOL diverse molar ratios between the hydroxyl groups of the EOL and PO. Further, Table 3-3 summarizes $M_n$, $M_w$, and PDI of the oxypropylated EOLs.

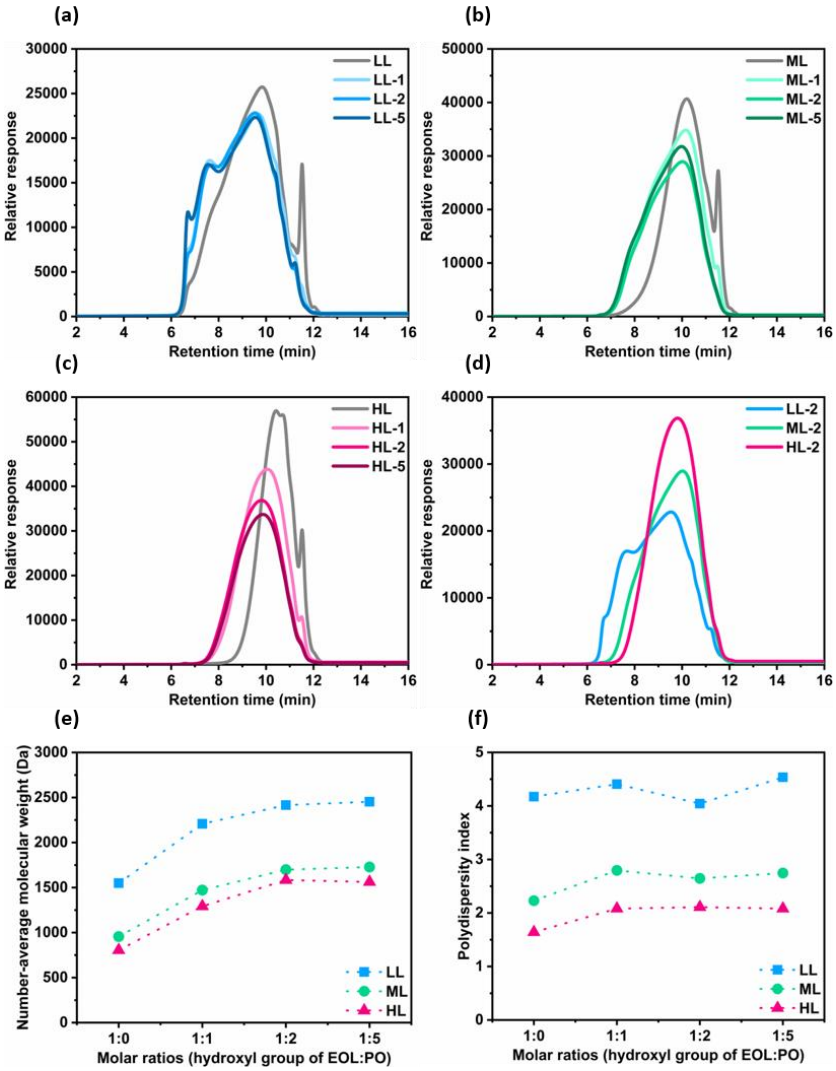


Figure 3-1. The representative GPC chromatogram with the number-average molecular weight and PDI of oxypropylated EOLs. (a) The oxypropylated LL. (b) The oxypropylated ML. (c) The oxypropylated HL. (d) The oxypropylated EOLs with a molar ratio of 1:2 (hydroxyl group of EOL:PO). (e) The number-average molecular weight of the oxypropylated EOLs. (f) PDI of the oxypropylated EOLs.

Table 3-3. Molecular weight and the polydispersity index of the oxypropylated EOLs

| | Molecular weight (Da) | | Polydispersity index ($M_w/M_n$) |
|---|---|---|---|
| | $M_n$ | $M_w$ | |
| LL | 1550 | 6470 | 4.17 |
| LL-1 | 2210 | 9730 | 4.41 |
| LL-2 | 2420 | 9770 | 4.04 |
| LL-5 | 2450 | 11130 | 4.54 |
| ML | 960 | 2130 | 2.23 |
| ML-1 | 1470 | 4110 | 2.80 |
| ML-2 | 1700 | 4500 | 2.65 |
| ML-5 | 1730 | 4750 | 2.75 |
| HL | 810 | 1320 | 1.64 |
| HL-1 | 1290 | 2690 | 2.08 |
| HL-2 | 1580 | 3340 | 2.11 |
| HL-5 | 1560 | 3250 | 2.08 |

As shown in Figure 3-1, the oxypropylated EOLs exhibited increased molecular weight compared to the corresponding unmodified EOLs, showing that the retention time was shifted forward. The molecular weight of oxypropylated EOL grew steeply as the mole ratio of PO increased until a 1:2 (hydroxyl group of EOL:PO) molar ratio, then flatten out (Figure 3-1(e)). This implies that the efficiency of ring-opening polymerization of PO decreases after PO is introduced into the hydroxyl group of lignin to some extent (Cateto et al., 2009). In particular, for the LL extracted under relatively mild conditions, the overall retention time of oxypropylated LL in the GPC chromatogram is not significantly different from that of unmodified LL. However, the intensity of the peak in the region corresponding to the high molecular weight (early retention time) increased, instead of the decrease in the peak intensity (late retention time) in the low molecular weight region. During the organosolv extraction, the aryl-ether bonds, the most dominant lignin bonds, are decomposed, and hydroxyl groups are concomitantly introduced in the form of an aliphatic hydroxyl group on the side chain or a phenolic hydroxyl group on the aromatic ring (Zhang et al., 2016b). The hydroxyl group of lignin introduced via this route initiates the ring-opening polymerization (Sadeghifar et al., 2012). The modification of lignin is significantly influenced by the accessibility to its functional groups. Typically, the phenolic hydroxyl group of lignin has a low reactivity, attributed to the steric hindrance caused by the high substitution of the methoxy group in C3 and/or C5 sites. As shown in Figure 3-1(e) and Table 3-3, the molecular weight increased more steeply with EOL extracted under mild conditions. It is considered that the reactivity of lignin with a low molecular weight and condensed structure is impaired by steric hindrance (Ding et al., 2018).

After the oxypropylation, the polydispersity index of the oxypropylated EOLs slightly increased compared to those of the unmodified EOLs, as the molecular weight increased, although the difference was not significant. On the

other hand, the oxypropylated LL had a smaller PDI value than that of the initial LL even after oxypropylation. The LL extracted under mild conditions has many aryl-ether bonds that are not decomposed in the macromolecular structure. Such aryl-ether bonds can be decomposed under alkaline conditions in the oxypropylation process, affording a more uniform structure (Li & Ragauskas, 2012).

### 3.1.2. Hydroxyl group and modified methyl group content of the oxypropylated EOLs

Lignin macromolecules have a large number of hydroxyl groups in their structure, including aliphatic and phenolic hydroxyl groups. The distribution of phenolic hydroxyl groups and aliphatic hydroxyl groups is strongly influenced by the extraction conditions. These hydroxyl groups of lignin form inter- and intramolecular hydrogen bonding, resulting in different physicochemical properties. The high frequency of intermolecular hydrogen bond interactions limits the thermal mobility of lignin (Thakur et al., 2014). In addition, the phenolic hydroxyl groups in the phenyl propane unit show inhibited reactivity, attributed to the steric hindrance caused by the high degree of substitution by the methoxyl group and abundant intra- and intermolecular hydrogen bonds (Guo & Gandini, 1991; Saito et al., 2012). The undesirable properties of lignin can be improved by replacing the phenolic hydroxyl group with an aliphatic hydroxyl group through oxypropylation and increasing the length of the side chain. Figure 3-2 describes the 31P NMR spectra of three types of EOL oxypropylated with diverse molar ratios. Additionally, Figure 3-3 and Table 3-4 summarize the quantification of the aliphatic and phenolic hydroxyl groups of the oxypropylated EOLs.

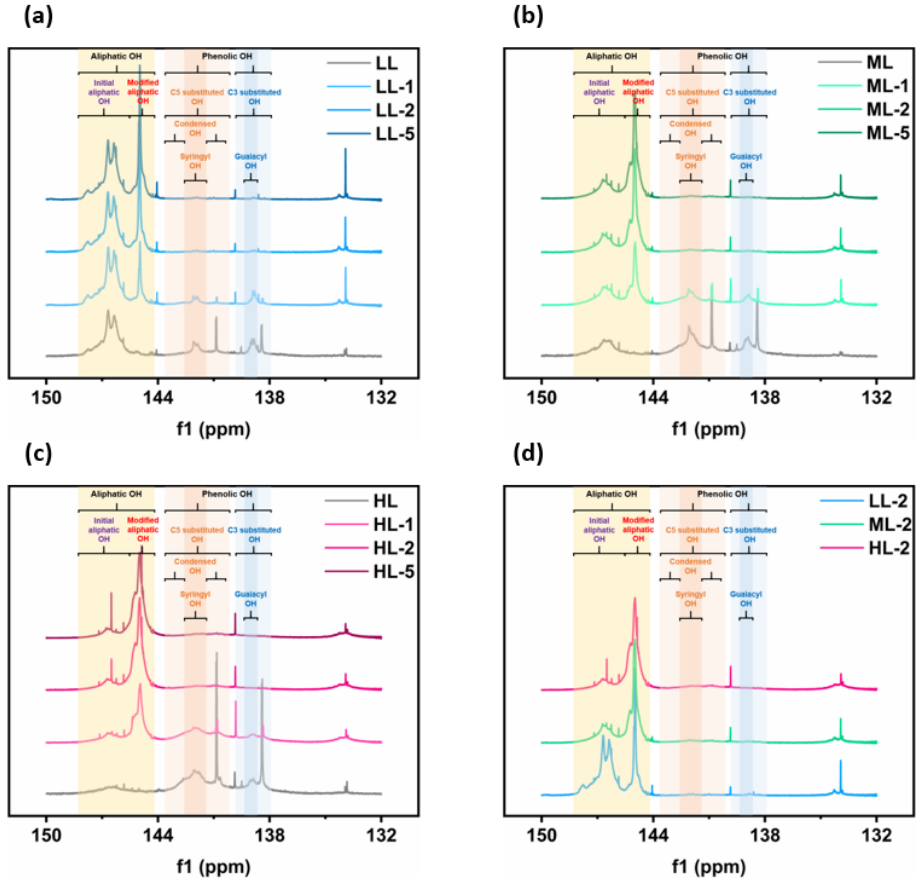


Figure 3-2. The representative 31P NMR spectra of the oxypropylated EOLs with diverse molar ratios between the hydroxyl groups of EOL and PO. (a) 31P NMR spectra of the oxypropylated LL. (b) 31P NMR spectra of the oxypropylated ML. (c) 31P NMR spectra of HL. (d) 31P NMR spectra of the oxypropylated EOLs with a molar ratio of 1:2 (hydroxyl group of EOL:PO).

After oxypropylation, the intensities of the peaks of the aliphatic hydroxyl group region increased in the 31P NMR spectra of three types of EOL, compared to the region of the initial aliphatic hydroxyl group. The shape and intensity of the original peaks, observed in the aliphatic hydroxyl group region of each unmodified EOLs, showed minor alteration, although the oxypropylation generated a new peak at ~145 ppm (Figure 3-2). This indicates that the oxypropylation exhibits higher selectivity in aromatic hydroxyl groups than in aliphatic hydroxyl groups of lignin. (Sadeghifar et al., 2012). These results are highly correlated with the pKa values of the aliphatic and aromatic hydroxyl groups in the lignin structure. In general, the pKa value of the aromatic hydroxyl group of lignin is lower than that of the aliphatic hydroxyl group. Moreover, the dissociation of hydrogen occurs more effectively under alkaline conditions, which causes dominant oxypropylation in the aromatic hydroxyl group (Silva et al., 2009).

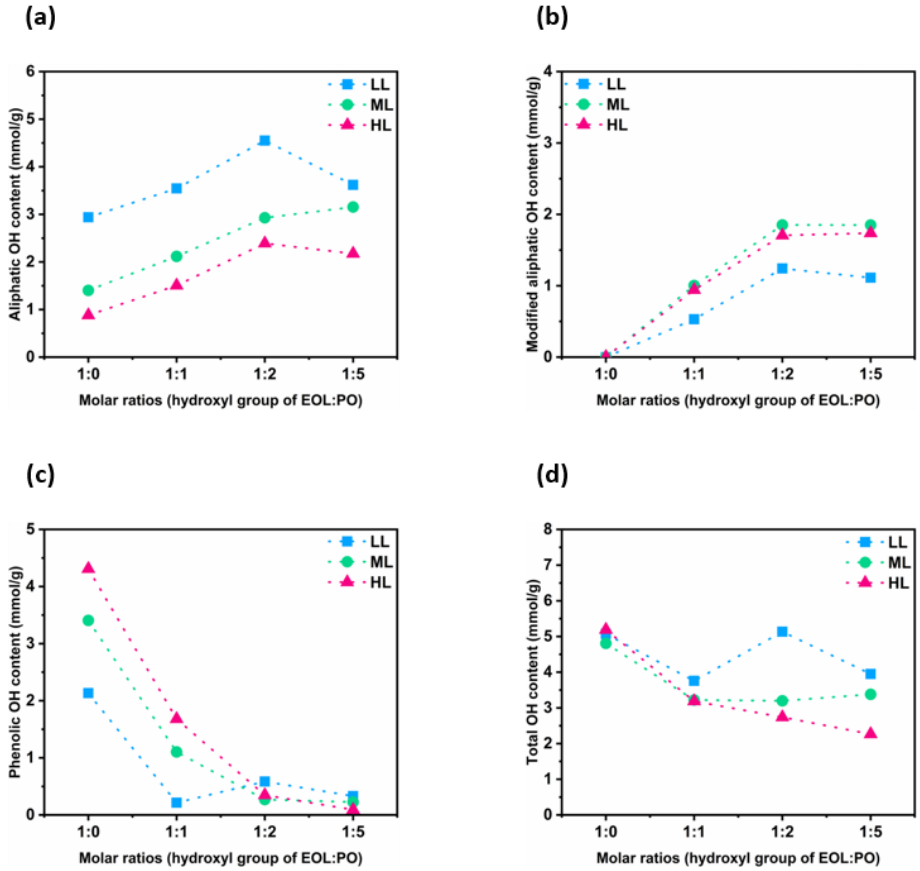


Figure 3-3. Quantification of the hydroxyl groups of the oxypropylated EOLs with diverse molar ratios between the hydroxyl groups of EOL and PO. (a) Aliphatic hydroxyl group content. (b) Modified aliphatic hydroxyl group content. (c) Phenolic hydroxyl group content. (d) Total hydroxyl group content.

Table 3-4. Quantification of the hydroxyl groups and modified methyl groups of the oxypropylated EOLs

| mmol/g | Aliphatic OH | | Phenolic OH | Total OH | Modified $CH_3$ |
|---|---|---|---|---|---|
| | Initial aliphatic OH | Modified aliphatic OH | | | |
| LL | 2.94 | 0.00 | 2.13 | 5.07 | 0.00 |
| LL-1 | 3.01 | 0.53 | 0.21 | 3.76 | 5.93 |
| LL-2 | 3.31 | 1.24 | 0.59 | 5.14 | 7.00 |
| LL-5 | 2.50 | 1.11 | 0.33 | 3.95 | 9.29 |
| ML | 1.40 | 0.00 | 3.41 | 4.81 | 0.00 |
| ML-1 | 1.11 | 1.00 | 1.10 | 3.22 | 9.79 |
| ML-2 | 1.08 | 1.85 | 0.27 | 3.20 | 11.65 |
| ML-5 | 1.30 | 1.85 | 0.23 | 3.38 | 13.89 |
| HL | 0.88 | 0.00 | 4.31 | 5.19 | 0.00 |
| HL-1 | 0.56 | 0.94 | 1.68 | 3.19 | 8.56 |
| HL-2 | 0.68 | 1.71 | 0.35 | 2.74 | 11.26 |
| HL-5 | 0.44 | 1.74 | 0.09 | 2.27 | 14.25 |

The intensity of the new peak increases steeply as the molar ratio of PO increases and subsequently flattens out over the 1:2 ratio (Figure 3-3(b)). These results are consistent with the results of the aromatic hydroxyl group content (Figure 3-3(c)). The peak for the aromatic hydroxyl group almost disappeared at the ratio of 1:2 by oxypropylation. This can also be confirmed in the quantification table of aliphatic and phenolic hydroxyl groups of three types of EOL (Table 3-4). The contents of the phenolic OH region rapidly decrease, after which the residual contents almost approach zero at a 1:2 ratio. Therefore, oxypropylation occurs effectively until the content of aromatic hydroxyl groups that can be substituted with aliphatic hydroxyl groups remains. In contrast, the content of methyl groups introduced through oxypropylation continued to increase (Figure 3-4). The ring-opening polymerization of PO, which was initiated by the hydroxyl group of lignin, continues as a chain reaction even though all of the aromatic hydroxyl groups to be substituted are consumed (Cateto et al., 2009).

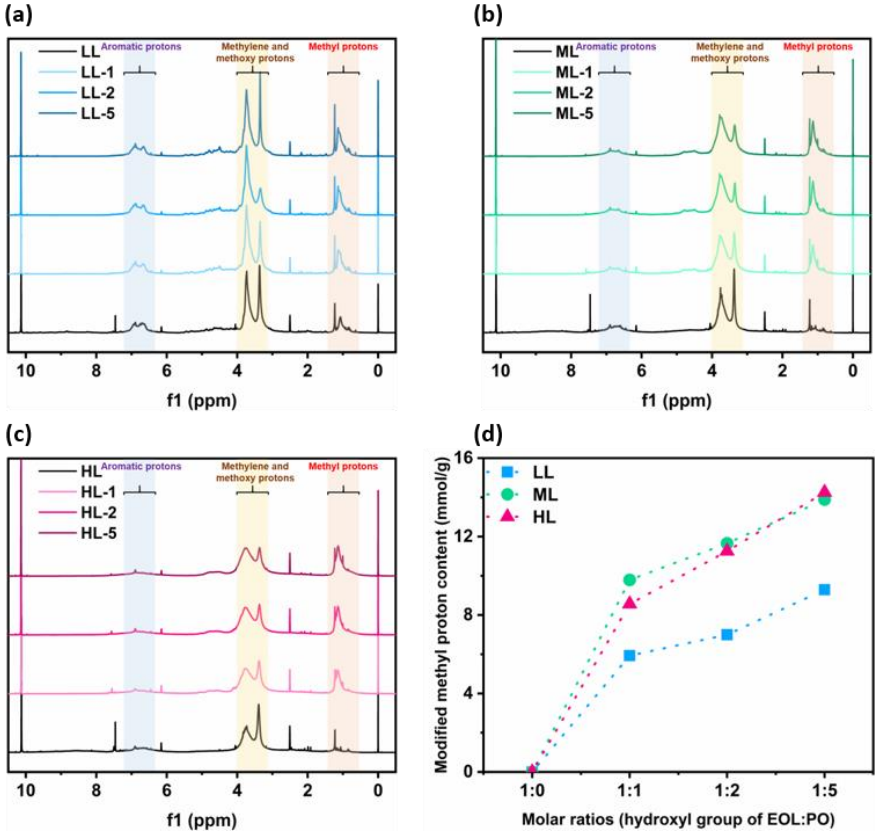


Figure 3-4. The representative 1H NMR spectra and modified methyl group content of the oxypropylated EOLs. (a) 1H NMR spectra of the oxypropylated LL. (b) 1H NMR spectra of the oxypropylated ML. (c) 1H NMR spectra of the oxypropylated HL. (d) Modified methyl group content of the oxypropylated EOLs with diverse molar ratios.

Meanwhile, the total hydroxyl group content, including aliphatic and aromatic hydroxyl groups, tended to decrease as the molar ratio of PO increased during oxypropylation. In addition, the decrease in the aliphatic hydroxyl group content, compared to contents of the initial samples, was observed in ML and HL. The total hydroxyl group content of the oxypropylated EOLs was relatively low, because of the molecular weight increase caused by the oxypropylation. Although the initial hydroxyl group content of the oxypropylated LL was higher than that of the unmodified LL. The LL contains many aryl-ether bonds that are easy to decompose under alkaline conditions in the macromolecule structure. These bonds can be degraded, introducing the hydroxyl groups into the oxypropylation process (Ma'ruf et al., 2017).

### 3.1.3. DS and DP of the oxypropylated EOLs

The DS and DP of the oxypropylated EOLs are important factors determining the blending compatibility with plastic polymers (Wei et al., 2006). Figure 3-5(a) illustrates the DS of the oxypropylated EOLs with diverse molar ratios between the hydroxyl group of lignin and PO. The DS of the oxypropylated EOLs gradually increased as the molar ratio of the injected PO increased, after which it flattened at a certain level (1:2). The HL extracted under the harshest condition showed the highest DS value, whereas the LL extracted under the mildest condition showed the lowest DS. In particular, the DS values of HL and ML were similar up to the 1:2 ratio; however, the gap widened at the 1:5 ratio. Since oxypropylation is selectively introduced in the aromatic hydroxyl group, the increase in the DS of ML was stagnant when all the aromatic hydroxyl groups for modification were consumed. For the DS of LL, the generation of a hydroxyl group by the decomposition of the aryl-ether bonds and the substitution of the hydroxyl group by PO occurred simultaneously, which smoothened the DS slope of LL.

Oxypropylated lignin has been widely used as a lignin macromonomer for macromoleculization. In this process, the side chain length of the oxypropylated lignin is one of the major factors determining its reactivity (Nadji et al., 2005). In addition, the oxypropylated lignin will increase the average molecular weight between crosslinks as the side-chain length increases, which can lead to a decrease in the crosslinking density of the copolymers (Upton & Kasko, 2016).

The DP of the oxypropylated EOLs having different characteristics is shown in Figure 3-5(b). The highest DP of the oxypropylated lignin was observed at a 1:1 ratio, and the value decreased at a 1:2 ratio, after which it increased again at a 1:5 ratio. The DP of the oxypropylated EOLs at a 1:1 ratio was 11.2 (LL), 5.6 (ML), and 8.4 (HL). The unmodified LL had a low DS value, due to the low

content of aromatic hydroxyl groups, which are the target of oxypropylation in the lignin structure. Therefore, it is considered that a relatively large mole of PO was polymerized at the narrow site of the phenolic hydroxyl group, resulting in a long side chain. Conversely, the DP at the ratio of 1:2 is lower than that at the ratio of 1:1. The oxypropylation of EOL is performed in a 0.5 M NaOH aqueous solution (pH 14). In this circumstance, the proton of the phenolic hydroxyl group with a low pKa value dissociates to form phenoxide, and the ring-opening polymerization of propylene oxide is initiated and accelerated by this nucleophilic site. In the oxypropylation process under alkaline conditions, the substitution of aromatic hydroxyl groups with aliphatic hydroxyl groups is preferred over the growth of side chains. Therefore, the DS increases continuously as the molar ratio of PO increases; however, the DP decreases until the aromatic hydroxyl group is saturated with the aliphatic hydroxyl group. Therefore, under the 1:2 ratio condition where the substitution did not achieve saturation, the DP decreased compared to that under the 1:1 ratio condition and subsequently increased upon reaching saturation.

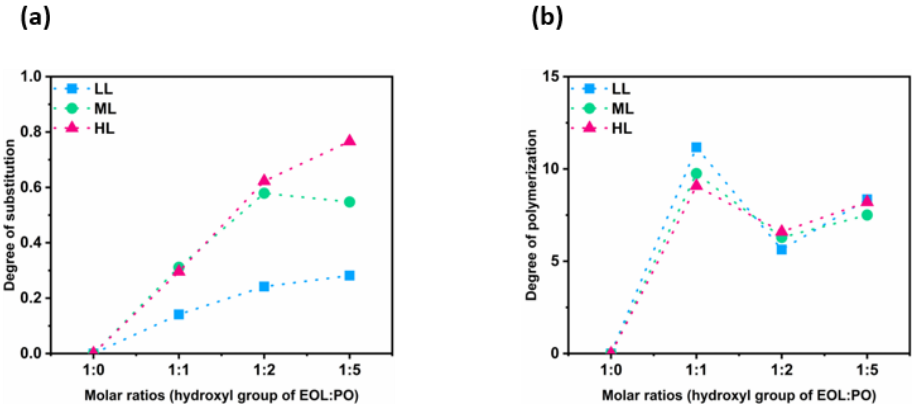


Figure 3-5. The DS and DP of the oxypropylated EOLs with diverse molar ratios. (a) The DS of the oxypropylated EOLs. (b) The DP of the oxypropylated EOLs.

## 3.2. Thermal properties of oxypropylated EOLs based on its structural characteristics

### 3.2.1. Thermal decomposition behavior of the oxypropylated EOL based on its structural characteristics

In general, lignin exhibits relatively high thermal stability compared to other natural polymers at high temperatures and has a high $T_g$ (Irvine, 1985). In particular, lignin has a double-sided thermal property, i.e., both thermoplastic and thermosetting properties. The rigid aromatic structure and the formation of cross-linkages at high temperatures induce the thermosetting properties, while the thermoplastic properties are caused by its amorphous structure and intermolecular hydrogen bonding (Jeong et al., 2013). The thermal properties of lignin differ depending on its structural characteristics.

The oxypropylation induced appreciable changes to the thermal properties of the EOLs. The thermal decomposition behaviors of the oxypropylated EOLs are shown in Figure 3-6. The distinct change in the thermal decomposition behavior of oxypropylated EOLs compared to those of the initial EOLs is indicated by a distinct double-shoulder peak, generated around 600 °C on the DTG curve. The former peak of the double-shoulder peak is indicative of the rapid mass loss due to the thermal decomposition initiated by the hydroxyl groups and ether bonds of lignin. The hydroxyl group is regarded as a functional group with low thermal stability and is easily eliminated through dehydration during pyrolysis, thereby reducing the thermal stability of lignin (Li et al., 2014). In general, the hydroxyl group begins to decompose at a lower temperature than that for the ether bond. From this viewpoint, it was observed in the TGA curve that the initial decomposition of the oxypropylated EOLs, whose hydroxyl concentrations were relatively low due to the increase in the molecular weight,

occurred slowly compared to that of the initial EOLs (Cui et al., 2013). The initial decomposition starting points and rates of LL and ML, which have a high aliphatic hydroxyl concentration due to the mild extraction conditions and poor thermal stability, were remarkably changed, compared to those for the initial EOLs. Contrarily, in the latter half of the decomposition above 400 °C, the decomposition rate of the initial EOL decreases, while that of the oxypropylated EOLs increases owing to the decomposition of the newly formed propyl side chains, indicating the reversal of the decomposition pattern.

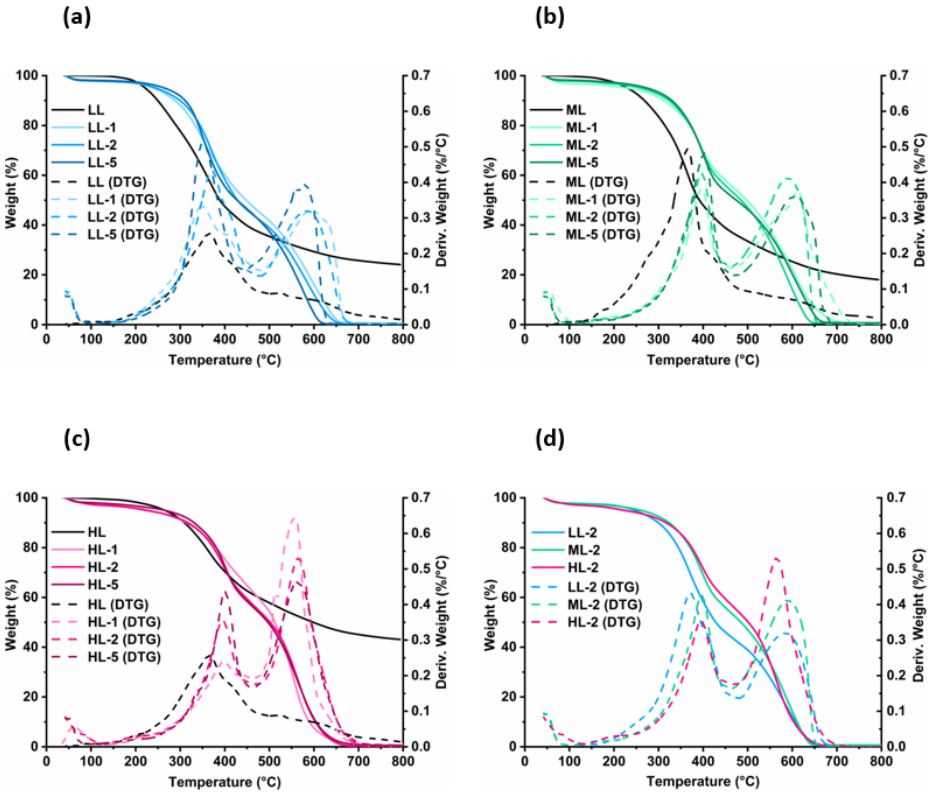


Figure 3-6. The representative TGA curve of the oxypropylated EOLs. (a) TGA curve of the oxypropylated LL. (b) TGA curve of the oxypropylated ML. (c) TGA curve of the oxypropylated HL. (d) TGA curve of the oxypropylated EOLs with a molar ratio of 1:2 (hydroxyl group of EOL:PO).

In addition, the char yield of the oxypropylated EOLs was significantly reduced compared to that of the initial EOLs, resulting in the generation of the following peak. Although the char yield of the initial EOLs differs depending on the hydroxyl content in the structure and the intermolecular bond structure, it was determined to be ~20% or more. Conversely, the oxypropylated EOLs lost most of their mass by thermal decomposition at ~650 °C, resulting in a char yield approaching 0%. This implies that the oxypropylated lignin displays diminished thermosetting properties, which result in a high char yield through crosslinking at high temperatures. Lignin usually forms high-density crosslinks at high temperatures by frequent hydrogen bonding interactions in the structure, which account for the thermosetting properties (Brodin et al., 2010). However, the introduction of side chains by oxypropylation not only increases the physical distance between the functional groups in the lignin structure but also interferes with the crosslinking of functional groups due to steric hindrance. This weakens the thermosetting properties of lignin, resulting in a decrease in the char yield (Hosoya et al., 2009). In the TGA curve of the oxypropylated EOLs with a molar ratio of 1:2, oxypropylated HL, which has a high DS and a low total hydroxyl content, has a low thermal decomposition starting point and rate.

### 3.2.2. DSC analysis of the oxypropylated EOL based on its structural characteristics

Lignin is generally known to have a high $T_g$, and the range of the $T_g$ is distributed according to the structure derived from the extraction process (Irvine, 1985). $T_g$ is not only an important factor in determining the thermal properties of a polymer but also a major factor in predicting the compatibility with the matrix polymer to form a thermoplastic. In the melt-blending process, the compatibility tends to increase as the $T_g$ of the heterogeneous polymers approaches (Mousavioun et al., 2010). Figure 3-7 illustrates the DSC analysis results of the oxypropylated EOLs.

The initial EOLs under different extraction conditions had different $T_g$ values depending on their structural characteristics. The HL, which had a low molecular weight, high phenolic hydroxyl content, and condensed structure, exhibited the highest $T_g$ among three types of EOL. After the oxypropylation, for the LL and ML extracted under relatively mild conditions, a new $T_g$ was observed between 55 and 60 °C. After oxypropylation, the $T_g$ of the EOLs gradually decreased as the molar ratio of the added PO increased. The fully oxypropylated lignin only has an aliphatic hydroxyl group in its structure, in which the aromatic hydroxyl group is substituted with the secondary aliphatic hydroxyl group. In addition, aliphatic hydroxyl groups are converted into branched forms with extended side chains, resulting in a decrease in the $T_g$ (Kelley et al., 1988b). Thus, the oxypropylated EOL is free from hydrogen bonds; this results in reduced $T_g$, which can lead to increased compatibility for melting blends (Lisperguer et al., 2009).

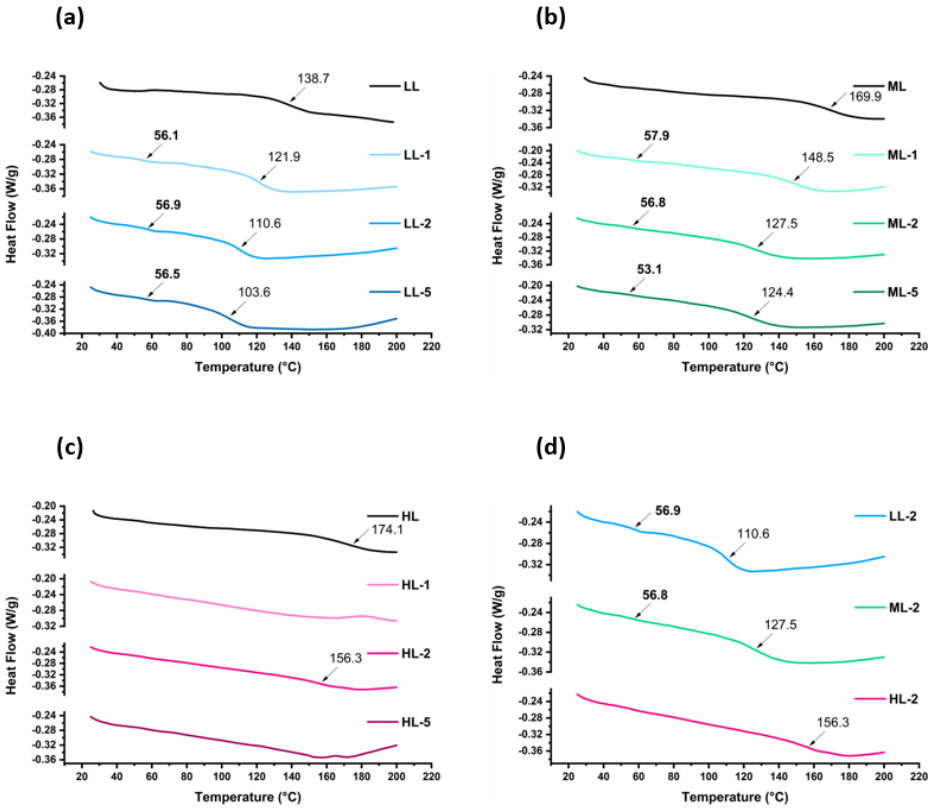


Figure 3-7. The representative DSC curve of oxypropylated EOLs. (a) DSC curve of the oxypropylated LL. (b) DSC curve of the oxypropylated ML. (c) DSC curve of the oxypropylated HL. (d) DSC curve of the oxypropylated EOLs with a molar ratio of 1:2 (hydroxyl group of EOL:PO).

Conversely, the thermal event of oxypropylated lignin observed after 100 °C is considered the melting point. In general, polymers have a distinct range of $T_g$, and it is a major factor in determining the physicochemical properties of the material. From this point of view, it was strange that two $T_g$ values were observed in two regions in the DSC curve of oxypropylated lignin. Figure 3-8 shows the oxypropylated EOLs exposed on a hot plate at 200 °C for 5 min. Melting was observed in the oxypropylated LL and ML; particularly, for the oxypropylated LL, melting was observed even at a 1:1 ratio, and fluidity was achieved. In addition, the SDT analysis performed in air revealed broad melting points of 134.2 °C and 154.5 °C in the DSC curves of LL-2 and ML-2, respectively (Figure 3-9). It is considered that LL and ML, which have a less condensed structure than HL, form a flexible structure with increased viscosity at a relatively low temperature as the intermolecular bonds are weakened by oxypropylation, resulting in increased thermoplasticity (Cateto et al., 2009; Hatakeyama et al., 2002; Saraf et al., 1985). Thus, it is evident that oxypropylation changes the thermal characteristics of the EOL; this change is largely dependent on the DP of the side chain, as well as the structural characteristics of the initial EOL.

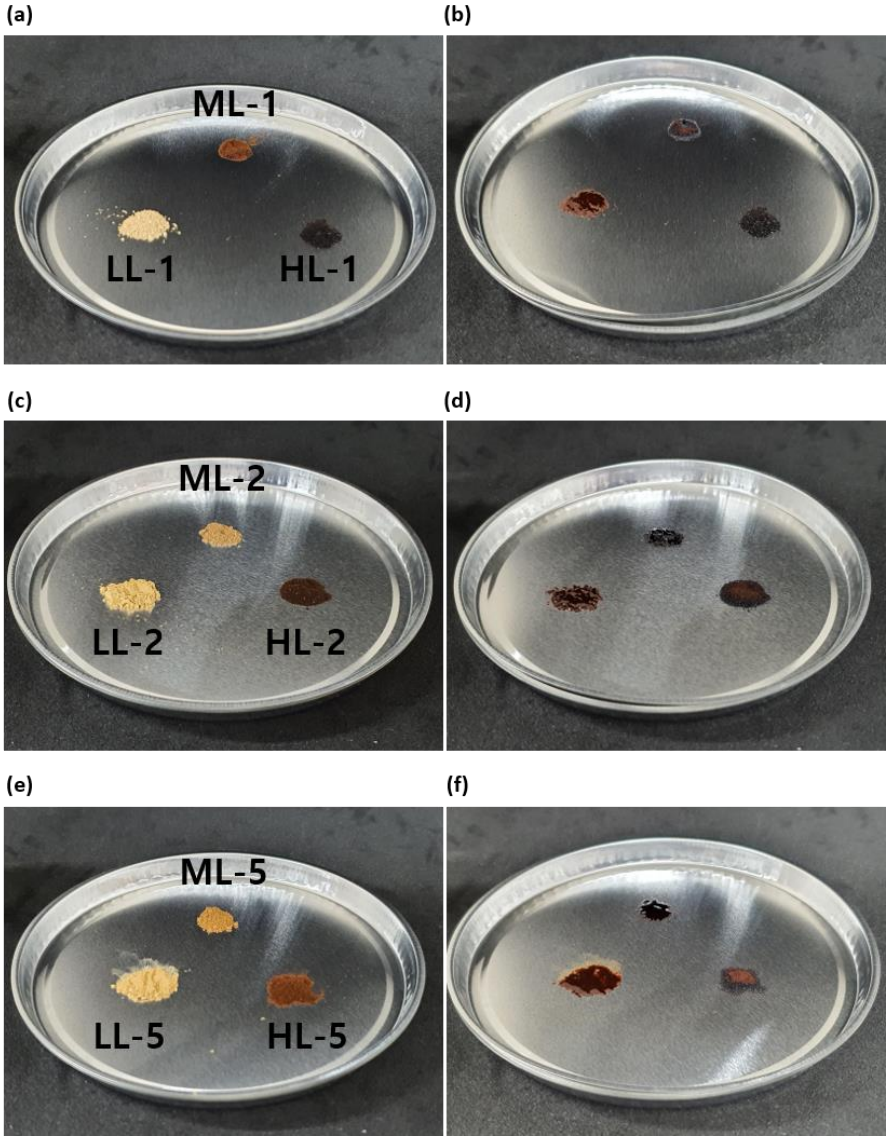


Figure 3-8. Melting test of the oxypropylated EOLs. (a) Oxypropylated EOL with a 1:1 ratio. (b) Heated oxypropylated EOL with a 1:1 ratio. (c) Oxypropylated EOL with a 1:2 ratio. (d) Heated oxypropylated EOL with a 1:2 ratio. (e) Oxypropylated EOL with a 1:5 ratio. (f) Heated oxypropylated EOL with a 1:5 ratio.

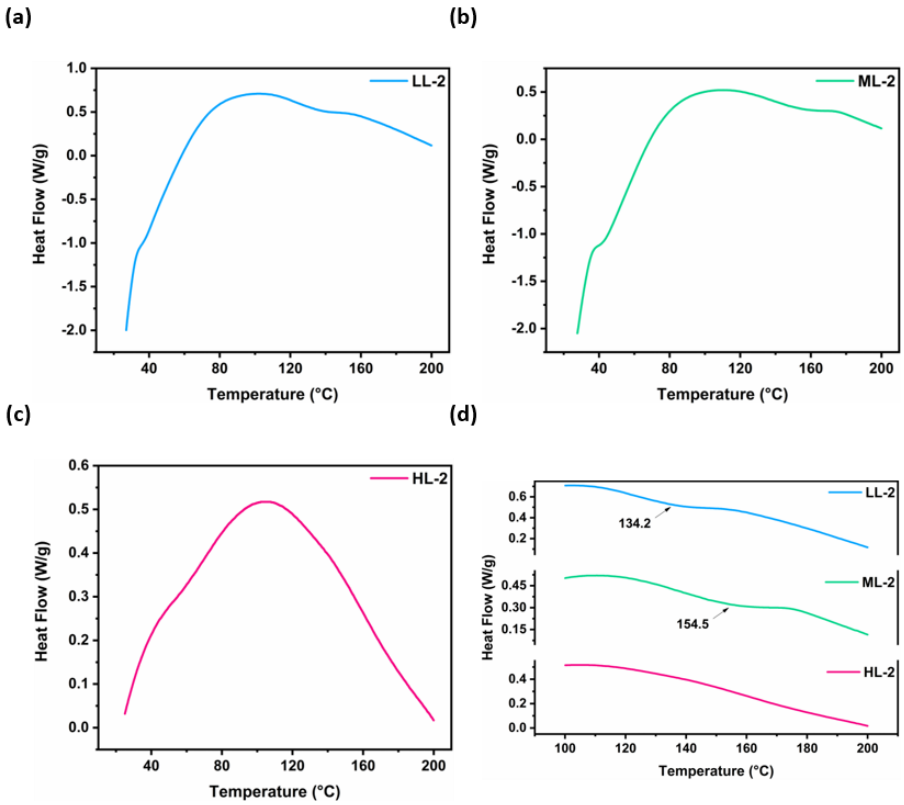


Figure 3-9. The representative DSC curve of the oxypropylated EOLs in the SDT analysis in air. (a) DSC curve of the oxypropylated LL in the SDT analysis under air flow. (b) DSC curve of the oxypropylated ML in the SDT analysis under air flow. (c) DSC curve of HL in the SDT analysis under air flow. (d) DSC curve of the oxypropylated EOLs with a molar ratio of 1:2 (hydroxyl group of EOL:PO) in the SDT analysis under air flow.

## 3.3. The properties of the oxypropylated EOL–PLA bioplastic

### 3.3.1. Morphologies of the EOL–PLA bioplastics

The morphological surface structures of the PLA bioplastics formed with the initial EOLs and oxypropylated EOLs are illustrated in Figures 3-10. The neat PLA had a very sleek and flat surface structure. In contrast, the initial EOL–PLA bioplastic comprising EOL particles embedded in the PLA matrix showed a rough and uneven surface structure. In the surface structure of the EOL–PLA bioplastic, EOL particles that aggregated to each other to form a large particle were irregularly distributed in the PLA matrix. In the SEM image of the aggregated EOL particles, the clumping of lignin droplets, which was easily observed in the surface structure of the pretreated wood powder after organosolv pretreatment, was observed (Koo et al., 2012). In the lignin-biopolyester bioplastic, lignin is easily self-aggregated by van der Waals attraction and inter- and intramolecular hydrogen bonding derived from various functional groups including oxygen (Chung et al., 2013). The aggregation of lignin particles can be promoted by the incompatibility of the matrix polymer of bioplastic and adversely affect the mechanical properties of the bioplastic (Collins et al., 2019b). It means that the initial EOLs has poor compatibility with PLA and are non-uniformly dispersed in the PLA matrix with implying a poor mechanical strength of bioplastic. In general, lignin macromolecules with a high molecular weight and long chain have a strong attractive force between the molecules, and an increase in this attractive force may cause aggregation in the thermo-bioplastic formed with a poorly compatible polymer matrix (Norgren et al., 2001). However, a relatively large amount of aggregated lignin was observed in the surface structure of the EOL–PLA bioplastic to which HL

was added, compared with those to which LL and ML were added. For HL, due to its condensed structure, the $T_g$ shows a large gap with that of PLA, which causes poor dispersion and agglomeration during the melt blending with PLA (Mousavioun et al., 2010).

Conversely, in the oxypropylated EOL–PLA bioplastic, the amount and size of aggregated EOL particles in the surface structure were markedly reduced, suggesting that the dispersibility was improved. The magnification images of the oxypropylated EOL–PLA bioplastics showed a much smoother and flatter surface structure compared to that of the initial EOL–PLA. The surface properties of EOL were modified by growing side chains length through a chain ring cleavage reaction with increasing its hydrophobicity (Chen et al., 1996). And, the hydroxyl group content of EOL was relatively decreased by increasing molecular weight. In this regard, the modified surface properties and chemical structure of EOL contributed to improving the compatibility with the PLA matrix. In particular, LL and ML exhibited higher dispersibility than that of the oxypropylated HL, despite their large molecular weights. The oxypropylated LL and ML, which exhibit a similar range of $T_g$ to that of PLA, exhibited significantly increased compatibility with PLA. In addition, their melting properties prevented agglomeration during the melt-blending process, which contributed to the uniform dispersion and small particle size.

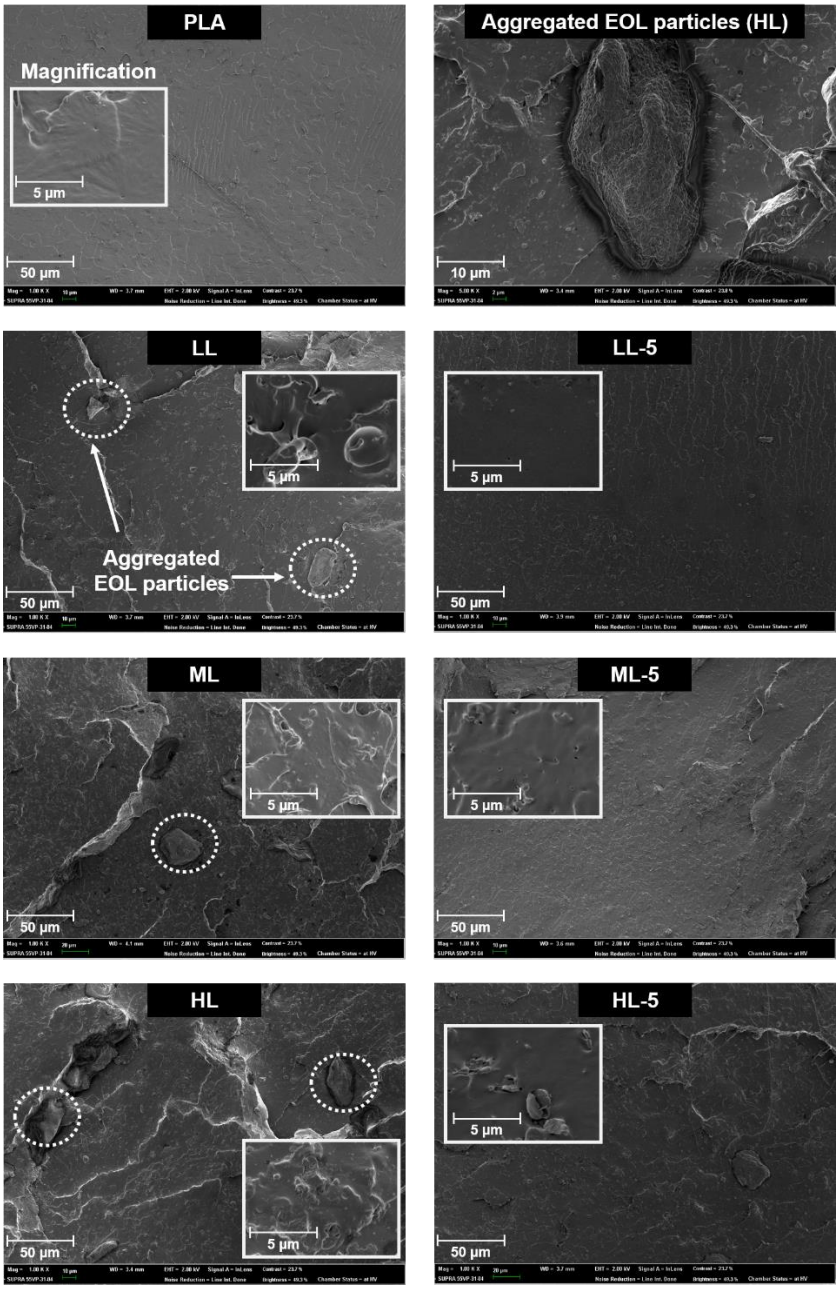


Figure 3-10. FE-SEM images of PLA, the initial and oxypropylated EOL–PLA bioplastics, and aggregated EOL particle (HL) with magnified images in white squares.

### 3.3.2. Thermal properties of the oxypropylated EOL–PLA bioplastics

Depending on the compatibility of lignin with the matrix polymer, the lignin-containing thermo-bioplastic may be unstable or phase-separated (Collins et al., 2019a). The compatibility of lignin with PLA can be improved by oxypropylation. Figure 3-11 shows the thermal decomposition characteristics of the oxypropylated EOL–PLA bioplastics. As mentioned in Section 3.3 of Chapter 2, the initial EOL–PLA bioplastics exhibited improved thermal stability compared to that of the neat PLA. Lignin, which exhibits relatively high thermal stability at high temperatures, can impart thermal stability to PLA. The thermal properties of EOLs, which changed after oxypropylation, also affect the thermal properties of EOL–PLA bioplastics. The oxypropylated EOL–PLA bioplastics exhibited reduced thermal stability compared to that of the initial EOL–PLA bioplastics. For the LL and ML extracted under relatively mild conditions, the thermal decomposition of the bioplastic prepared using oxypropylated EOL was accelerated. In contrast, the bioplastic containing the oxypropylated HL exhibited lower thermal stability than that containing the initial HL, but higher or similar stability to that of the neat PLA. Due to the introduction of the propyl side chain, the oxypropylated lignin has a small proportion of the rigid aromatic moiety in its structure, which imparts poor thermal stability at high temperatures (Thakur et al., 2014).

In the case of EOL–PLA bioplastic, the thermal decomposition of the oxypropylated EOL–PLA bioplastics proceeded faster than that of the initial EOL–PLA bioplastics, although oxypropylated EOLs had slower initial thermal decomposition rate than that of initial EOLs. Oxypropylated EOL has a slow initial thermal decomposition rate due to a relatively decrease in hydroxyl groups compared to the initial EOL, but the weight loss is accelerated above

350 °C. This phenomenon is due to the weakened thermosetting that forms crosslinks at high temperatures and the reduced relative proportion of heat-resistant aromatic rings in the molecular structure. On the other hand, PLA hardly observed the weight loss before 350 °C observed in EOL. Therefore, it is considered that when PLA starts to decompose above 350 °C, oxypropylated EOLs rapidly decompose along with PLA, accelerating the weight loss. However, thermal decomposition start temperature of oxypropylated HL reduced relatively less than oxypropylated LL and ML due to the excellent thermal stability of the initial HL.

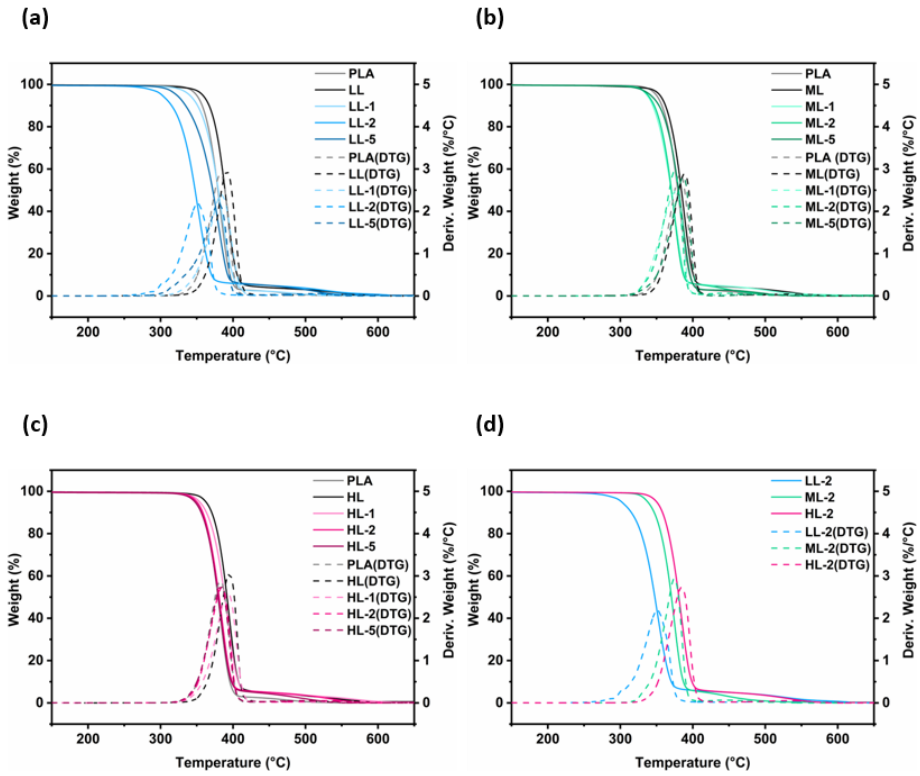


Figure 3-11. The representative TGA curve of the oxypropylated EOL–PLA bioplastics. (a) TGA curve of the oxypropylated LL–PLA bioplastics. (b) TGA curve of the oxypropylated ML–PLA bioplastics. (c) TGA curve of the oxypropylated HL–PLA bioplastics. (d) TGA curve of the oxypropylated EOLs with a molar ratio of 1:2 (hydroxyl group of EOL:PO).

Figure 3-12 shows the results of the DSC analysis of the oxypropylated EOL–PLA bioplastics. The $T_g$ and melting temperature of the oxypropylated EOL–PLA bioplastics exhibited no significant change compared to those of the neat PLA. However, the cold crystallization enthalpy ($\triangle H_{cc}$) and melting enthalpy ($\triangle H_m$) gradually increased as the molar ratio of PO increased. This implies that the arrangement of the PLA chain by the addition of the oxypropylated EOL (amorphous structure) consumes a significant amount of energy, and an even higher amount of energy is required for the phase changes (Jia et al., 2017). In addition, the oxypropylated EOL with a high molar ratio of PO may interfere with the arrangement and phase change of PLA due to steric hindrance caused by the increased molecular weight and side-chain length.

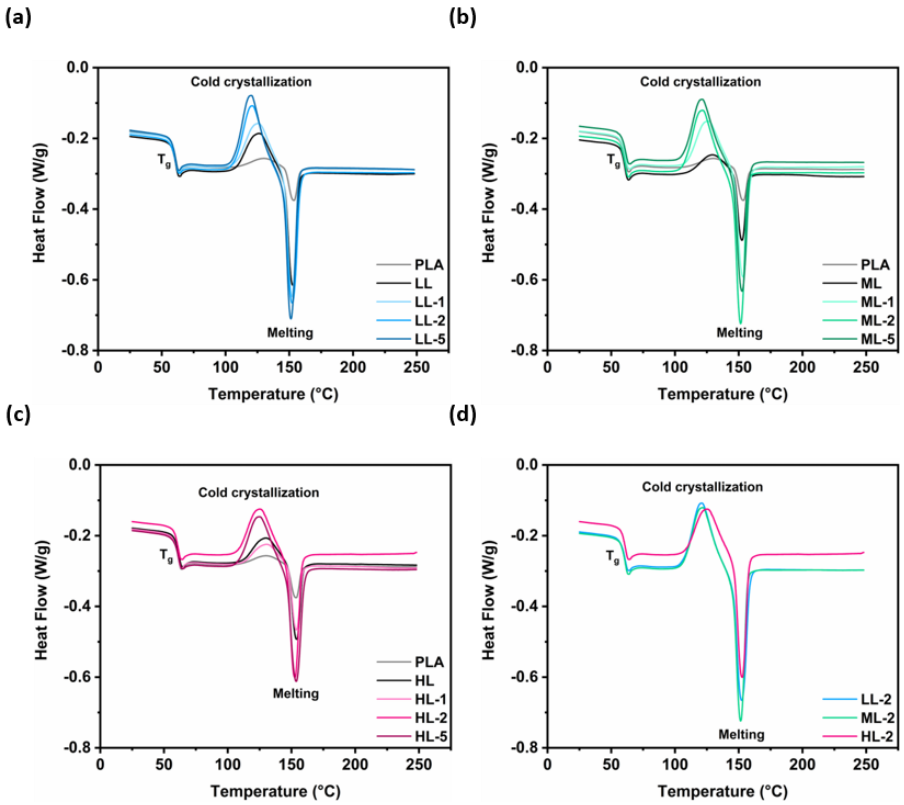


Figure 3-12. The representative DSC curve of the oxypropylated EOL–PLA bioplastics. (a) DSC curve of the oxypropylated LL–PLA bioplastics. (b) DSC curve of the oxypropylated ML–PLA bioplastics. (c) DSC curve of the oxypropylated HL–PLA bioplastics. (d) DSC curve of the oxypropylated EOLs with a molar ratio of 1:2 (hydroxyl group of EOL:PO).

### 3.3.3. Mechanical properties of the oxypropylated EOL–PLA bioplastics

Many studies have been conducted that the addition of lignin reduces the mechanical strength, including the tensile strength and elongation of biopolyester (Anwer et al., 2015; Yang et al., 2015). This phenomenon was also confirmed in Section 3.3.2 of Chapter 2 of this study. As mentioned above, the typical cause of the mechanical strength reduction by the addition of lignin is poor compatibility with the matrix polymer. Figure 3-13 shows the stress–strain curve of the oxypropylated EOL–PLA bioplastics.

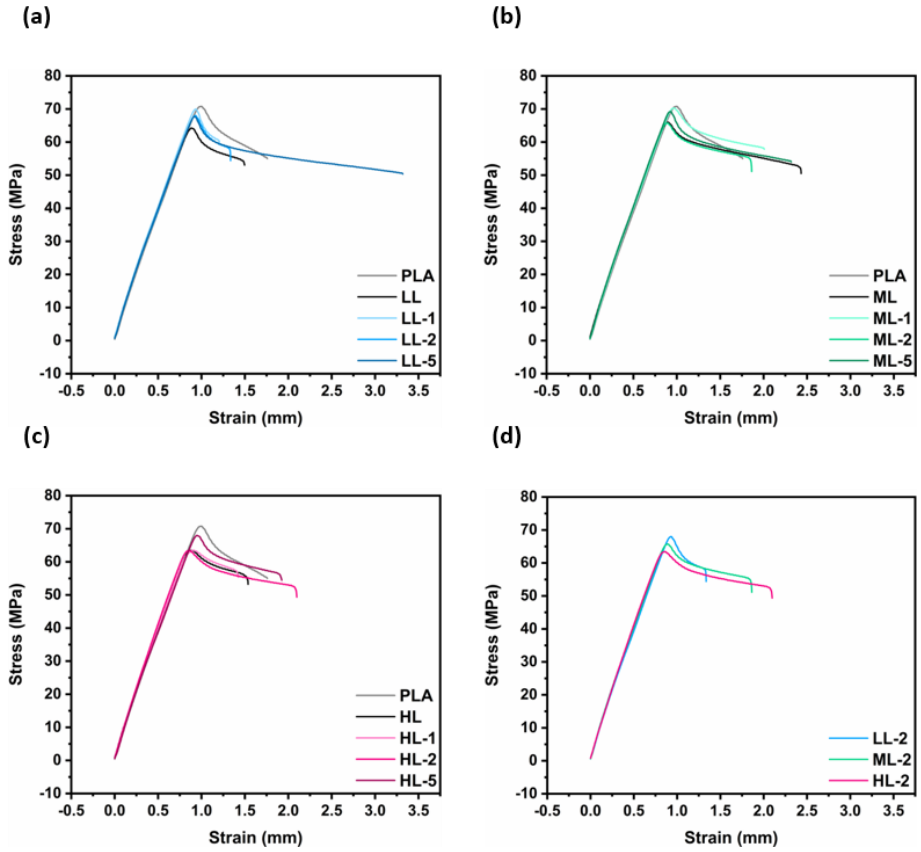


Figure 3-13. The representative stress–strain curve of the oxypropylated EOL–PLA bioplastics. (a) Stress–strain curve of the oxypropylated LL–PLA bioplastics. (b) Stress–strain curve of the oxypropylated ML–PLA bioplastics. (c) Stress–strain curve of the oxypropylated HL–PLA bioplastics. (d) Stress–strain curve of the oxypropylated EOLs with a molar ratio of 1:2 (hydroxyl group of EOL:PO).

The stress–strain curve of the EOL–PLA bioplastics containing 5% of oxypropylated EOL showed similar slope and shape to those for the neat PLA. The observed tensile strength was between that of the neat PLA and that of each of the initial EOL–PLA bioplastics, implying an increase in the compatibility of each oxypropylated EOL and PLA. Contrarily, the tensile strength of the bioplastics based on unmodified lignin significantly decreased compared to that of the neat PLA. The blending of PLA with unmodified EOL (LL, ML, and HL) reduced the tensile strength of PLA from 70.9 MPa to 64.0 (LL), 65.5 (ML), and 63.2 (HL) MPa. The EOL–PLA bioplastic with HL, extracted under the high severity conditions, had the lowest tensile strength, and the EOL–PLA bioplastic with ML, extracted under the moderate severity conditions, showed the least reduced tensile strength, although the value was not significant. As shown in Figure 3-7, the $T_g$ of HL is higher than those of the other two types of EOLs, and it has the largest gap from the $T_g$ of PLA. This results in the incompatibility of HL and PLA and leads to poor dispersibility within the thermo-bioplastic (Figures 3-10).

However, the tensile strength of the EOL–PLA bioplastics containing 5% oxypropylated EOL differs significantly depending on the types of EOL. The thermo-bioplastics with each type of oxypropylated EOL tended to have a higher tensile strength than those with the unmodified EOL, although the transitional aspect varied depending on the types of EOL. Moreover, the tensile strengths of ML and LL were similar to that of the neat PLA at a 1:1 ratio; they decreased at the ratio of 1:2 and subsequently increased at the ratio of 1:5. These patterns of the tensile strength shown in Figure 3-14(a) are similar to those of the DP, shown in Figure 3-5(b). Regarding the results, the tensile strength of the thermo-bioplastic has a significant relationship with the substituted side-chain length. This implies that the longer the side chains modified by oxypropylation, the greater the compatibility with PLA and the greater the

interfacial adhesion between the two heterogeneous polymers (Kazzaz et al., 2019; Wei et al., 2006).

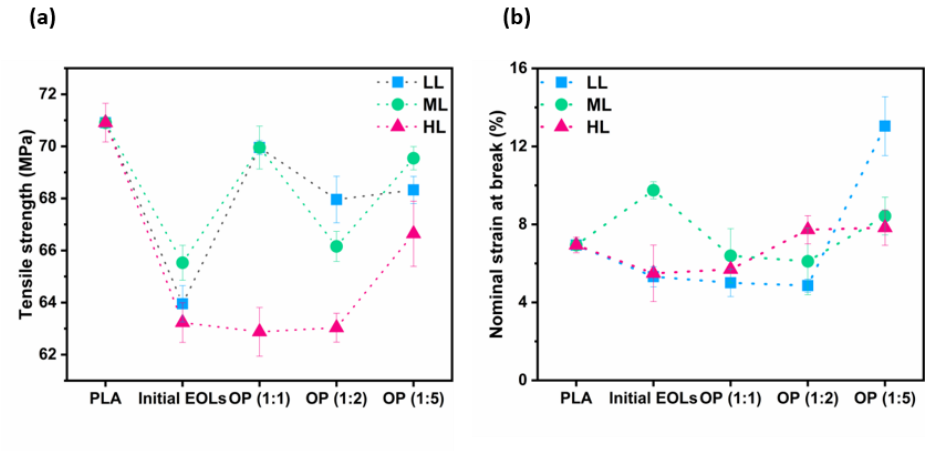


Figure 3-14. Tensile strength and nominal strain at break of the oxypropylated EOL–PLA bioplastics (a) Tensile strength of the oxypropylated EOL–PLA bioplastics (b) Nominal strain at the break of the oxypropylated EOL–PLA bioplastics.

For HL, despite having the highest DP at a 1:1 ratio, it showed similar tensile strength to that of the unmodified HL, and the tensile strength increased as the mole ratio of PO increased. Unlike the other two oxypropylated EOLs, HL, which has a high phenolic OH group content and a condensed structure, did not show $T_g$ below 60 °C after oxypropylation. Moreover, the melting was not clearly observed as shown in Figure 3-7(d) of Section 3.2.2. In this regard, the oxypropylated HL could not be uniformly mixed through melting, compared to the cases with LL and ML. Thus, a weak interaction was formed between the propyl side chain and the PLA chains, resulting in poor tensile strength (Mousavioun et al., 2010). Therefore, the reduction of the tensile strength of the lignin-containing thermo-bioplastic can be supplemented by oxypropylation, which can improve the compatibility with PLA. Additionally, the compatibility of the oxypropylated EOL with PLA is thought to be significantly influenced by the DP of the side chain, as well as the properties of the initial lignin.

On the other hand, the thermo-bioplastic using oxypropylated EOLs with a high PO ratio tended to exhibit a high value of nominal strain at break (Figure 3-14(b)). The oxypropylated EOL was evenly dispersed in the PLA matrix due to the increased PLA compatibility. In particular, the oxypropylated LL, modified at a molar ratio of 1:5, showed a remarkably smooth and flat surface structure, implying excellent compatibility with PLA (Figure 3-10). As mentioned above, the compatibility has a significant effect on the elongation. The oxypropylated EOL, which has increased compatibility, can form a structure that promotes energy dispersion by strong entanglement with PLA chains, since the DP of the side chain is increased.

### 3.3.4. Thermodynamic properties of the oxypropylated EOL–PLA bioplastics

Plastics are also usually exposed to relatively low temperatures below 100 °C, not just high temperatures. Therefore, to evaluate the practical heat resistance of plastics, it is necessary to predict their mechanical properties as a function of the temperature change. The thermodynamic properties of viscoelastic polymers change with the temperature of the material. The mechanical properties of a polymer change according to the degree of movement of the polymer chain. As the temperature increases, the movement of the polymer chain increases, which causes a decrease in the storage modulus. In particular, near the $T_g$, the deterioration of the mechanical properties becomes significant. Tan delta is the ratio of the loss modulus to the storage modulus, and when the tan delta reaches a maximum value, the phase transition is maximized (Saba et al., 2016; Young & Lovell, 2011). This evidences that the phase of the material is changing, and the maximum point of the tan delta is defined as the $T_g$ of the polymer (Gracia-Fernández et al., 2010).

Figure 3-15 shows the results of dynamic mechanical analysis (DMA) performed in the double cantilever mode to predict the change in the mechanical properties of the thermo-bioplastic from room temperature to 130 °C. The storage modulus of all the thermo-bioplastics decreased with increasing temperature. The initial EOL–PLA bioplastic exhibited a lower initial storage modulus at room temperature than that of the neat PLA. Conversely, the oxypropylated EOL–PLA bioplastic tended to show an improved initial storage modulus compared to that of the initial EOL–PLA bioplastic. This is consistent with the discussion on the mechanical properties of the oxypropylated EOL–PLA bioplastic in Section 3.3.2, implying that the

mechanical strength of the thermo-bioplastic increased due to the improved compatibility of EOL with PLA by oxypropylation.

The storage modulus of PLA rapidly decreased after 60 °C, and the tan delta reached a maximum value at 74.6 °C. Contrarily, a sharp decline in the storage modulus of the EOL–PLA bioplastic and the maximum tan delta were observed at higher temperatures than those for the neat PLA. This implies that the $T_g$ of the EOL–PLA bioplastic was increased compared to that of the neat PLA from a thermodynamic perspective. Furthermore, it indicates that the addition of the oxypropylated EOL improves the mechanical performance of PLA at temperatures above the $T_g$ (Gordobil et al., 2015; Jonoobi et al., 2010). As shown in the DMA results of three types of thermo-bioplastic prepared using the EOL oxypropylated at a ratio of 1:5, the EOL–PLA bioplastic of LL-5 had the highest $T_g$, while the EOL–PLA bioplastic of HL-5 showed the lowest $T_g$. As mentioned above, the compatibility of LL and ML with PLA was improved by oxypropylation. This improved compatibility enables the production of a more uniform thermo-bioplastic and the dispersion of the energy derived from external forces by the formation of a strong entanglement with a matrix polymer (Saïd Azizi Samir et al., 2004). Therefore, the EOL–PLA bioplastics of LL-5 and ML-5 have a higher $T_g$ than that of HL-5.

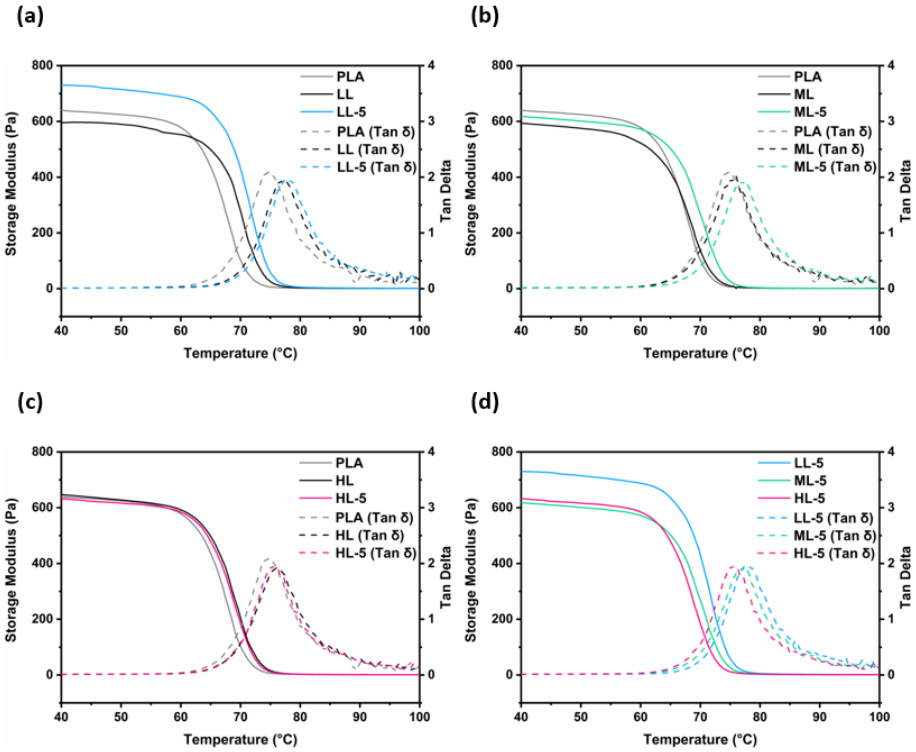


Figure 3-15. The representative DMA thermal scan of the oxypropylated EOL–PLA bioplastics. (a) DMA thermal scan of the oxypropylated LL–PLA bioplastics. (b) DMA thermal scan of the oxypropylated ML–PLA bioplastics. (c) DMA thermal scan of the oxypropylated HL–PLA bioplastics. (d) DMA thermal scan of the oxypropylated EOLs with a molar ratio of 1:5 (hydroxyl group of EOL:PO).

# 4. Summary

In this chapter, the effect of oxypropylation on the compatibility with PLA depending on the structural characteristics of EOL was investigated. Three types of EOLs with different structural characteristics were modified with various molar ratios of the hydroxyl groups of lignin to PO. The structural characteristics of the oxypropylated EOLs were highly dependent on the types of the initial EOL. During the oxypropylation, the DS and DP of the propyl side chain were affected by the distribution of the hydroxyl groups of the initial lignin. HL with a high aromatic hydroxyl group content (4.31 mmol/g) exhibited a high DS (0.77), and LL with a high aliphatic hydroxyl group content (2.94 mmol/g) exhibited a high DP (11.17).

The oxypropylated EOLs with different structural characteristics exhibited varying thermal properties. In particular, a new $T_g$ between 55 and 60 °C was observed in the oxypropylated LL and ML. Further, melting was observed according to the types of oxypropylated EOL, which improved the thermoplasticity. The thermal properties of the oxypropylated EOLs influenced the thermal and mechanical properties of the EOL–PLA bioplastics. The introduction of side chains accelerated the thermal decomposition of the oxypropylated EOL–PLA bioplastics by decreasing the relative proportion of aromatic moieties in the structure. However, the compatibility of EOL with PLA was successfully improved by oxypropylation. In particular, the oxypropylated LL and ML exhibited improved thermoplasticity and compatibility, resulting in the slick and flat surface structures observed in the thermo-bioplastics. The increased compatibility of EOL with PLA increased the tensile strength of the oxypropylated EOL–PLA bioplastic to a similar level to that of the neat PLA, and the nominal strain was increased to a higher level than that of the neat PLA. In addition, the $T_g$ of the EOL–PLA bioplastic was

increased compared to that of the neat PLA in a thermodynamic perspective, implying the improved mechanical properties of the oxypropylated EOL–PLA bioplastic at temperatures above the $T_g$ of the neat PLA. Thermodynamic analysis revealed that the $T_g$ of PLA (74.6 °C) was increased to 77.8 (LL-5), 77.7 (ML-5), and 75.5 °C (HL-5), by blending with unmodified EOLs, and it further increased upon blending with oxypropylated EOLs. Therefore, the physicochemical properties of the EOL–PLA bioplastic were improved by successfully enhancing the compatibility with PLA and thermoplasticity of EOL through oxypropylation. The compatibility and thermoplasticity were found to be significantly influenced not only by the DP of the side chains but also by the lignin structure.

# *Chapter 4*

## Preparation and characterization of lignopolyurethanes using different types of EOL

# 1. Introduction

Biopolyurethane is a synthetic or biodegradable urethane produced using biomass-derived raw materials containing isocyanates or polyols. Thus far, many studies have been conducted to develop biopolyurethane by synthesizing petrochemical-derived isocyanates and biomass-derived polyols. Biomass-derived polyols include biopolyether polyols and biopolyester polyols. As the polyether polyol, sucrose and sorbitol are used in the rigid polyurethane foam, and the content of these polyols is 30% or less. In addition, 1,3-propanediol, obtained by the fermentation of corn sugar, is used in the manufacture of polytrimethylene ether glycol, which is used in the softening segment of elastomers and spandex fibers (Shen et al., 2009). Meanwhile, for biopolyester polyol, some of the polyester polyols may be biomaterials. Dibasic acid is a fermented product, e.g., succinic acid and adipic acid, and ethylene oxide (EO) and 1,2-propanediol (propylene glycol, PG), which are raw materials for polyols, can also be biosynthesized. However, biopolyether polyols and biopolyester polyols are considered not economical because they require additional processes for production and purification. Therefore, to ensure the economic feasibility of biopolyurethane, it is necessary to use an inexpensive raw material derived from biomass that is obtained as a by-product in traditional industries.

Lignin, which has a molecular weight in the range of several thousand Da and multiple functional groups per molecule, is suitable for use as a macromonomer for the lignin macromolecular complex. This can be achieved by inducing cross-linked bonds between lignin macromolecules using a bifunctional crosslinking agent. The lignin macromolecular complex may have a linear or branched copolymer structure depending on the ratio of the functional group of lignin and the dose of the bifunctional crosslinking agent.

Lignin macromolecules can react with a diisocyanate to form thermosetting polyurethane resin. The thermosetting lignopolyurethane has excellent heat resistance due to its rigid structure, which is composed of a 3D cross-linking of polymer chains; therefore, it has a high application potential in the bioplastic industry. The mechanical properties of lignopolyurethane are significantly influenced by the network crosslinking density, which depends on the molecular weight and hydroxyl content of the lignin macromolecule participating in the crosslinking (Trzebiatowska et al., 2018). Studies involving the synthesis of lignopolyurethane have shown that the higher the lignin content, the higher the density of the crosslink due to the increase in the molar ratio of hydroxy groups, which leads to an increase in tensile strength and a decrease in elongation (Das et al., 2015; Tavares et al., 2016). The thermal properties of polyurethane also depend considerably on the crosslink density. An increase in the crosslink density results in a decrease in the molecular mobility, increasing $T_g$ (Gouveia et al., 2019). In a study in which lignopolyurethane was synthesized using ethanol organosolv lignin (EOL), the $T_g$ increased with the lignin content, and this phenomenon was attributed to an increase in the crosslinking density and rigidity of lignin (Avelino et al., 2018).

The mechanical properties of the lignin macromolecular complex largely depend on the network crosslinking density, and the molecular weight of the lignin macromolecule between crosslinking agents and the number of functional groups contained in its chemical structure are general factors influencing the crosslinking density. The crosslink density tends to be inversely proportional to the molecular weight between crosslinks and directly proportional to the number of lignin functional groups (Flory & Rehner Jr, 1943). Therefore, it is considered that the crosslink density and properties of the lignopolyurethane can be regulated by controlling the properties of the lignin macromolecule.

However, most researches related to lignopolyurethane have focused on controlling the physicochemical properties by simply changing the amount of lignin added or modifying the synthesis method. In addition, lignin exhibits various physicochemical properties due to its complex bonding structures and functional groups, which makes it difficult to predict reactivity and final properties in bioplastic applications. Therefore, it is necessary to predict the crosslinking density of lignopolyurethane according to reactivity derived from lignin structures and to evaluate the thermal and mechanical properties of the final product. In this chapter, thermosetting lignopolyurethane was developed using three types of oxypropylated EOLs having different structural characteristics. The crosslinking density and properties of the prepared lignopolyurethane were evaluated with a focus on the structural characteristics and properties of the EOLs.

# 2. Materials and methods

## 2.1. EOL and oxypropylated EOL preparation

### 2.1.1. Raw materials

The raw material of this study, a jolcham oak (*Quercus serrata*), was described circumstantially in Section 2.1.1 of Chapter 2.

### 2.1.2. Extraction of EOL

Three types of EOLs with different structural characteristics were extracted as described in Section 2.1.2 of Chapter 3. The characteristics of three types of EOL are provided in Table 3-2.

### 2.1.3. Oxypropylation of EOL

The oxypropylation of three types of EOL was conducted as described in Section 2.2.1 of Chapter 3. The extraction and oxypropylation conditions are shown in Table 4-1. Moreover, the characteristics of the oxypropylated EOLs are shown in Table 4-2.

Table 4-1. Extraction and oxypropylation conditions of the oxypropylated EOLs

| | | LL-2 | ML-2 | HL-2 |
|---|---|---|---|---|
| Extraction condition | Reaction temp. (°C) | 140 | 160 | 180 |
| | Reaction time (min) | 5 | 5 | 5 |
| | Sulfuric acid conc. (%) | 0.5 | 1 | 1.5 |
| | Ethanol conc. (%) | 80 | 60 | 40 |
| Oxypropylation condition | Reaction temp. (°C) | 40 | 40 | 40 |
| | Reaction time (h) | 18 | 18 | 18 |
| | Molar ratio (Hydroxyl group:Propylene oxide) | 1:2 | 1:2 | 1:2 |

Table 4-2. The characteristics of the oxypropylated EOLs

| | LL-2 | ML-2 | HL-2 |
|---|---|---|---|
| Molecular weight ($M_n$, Da) | 2416 | 1699 | 1584 |
| Molecular weight ($M_w$, Da) | 9771 | 4495 | 3343 |
| PDI | 4.04 | 2.65 | 2.11 |
| Aliphatic OH (mmol/g) | 4.55 | 2.93 | 2.39 |
| Phenolic OH (mmol/g) | 0.59 | 0.27 | 0.35 |
| Total OH (mmol/g) | 5.14 | 3.20 | 2.74 |
| $T_g$ (°C) | 56.9 | 56.8 | 156.3 |
| Melting point (°C) | 110.6 | 127.5 | - |

## 2.2. Lignopolyurethane preparation

### 2.2.1. Urethane synthesis for lignopolyurethane

The lignopolyurethane was prepared following previously reported procedures (Evtuguin et al., 1998; Saito et al., 2013). The oxypropylated EOLs were adopted as a polyol. The oxypropylated EOLs and polyethylene glycol (PEG) 6000 were dissolved in tetrahydrofuran (THF) at weight ratios (EOL:PEG) of 0:10, 5:5, and 10:0. The mixture was stirred at 60 °C until complete dissolution was achieved. Thereafter, the same amount of hexamethylene diisocyanate (HDI) was added to the solution. After the mixture had stabilized, dibutyltin dilaurate was added as a catalyst. The mixture with all reagents added was reacted at 60 °C. The lignopolyurethane for structural analysis was reacted for 12 h to complete the urethane synthesis of all the EOLs and HDI. After the reaction, the lignopolyurethane was recovered by precipitation in an 80% methanol solution. The obtained lignopolyurethane was washed with 80% methanol and water to remove unreacted reagents, followed by freeze-drying. The lignopolyurethane was named according to the type and content of EOL used. For example, a lignopolyurethane synthesized at a 5:5 weight ratio using oxypropylated LL was named LL-P5, and a lignopolyurethane synthesized at a 10:0 weight ratio using oxypropylated LL was named LL-P10.

### 2.2.2. Lignopolyurethane film preparation

For the lignopolyurethane film preparation, the polyol mixed in weight ratios (EOL:PEG = 0:10, 5:5, 2:8, and 10:0) was reacted with HDI at 60 °C for 1 h to prevent excessive crosslink formation. After the reaction, the reactants were

cast on a stainless-steel weighing dish. The cast lignopolyurethane was dried at 65 °C in an oven for 12 h.

## 2.3. Structural characteristics of lignopolyurethane

### 2.3.1. Elementary analysis of lignopolyurethane

The lignopolyurethane was analyzed using an elemental analyzer (Flash EA 1112, Thermo Electron Corporation, USA) to determine the weight percentages of C, H, N, and O. The oxygen content was evaluated using the difference.

### 2.3.2. FT-IR analysis of lignopolyurethane

The chemical structure and functional groups of lignopolyurethane were determined by Fourier transform infrared (FT-IR) spectroscopy (Nicolet 6700, Thermo Scientific, USA) coupled with attenuated total reflectance (ATR, ATR Acc. (window AnSe/Diamond)). Each experiment was performed with the following parameters: scans, 32; resolution, 8; wavenumber range, 4000–650 $cm^{-1}$.

## 2.4. The properties of lignopolyurethane

### 2.4.1. Thermal properties of lignopolyurethane

The thermal decomposition characteristics of lignopolyurethane were analyzed as described in Section 2.2.2.4 of Chapter 3. Differential scanning calorimetry (DSC) analysis was performed using the same instrument described in Section 2.2.2.4 of Chapter 3, although the analysis conditions were slightly different. The first heating scan was performed in a temperature range of 25–200 °C at a heating rate of 10 °C/min, and this temperature was held for 2 min to exclude the thermal history. Next, the temperature of the furnace was reduced to −25 °C and held for 10 min. For the second heating scan, the temperature was increased from −25 to 350 °C at the same heating rate of the first scan. The $T_g$ and melting temperature of lignopolyurethane were determined using the second heating scan data.

### 2.4.2. Mechanical properties of lignopolyurethane film

The tensile strength and elongation of lignopolyurethane films were determined according to ASTM D638 with a tensile testing machine (Low Force Universal Testing Systems, Intron, USA). The test was performed with a gap between the grips of 20 mm and a constant strain rate of 5 mm/min.

# 3. Results and Discussion

## 3.1. Structural characteristics of lignopolyurethane

### 3.1.1. Urethane synthesis for lignopolyurethane

The polyols used in the synthesis of polyurethanes have different reactivities depending on their structural characteristics, including molecular weight and hydroxyl group content (Li et al., 2015). Figure 4-1 shows the yield of three types of lignopolyurethanes based on the reaction time. The yield of lignopolyurethane of the oxypropylated EOLs was improved as the reaction time increased; however, the pattern of the increase was significantly different depending on the types of EOL. For ML-2 and HL-2, a low yield of less than 20% was observed until a reaction time of 4 h, indicating a low reaction rate. In contrast, LL-2 showed a yield of 70% or more even at a reaction time of 1 h, implying a higher reaction rate than those of the other two EOLs. In particular, HL showed the lowest rate of increase in the yield of lignopolyurethane according to the increase in the reaction time. HL, which is extracted under severe conditions compared to LL and ML, has a low molecular weight and a high proportion of aromatic hydroxyl groups. The oxypropylated HL exhibits a lower molecular weight and lower hydroxyl group content than those of oxypropylated LL and ML. Lignin exhibits low reactivity due to steric hindrance, which is attributed to its complex molecular structure and inter- and intramolecular hydrogen bonds (Duval & Lawoko, 2014). In particular, aromatic hydroxyl groups exhibit significantly lower reactivity compared to aliphatic hydroxyl groups (Alinejad et al., 2019; Evtuguin et al., 1998). In this study, to increase the reactivity of lignin, the functional group of EOL was modified through oxypropylation. After oxypropylation, the aromatic hydroxyl

group of lignin was substituted with a secondary aliphatic hydroxyl group, and the length of the side chain was increased. Consequently, the reactivity was improved in the order of LL-2, ML-2, and HL-2. The chain length and content of a functional group of polyols significantly contribute to the reactivity during polyurethane synthesis (Das et al., 2015; Tavares et al., 2016). Oxypropylated HL has a lower total hydroxyl group content than LL and ML. In particular, considering the relatively low molecular weight of HL, the number of hydroxyl groups per molecule is significantly reduced. Therefore, the amount of oxypropylated HL that can be employed as polyols in urethane synthesis is relatively small, which causes a decrease in the reaction rate.

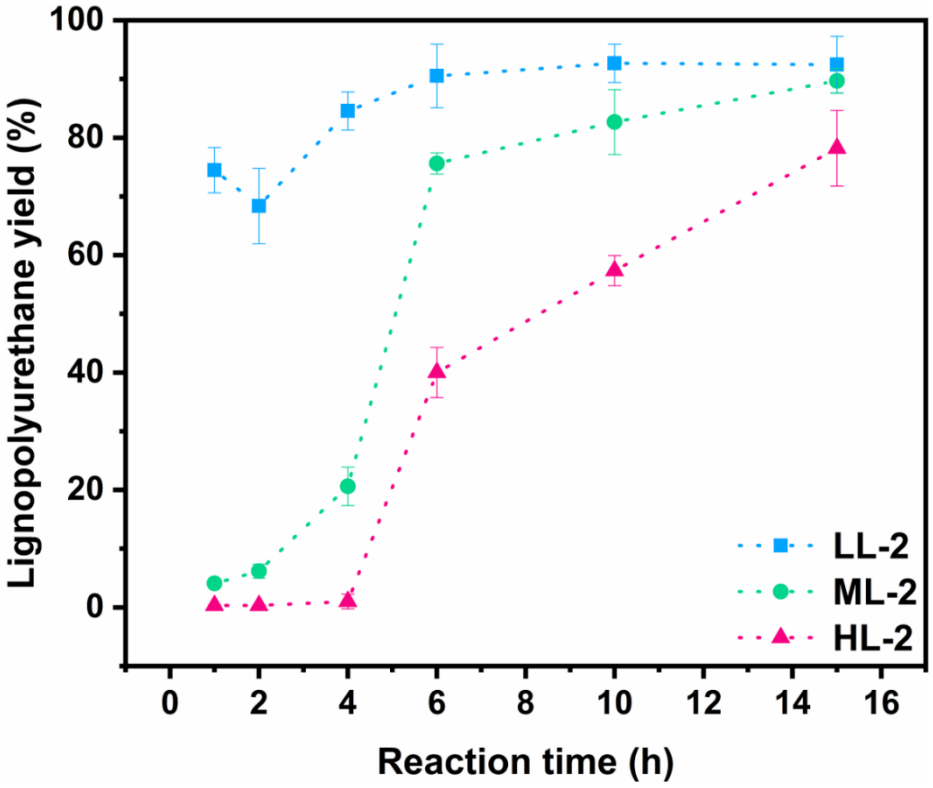


Figure 4-1. The lignopolyurethane yield of the oxypropylated EOLs as a function of the reaction time.

On the other hand, Table 4-3 summarizes the elemental components of three types of initial EOL, oxypropylated EOLs, and lignopolyurethanes. Three polyurethanes were obtained by synthesizing each of the corresponding oxypropylated EOL for 15 h without the addition of PEG 6000. From the elemental analysis results, nitrogen was not detected in the initial EOLs and oxypropylated EOLs, whereas it was detected in all the lignopolyurethanes. This implies that the hydroxyl group of oxypropylated lignin and the isocyanate group of HDI successfully formed a urethane bond.

Table 4-3. The elementary composition of the initial EOLs, oxypropylated EOLs, and lignopolyurethanes

| | N(wt%) | C(wt%) | H(wt%) | O(wt%) |
|---|---|---|---|---|
| LL | 0.05 | 58.55 | 6.09 | 35.31 |
| LL-2 | 0.00 | 60.88 | 6.67 | 32.45 |
| LL-P10 | 4.13 | 59.85 | 6.96 | 29.06 |
| ML | 0.08 | 60.06 | 5.51 | 34.35 |
| ML-2 | 0.01 | 61.82 | 6.42 | 31.75 |
| ML-P10 | 4.40 | 59.96 | 6.79 | 28.84 |
| HL | 0.02 | 60.02 | 4.96 | 35.00 |
| HL-2 | 0.00 | 61.06 | 6.11 | 32.82 |
| HL-P10 | 4.45 | 61.29 | 6.71 | 27.55 |

### 3.1.2. FT-IR analysis of lignopolyurethane

The coupling structure of the lignopolyurethanes synthesized using three types of oxypropylated EOL was investigated using FT-IR analysis. In polyurethane synthesis, the hydroxyl group of lignin reacts with the isocyanate group of HDI to form a urethane linkage (–RNHCOOR'–), which increases the intensity of the band corresponding to the carbonyl group and the secondary amide in the FT-IR spectra of lignin. Figure 4-2 shows the FT-IR spectra of the initial EOLs, oxypropylated EOLs, and lignopolyurethanes with 5:5 and 10:0 weight ratios (oxypropylated EOL:PEG) in the range of 1000–2000 $cm^{-1}$. The characteristic bands of lignopolyurethane are present in the spectra. In the FT-IR spectra, the 1700 $cm^{-1}$ band is assigned to the carbonyl group (C=O), and the band between 1550 and 1580 $cm^{-1}$ is assigned to the secondary amide (C–N).

In the FT-IR spectra of the lignopolyurethanes derived from the oxypropylated EOL, the strength of the band representing the carbonyl group was remarkably increased, and the intensity of the band tended to increase as the weight ratio of the lignin contained in lignopolyurethane increased. The increase in the intensity of the carbonyl group band indicates a high crosslinking density. The crosslinking density of polyurethane significantly depends on the molecular weight and hydroxyl content of the lignin macromolecule participating in the crosslinking. The oxypropylated EOLs have a higher proportion of polyols with a higher hydroxyl group content per molecule than those of PEG 6000. Therefore, the intensity of the 1700 $cm^{-1}$ band of lignopolyurethane prepared using only the oxypropylated EOL was higher than that of the lignopolyurethane prepared with a 5:5 ratio. Conversely, in the FT-IR spectra of the lignopolyurethane prepared using three types of oxypropylated EOLs, no significant difference was observed, which is consistent with the previous elemental analysis results.

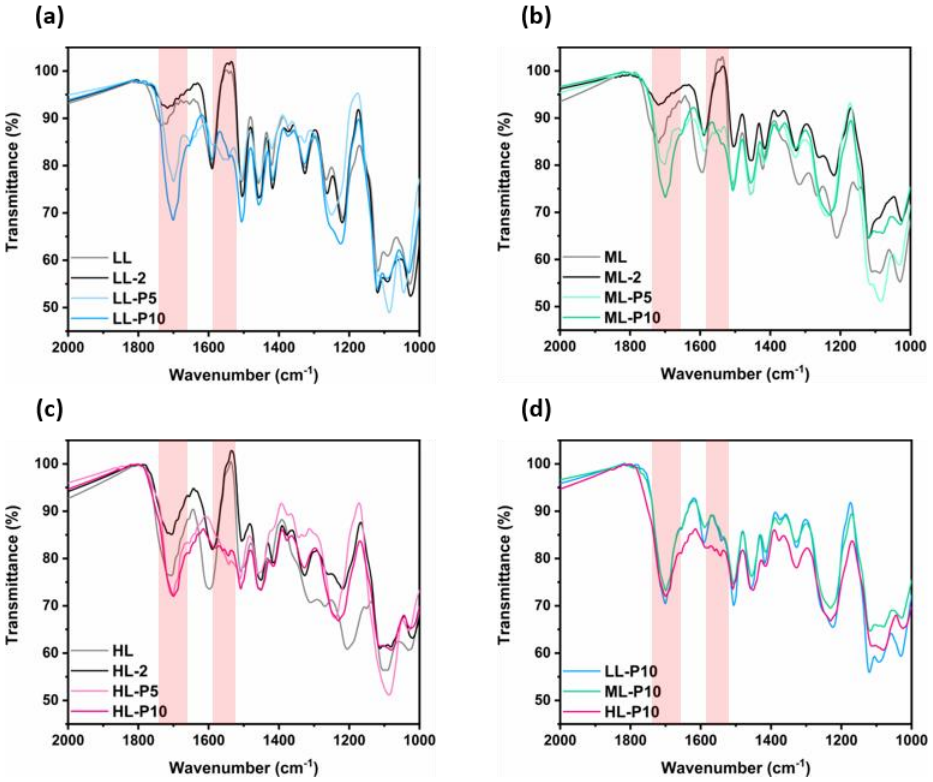


Figure 4-2. The representative FT-IR spectra of the initial EOLs, oxypropylated EOLs, and lignopolyurethanes with 5:5 and 10:0 weight ratios between the oxypropylated EOL and PEG 6000. (a) FT-IR spectra of LL. (b) FT-IR spectra of ML. (c) FT-IR spectra of HL. (d) FT-IR spectra of lignopolyurethanes with a 10:0 weight ratio (oxypropylated EOL:PEG 6000).

## 3.2. Properties of lignopolyurethane

### 3.2.1. TGA of lignopolyurethane

The thermal decomposition behavior of lignopolyurethanes is shown in Figure 4-3. The thermal decomposition behaviors of the initial EOLs, oxypropylated EOLs, and lignopolyurethanes are considerably different. The initial EOL tends to have a lower initial decomposition temperature and a high char yield than those of the oxypropylated EOL and lignopolyurethane. The oxypropylated EOL exhibits a higher thermal stability than that of the initial EOL at around 200 °C, which is the decomposition initiation temperature of the initial EOL, and shows a rapid weight loss after 400 °C.

Contrarily, lignopolyurethane showed a higher thermal decomposition initiation point compared to those of the unmodified EOL and oxypropylated EOL. In the lignopolyurethane synthesis, the hydroxyl groups of the oxypropylated EOL are consumed while forming urethane linkages with the isocyanate functional group. The hydroxyl group is known to have low thermal stability, and the decrease in the amount of hydroxyl group in the molecule increases the thermal stability at low temperatures (Li et al., 2014). Over 400 °C in the TGA curve, the difference according to the lignin content of lignopolyurethane can be clearly observed. It is evident that the higher the content of lignin in lignopolyurethane, the lower the rate of thermal decomposition over 400 °C. This implies that the lignin-derived polyurethane decomposes more slowly at high temperatures than the PEG-derived polyurethane. The PEG structure consists of ethylene glycol units repeatedly connected to ether bonds, and ether bonds have poor heat resistance compared to carbon–carbon bonds. Therefore, PEG-derived polyurethane has a higher

ether bond ratio than lignin-derived polyurethane, which causes a rapid weight reduction at high temperatures.

Figure 4-3(d) shows the TGA curve of the lignopolyurethane prepared using only three types of oxypropylated EOL without adding PEG. Three types of lignopolyurethane exhibited almost similar thermal decomposition behaviors over the entire temperature range; however, slight differences were observed over 400 °C. At high temperatures, the HL-derived polyurethane showed the lowest weight loss rate, while the LL-derived polyurethane showed the highest weight loss rate. HL has the most condensed structure among three types of initial EOL, and the thermal decomposition rate at high temperatures is relatively low compared to those of the others. Therefore, the thermal properties of lignopolyurethane depend on the thermal properties of each initial lignin.

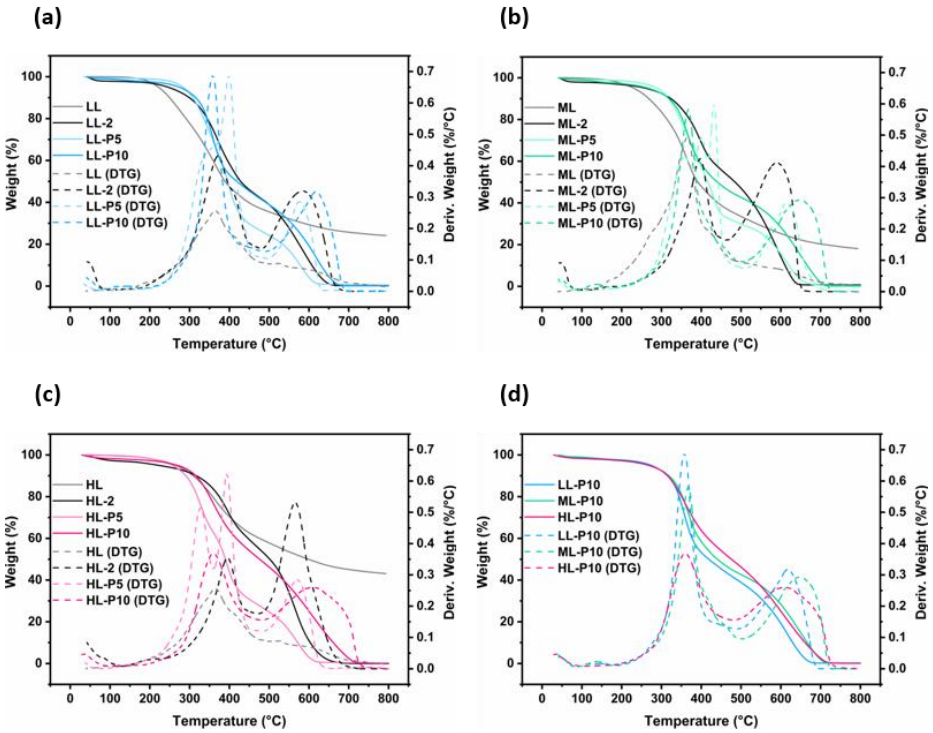


Figure 4-3. The representative TGA curve of the initial EOLs, oxypropylated EOLs, and lignopolyurethanes with 5:5 and 10:0 weight ratios, between the oxypropylated EOL and PEG 6000. (a) TGA curve of the LL and LL derivatives. (b) TGA curve of the ML and ML derivatives. (c) TGA curve of the HL and HL derivatives. (d) TGA curve of the lignopolyurethanes with a 10:0 weight ratio (oxypropylated EOL:PEG 6000).

### 3.2.2. DSC analysis of lignopolyurethane depending on its structural characteristics

Figure 4-4 exhibits the DSC curve of the initial EOLs, oxypropylated EOLs, and lignopolyurethanes with 5:5 and 10:0 weight ratios between the oxypropylated EOL and PEG 6000. Three types of initial EOL, which have different structural characteristics derived from different extraction conditions, showed different $T_g$ values. HL, extracted under the harshest conditions, showed the highest $T_g$, while LL, extracted under the mildest conditions, showed the lowest $T_g$. After the oxypropylation, the oxypropylated LL and ML showed a $T_g$ of less than 60 °C, due to an increase in the fluidity caused by an increase in the aliphatic side-chain length; however, no distinct $T_g$ was observed for HL. In contrast, for lignopolyurethane, $T_g$ was not observed in three types of polyurethane synthesized by mixing the oxypropylated EOL and PEG 6000 in equal proportions, whereas $T_g$ was observed in three types of polyurethane formed using only oxypropylated EOL. Three types of lignopolyurethane formed using only the oxypropylated lignin showed high $T_g$ values similar to those of the corresponding initial EOL. The formation of urethane linkages decreases molecular mobility and leads to increased stiffness and glassiness of the lignin macromolecular complex (Rials & Glasser, 1984; Yoshida et al., 1990).

In contrast, three types of lignopolyurethane showed different $T_g$ values. HL-P10 showed the highest $T_g$ (181.6 °C), while LL-P10 (149.0 °C) had the lowest $T_g$. In general, the thermal properties of polyurethane also depend considerably on the crosslink density. An increase in the crosslink density results in a decrease in the molecular mobility, increasing $T_g$ (Gouveia et al., 2019). The molecular weight of the lignin macromolecule between crosslinking agents and the number of functional groups contained in its chemical structure are general

factors influencing the crosslinking density. However, the elemental analysis of the oxypropylated EOLs revealed that there was no significant difference in the nitrogen content; thus, it is considered that they have similar crosslinking densities (Table 4-3). The relatively high hydroxyl content of LL-2 contributed to the high crosslink density, and the low average molecular weight of the oxypropylated HL led to an increase in the crosslink density during the urethane synthesis. Therefore, the high $T_g$ of the HL-derived polyurethane is due to the condensed structure of the initial HL.

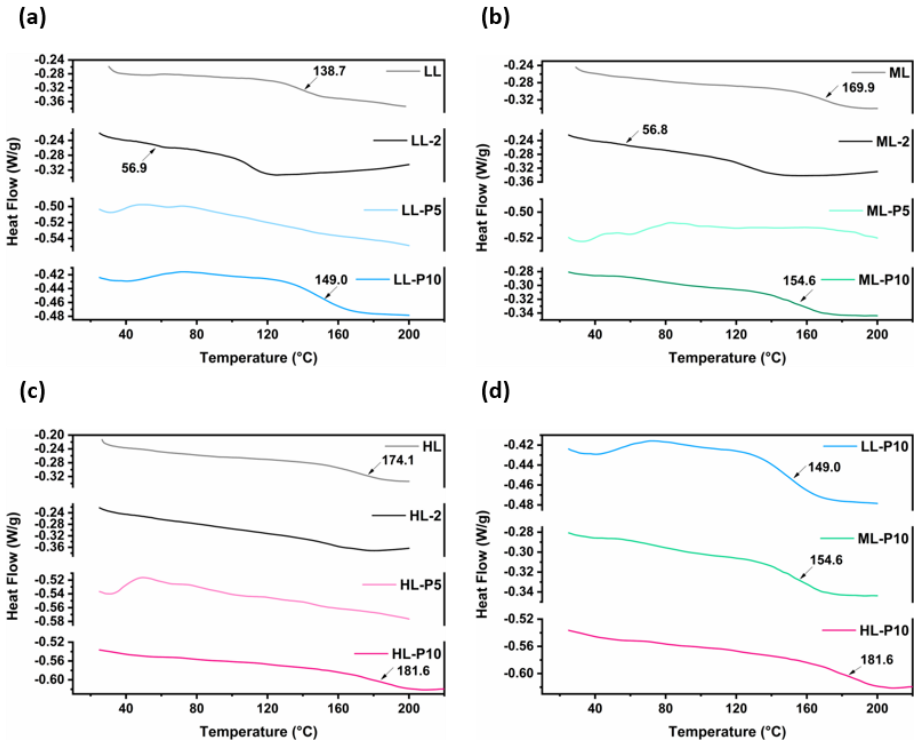


Figure 4-4. The representative DSC curve of the initial EOLs, oxypropylated EOLs, and lignopolyurethanes with 5:5 and 10:0 weight ratios between the oxypropylated EOL and PEG 6000. (a) DSC curve of the LL and LL derivatives. (b) DSC curve of the ML and ML derivatives. (c) DSC curve of the HL and HL derivatives. (d) DSC curve of the lignopolyurethanes with a 10:0 weight ratio (oxypropylated EOL:PEG 6000).

## 3.3. Lignopolyurethane film

### 3.3.1. Crosslinking density of lignopolyurethane film

Figure 4-5 shows the FT-IR spectroscopy of HDI, oxypropylated EOLs, and lignopolyurethane film. In the FT-IR spectrum of HDI, the distinct C=N=O stretch band of isocyanate was observed in the range of 2200 to 2300 $cm^{-1}$ (Ederer et al., 2017). On the other hand, in the oxypropylated EOL, a band at 2200 to 2300 $cm^{-1}$ was not observed, but a broad band due to a hydroxyl group was observed. During the manufacturing process of lignopolyurethane, the intensity of the C=N=O stretch band observed in the HDI spectra is decreased, attributed to the consumption for the urethane reaction. In the FT-IR spectra of lignopolyurethane, the intensity of the C=N=O stretch band depends on the content of unreacted HDI.

Among three types of lignopolyurethane, the intensities of the C=N=O stretch band differed depending on the types of oxypropylated EOL. ML-P10 showed the lowest intensity band, and HL-P10 showed the highest intensity band in the range of 2200–2300 $cm^{-1}$. This implies that the lignopolyurethane film derived from oxypropylated ML has the highest crosslinking density. In general, the crosslink density tends to be inversely proportional to the molecular weight between crosslinks (Flory & Rehner Jr, 1943). However, although the oxypropylated HL has a significantly lower molecular weight than those of the other two oxypropylated EOLs, HL-P10 has the lowest crosslink density. This is probably because it has the lowest average hydroxyl group content per molecule, resulting in low reactivity.

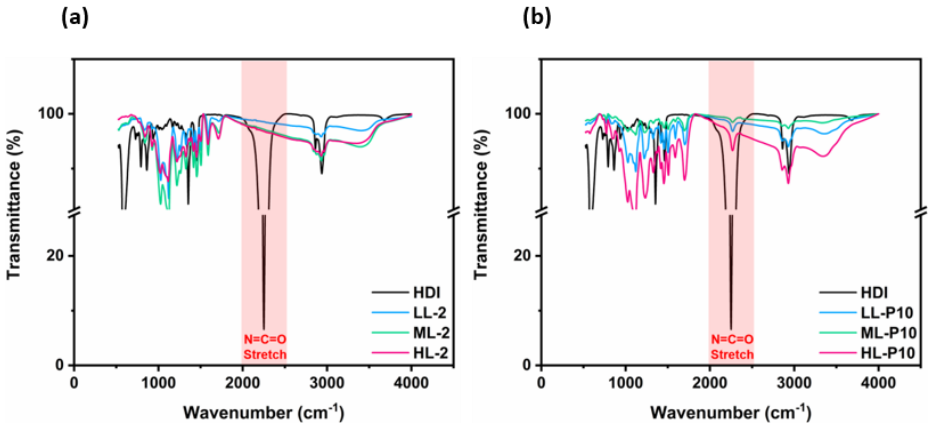


Figure 4-5. The representative FT-IR spectra of HDI, the oxypropylated EOLs, and the lignopolyurethane films. (a) FT-IR spectra of HDI and the oxypropylated EOLs. (b) FT-IR spectra of HDI and the lignopolyurethane films.

### 3.3.2. Mechanical properties of the lignopolyurethane film

Figure 4-6 shows the picture of the lignopolyurethane film and the representative stress–strain curve of the PEG 6000-derived polyurethane film and lignopolyurethane with 5:5, 8:2, and 10:0 weight ratios between the oxypropylated EOL and PEG 6000. The PEG 6000-derived polyurethane film exhibited a prominent elongation. Conversely, the lignopolyurethane with a 10:0 weight ratio between the oxypropylated EOL and PEG 6000 showed poor elongation and improved tensile strength. Lignin macromolecules have a complex 3D network structure with various intermolecular linkages, formed by enzymatic radical coupling polymerization (Boerjan et al., 2003). In addition, lignin has condensed rigid phenolic moieties and a high frequency of intermolecular hydrogen bond interactions (Irvine, 1985). These properties limit the mobility of lignin and impart brittleness. Furthermore, the mechanical properties of lignopolyurethane significantly depend on the network crosslinking density. The lignin macromolecule is a polyol containing two or more hydroxyl groups, which makes the crosslinking density of the lignin-derived polyurethane higher than that of the PEG 6000-derived polyurethane. According to studies involving the synthesis of lignopolyurethane, the higher the lignin content in the lignopolyurethane, the higher the density of the crosslink, due to the increase in the molar ratio of hydroxy groups, which leads to an increase in tensile strength and a decrease in elongation (Das et al., 2015; Tavares et al., 2016). Therefore, lignin-derived polyurethane exhibits higher brittleness than PEG 6000-derived polyurethane.

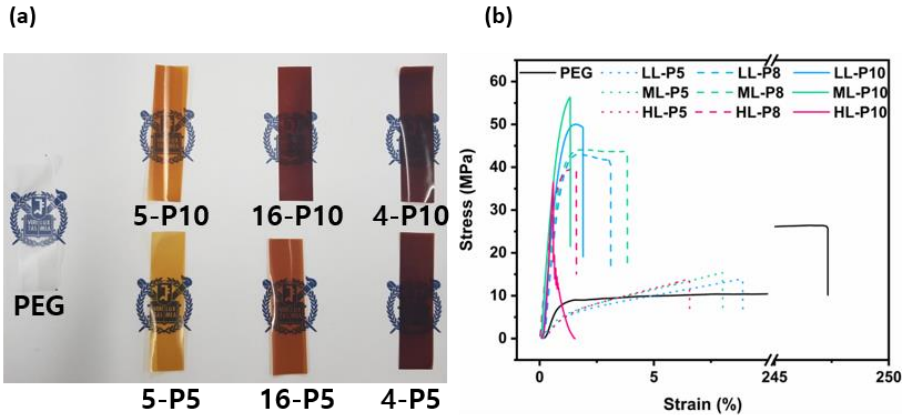


Figure 4-6. Picture of the lignopolyurethane film and the representative stress–strain curve of the PEG 6000-derived polyurethane film and lignopolyurethane with 5:5, 8:2, and 10:0 weight ratios between the oxypropylated EOL and PEG 6000. (a) Picture of the lignopolyurethane film. (b) Representative stress–strain curve of the PEG 6000-derived polyurethane film and lignopolyurethane.

Meanwhile, the tensile strength of the lignopolyurethane film with a 5:5 weight ratio between the oxypropylated EOL and PEG 6000 was lower than that of the lignopolyurethane film with a 10:0 weight ratio; however, the elongation was higher. In the lignopolyurethane film, the high ductility of PEG 6000 contributed to the brittleness relaxation (Wang et al., 2019). However, the decrease in the portion of the rigid structure of EOL and the amount of the crosslinking density due to the addition of PEG caused a decrease in the tensile strength. In addition, the non-uniform mixture of soft-segment heterogeneous polymers prevented the rearrangement of each polymer during elongation, resulting in severe strength reduction. The tensile strength of lignopolyurethane increased with increasing EOL content, while the elongation decreased with increasing lignin content.

Among three types of lignopolyurethane film, the LL and ML-derived lignopolyurethane films showed outstanding mechanical strengths with 5:5, 8:2, and 10:0 weight ratios, whereas the HL-derived lignopolyurethane exhibited poor mechanical strength (Figure 4-7). This phenomenon is more pronounced in the tensile strength results of the lignopolyurethane synthesized at a 10:0 weight ratio. The tensile strengths of LL-P10, ML-P10, and HL-P10 are 52.5, 56.5, and 36.5 MPa, respectively. HL has a low molecular weight and a highly condensed structure. These characteristics of the initial HL contribute to the brittleness of the HL-derived lignopolyurethane. In addition, HL has a low reactivity due to its low content of hydroxyl groups per molecule, resulting in the low crosslink density (Figure 4-5). This accounts for the poor mechanical properties of the HL-derived lignopolyurethane film. Contrarily, LL and ML have a high molecular weight and a less condensed structure. These characteristics of the initial EOLs contribute to the low brittleness of lignopolyurethane. The high reactivity due to the numerous hydroxyl groups per molecule contributed to the crosslinking density of lignopolyurethane, which resulted in a high tensile strength. In particular, LL-P10 and ML-P10

exhibited higher tensile strengths than those of the lignopolyurethane films in previous studies (4, 27.6, and 41.6 MPa) prepared using only lignin-derived precursors without the addition of other plasticizers (Jia et al., 2015; Saito et al., 2013; Wang et al., 2019). This indicates that it is possible to develop a high-strength lignopolyurethane film with a high bio-based content by controlling the structural characteristics of lignin according to the extraction conditions. Thus, the structural characteristics of the EOL used as a polyol have a significant effect on the mechanical properties of lignopolyurethane.

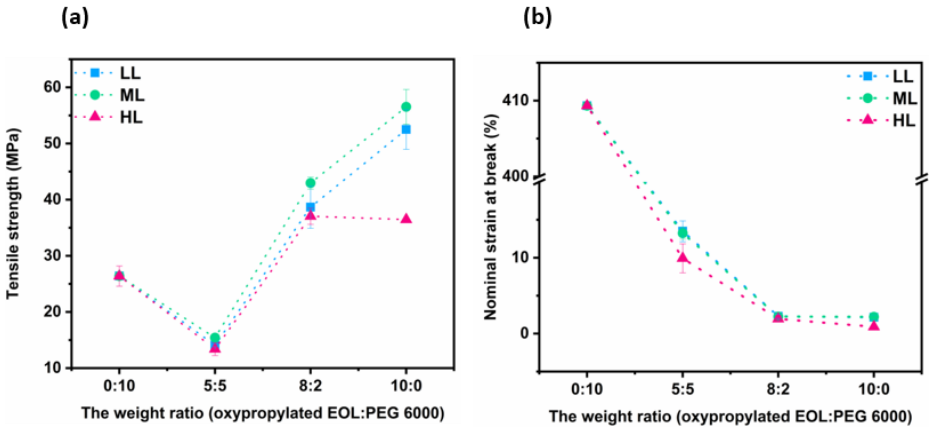


Figure 4-7. Tensile strength and elongation of the PEG 6000-derived polyurethane film and lignopolyurethane with 5:5 and 10:0 weight ratios between the oxypropylated EOL and PEG 6000. (a) Tensile strength of the lignopolyurethane film. (b) Elongation of the lignopolyurethane film.

# 4. Summary

In this chapter, lignopolyurethanes with different thermal and mechanical properties were developed depending on the types of EOL. The oxypropylated EOLs, which are extracted under different conditions, and PEG 6000 were used as the polyol for lignopolyurethane synthesis. The structural characteristics of lignopolyurethane highly depend on the structure of the oxypropylated EOL. The hydroxyl group distribution of the oxypropylated EOL influences the reaction rate of lignopolyurethane synthesis. The oxypropylated HL exhibits a lower molecular weight and lower hydroxyl group content than those of the oxypropylated LL and ML. The lignopolyurethane formed with the oxypropylated HL showed a low yield of less than 20% until a reaction time of 4 h, indicating the low reaction rate. Contrarily, the lignopolyurethane formed with oxypropylated LL showed a yield of 70% or more within 1 h, indicating the high reaction rate.

On the other hand, the physicochemical properties of lignopolyurethane differ depending on the types of oxypropylated EOL. All the types of lignopolyurethanes have increased thermal stability at low temperatures compared to those of the corresponding oxypropylated EOLs. However, at high temperatures, the thermal properties of lignopolyurethane depend on the thermal properties of the corresponding initial EOLs. In addition, the structural characteristics of the EOL used as a polyol have a significant effect on the crosslinking density of the lignopolyurethane film. The EOL with a low average hydroxyl content per molecule afforded a lignopolyurethane film with a low crosslink density due to its low reactivity.

The crosslinking density of the lignopolyurethane film impacts its mechanical properties. The ML and LL-derived lignopolyurethanes with high crosslinking densities exhibited competent mechanical strengths, whereas the

HL-derived lignopolyurethane with a low crosslinking density showed poor mechanical properties. In particular, LL-P10 and ML-P10 exhibited higher tensile strengths (52.5 and 56.5 MPa) than those of the lignopolyurethane films in previous studies (4, 27.6, and 41.6 MPa), implying the possibility of a high-strength lignopolyurethane film with a high bio-based content. Therefore, even if the lignin is chemically modified under the same conditions, the structural characteristics and properties of the lignopolyurethane would vary depending on the structural characteristics of the raw lignin.

# *Chapter 5*

Concluding remarks

As a bioplastic material, lignin, a naturally occurring polymer, has a high potential to overcome the drawbacks of biodegradable plastics, such as poor thermal or mechanical properties and low price-competitiveness. However, there are several obstacles to the utilization of lignin as a bioplastic material. First, lignin has unpredictable and non-uniform properties attributed to the diversity of its structural characteristics. Second, lignin exhibits poor compatibility with most thermoplastic biopolyesters because it has relatively polar surface characteristics, derived from the numerous hydroxyl groups in the molecular structure. Third, lignin has a low reactivity, derived from the lack of active sites and the steric hindrance caused by the high degree of substitution, which hinders the chemical modification of lignin into thermosetting plastic materials. Fourth, lignin has a rigid structure and undesirable properties, which reduces its processability. This study investigated the applicability of lignin as a bioplastic material by understanding the correlation between the structural characteristics and physicochemical properties of lignin. In addition, the application potential of lignin as a bioplastic material was improved by enhancing its thermoplastic or thermosetting properties through chemical modification.

To modulate the properties of lignin for commercial utilization, a systematic understanding of the correlation among the extraction conditions, structural characteristics, and properties is indispensable. The effect of the extraction conditions on the structural characteristics of EOL was investigated by response surface methodology (RSM). The structural characteristics of EOL (molecular weight, hydroxyl content, and intramolecular coupling structure) were significantly affected by the extraction conditions (temperature, sulfuric acid concentration, and ethanol concentration). Under the conditions set for the RSM analysis, as the severity of the extraction conditions increased, the EOL with low molecular weight, low PDI, and high phenolic hydroxyl content tended to be obtained. The correlation between the structural characteristics of

the EOL and the severity of the extraction conditions was confirmed by introducing the CSF value, and a clear correlation was derived.

In addition, the structural characteristics of the EOL derived from different extraction conditions influenced its thermal properties. The relevant correlations between the structural characteristics and thermal properties of EOL were determined. In particular, EOLs that had a low molecular weight, high phenolic hydroxyl content, and low aryl ether linkage content exhibited prominent thermal properties in terms of their initial decomposition rate and high $T_g$. For the prediction of the weight loss rate of EOL at 300 °C, the regression model with a reliable R-square value (0.837) was suggested. According to the p-values of each independent variable, the $M_w$ (0.009) was the most important variable, and the aliphatic hydroxyl content (0.676) was found to be the least important variable for the weight loss rate at 300 °C. Based on the regression model, the lower the molecular weight of the EOL extracted from the same biomass by EO extraction, the lower the rate of its thermal degradation.

Correspondingly, EOL–PLA bioplastics prepared using three EOL types exhibited improved thermal properties (starting point of thermal decomposition and maximum decomposition temperature) compared to that of the neat PLA and exhibited thermal decomposition behaviors coincident with the thermal properties of the constituent EOLs. Conversely, the mechanical properties of the EOL–PLA bioplastics differed depending on the types of EOL. The tensile strength of the EOL–PLA bioplastics showed a tendency to decrease as the content of lignin in the thermo-bioplastics increased, whereas the nominal strain at the break of the EOL–PLA bioplastics exhibited a different tendency depending on the types of EOL.

To ensure the commercial utilization of lignin as a thermoplastic material, the chemical modification should be performed to improve its compatibility with thermoplastic biopolyester. The effect of oxypropylation on the compatibility with PLA depending on the structural characteristics of EOL was

investigated. Three types of EOLs having different structural characteristics were obtained by controlling the severity of the extraction condition. Three types of EOL were modified in various molar ratios of the hydroxyl groups of lignin to PO. The structural characteristics of the oxypropylated EOLs was highly dependent on the types of the initial EOL. In the oxypropylation, the DS and DP of the propyl side chain highly depended on the distribution of the hydroxyl groups of the initial lignin. HL with a high aromatic hydroxyl group content exhibited a high DS, while LL with a high aliphatic hydroxyl group content showed a high DP under the same oxypropylation condition. The oxypropylated EOLs exhibited different thermal properties depending on their structural characteristics.

After the oxypropylation, a new $T_g$ between 55 and 60 °C was observed for the oxypropylated LL and ML. In addition, melting was observed according to the types of oxypropylated EOL, which improved the thermoplasticity. The thermal properties of the oxypropylated EOLs influenced the thermal and mechanical properties of the EOL–PLA bioplastics. The introduction of side chains accelerated the thermal decomposition of the oxypropylated EOL–PLA bioplastics by decreasing the relative proportion of aromatic moieties in the structure.

However, the compatibility of EOL with PLA was successfully improved by oxypropylation. In particular, the oxypropylated LL and ML exhibited improved thermoplasticity and compatibility with PLA, resulting in the slick and flat surface structure observed in the thermo-bioplastics. The increased compatibility of EOL with PLA induced the improvement of the tensile strength of the oxypropylated EOL–PLA bioplastic to a similar level to that of the neat PLA, and the nominal strain was improved to a higher level than that of the neat PLA. In addition, the $T_g$ of the EOL–PLA bioplastic was increased compared to that of the neat PLA in a thermodynamic perspective, implying the improved mechanical properties of the oxypropylated EOL–PLA bioplastic at

temperatures above the $T_g$ of the neat PLA. The $T_g$ of PLA (74.6 °C) increased to 77.8 (LL-5), 77.7 (ML-5), and 75.5 (HL-5), by blending with unmodified EOLs, and it further increased upon blending with oxypropylated EOLs. Therefore, the physicochemical properties of the EOL–PLA bioplastic were improved by successfully enhancing the compatibility with PLA and thermoplasticity of EOL through oxypropylation. Moreover, the thermoplasticity and compatibility with PLA were found to be significantly influenced not only by the DP of the side chains but also by the lignin structure.

To develop lignopolyurethane with different thermal and mechanical properties, the oxypropylated EOLs, which are extracted under different conditions, and PEG 6000 were used as the polyol for lignopolyurethane synthesis. The mechanical properties of the lignopolyurethane were significantly influenced by the network crosslinking density, which depends on the molecular weight and hydroxyl content of the lignin macromolecule participating in the crosslinking. The structure of lignopolyurethane highly depended on the structural characteristics of the oxypropylated EOL. The hydroxyl group distribution of the oxypropylated EOL influenced the reaction rate of the lignopolyurethane synthesis.

On the other hand, the physicochemical properties of lignopolyurethane differed depending on the types of oxypropylated EOL. All the different types of lignopolyurethanes exhibited increased thermal stability at low temperatures compared to those of the corresponding oxypropylated EOLs. However, at high temperatures, the thermal properties of lignopolyurethane relied on the thermal properties of the corresponding initial EOLs. In addition, the structural characteristics of the EOL used as a polyol had a significant effect on the crosslinking density of the lignopolyurethane film. The EOL with a low average hydroxyl content per molecule led to a lignopolyurethane film with a low crosslink density, due to its low reactivity. The crosslinking density of the lignopolyurethane film influenced its mechanical properties. The ML and LL-

derived lignopolyurethanes exhibited outstanding mechanical strength, whereas the HL-derived lignopolyurethane showed poor mechanical properties. In particular, the tensile strengths of LL-P10 (52.5 MPa) and ML-P10 (56.5 MPa) were higher than those of the lignopolyurethane films in previous studies (4, 27.6, and 41.6 MPa), prepared using only lignin-derived precursors without the addition of other plasticizers.

To sum up, the structural characteristics of lignin was highly dependent on the extraction conditions, and the thermal properties of lignin could be predicted to some extent by controlling its structural characteristics. This implies that different properties can be conferred within the thermo-bioplastic by controlling the lignin structure. In addition, the compatibility and thermoplasticity of lignin can be improved by oxypropylation, and the properties of the oxypropylated lignin significantly depend on the structural characteristics of the initial lignin. Furthermore, the reactivity characteristics and properties of lignopolyurethane can be regulated depending on the structural characteristics of the lignin macromolecule. The properties of the lignopolyurethane film are significantly influenced by the network crosslinking density, which depends on the EOL structure participating in the crosslinking.

# *References*

Ahmed, J., Zhang, J.-X., Song, Z., Varshney, S. 2009. Thermal properties of polylactides. *Journal of Thermal Analysis and Calorimetry*, **95**(3), 957-964.

Alinejad, M., Henry, C., Nikafshar, S., Gondaliya, A., Bagheri, S., Chen, N., Singh, S.K., Hodge, D.B., Nejad, M. 2019. Lignin-based polyurethanes: opportunities for bio-based foams, elastomers, coatings and adhesives. *Polymers*, **11**(7), 1202.

Alonso, M., Oliet, M., Rodriguez, F., Astarloa, G., Echeverría, J. 2004. Use of a methylolated softwood ammonium lignosulfonate as partial substitute of phenol in resol resins manufacture. *Journal of Applied Polymer Science*, **94**(2), 643-650.

Amiri, M.T., Bertella, S., Questell-Santiago, Y.M., Luterbacher, J.S. 2019. Establishing lignin structure-upgradeability relationships using quantitative 1 H–13 C heteronuclear single quantum coherence nuclear magnetic resonance (HSQC-NMR) spectroscopy. *Chemical science*, **10**(35), 8135-8142.

Anwer, M.A., Naguib, H.E., Celzard, A., Fierro, V. 2015. Comparison of the thermal, dynamic mechanical and morphological properties of PLA-Lignin & PLA-Tannin particulate green composites. *Composites Part B: Engineering*, **82**, 92-99.

Auras, R.A., Lim, L.-T., Selke, S.E., Tsuji, H. 2011. *Poly (lactic acid): synthesis, structures, properties, processing, and applications*. John Wiley & Sons.

Avelino, F., Almeida, S.L., Duarte, E.B., Sousa, J.R., Mazzetto, S.E., de Souza, M.d.S.M. 2018. Thermal and mechanical properties of coconut shell lignin-based polyurethanes synthesized by solvent-free polymerization. *Journal of Materials Science*, **53**(2), 1470-1486.

Baeurle, S.A., Hotta, A., Gusev, A.A. 2006. On the glassy state of multiphase and pure polymer materials. *Polymer*, **47**(17), 6243-6253.

Baumberger, S., Abaecherli, A., Fasching, M., Gellerstedt, G., Gosselink, R., Hortling, B., Li, J., Saake, B., de Jong, E. 2007. Molar mass determination of lignins by size-exclusion chromatography: towards standardisation of the method. *Holzforschung*, **61**(4), 459-468.

Baumberger, S., Dole, P., Lapierre, C. 2002. Using transgenic poplars to

elucidate the relationship between the structure and the thermal properties of lignins. *Journal of agricultural and food chemistry*, **50**(8), 2450-2453.

Boerjan, W., Ralph, J., Baucher, M. 2003. Lignin biosynthesis. *Annual review of plant biology*, **54**(1), 519-546.

Braaten, S.M., Christensen, B.E., Fredheim, G.E. 2003. Comparison of molecular weight and molecular weight distributions of softwood and hardwood lignosulfonates. *Journal of wood chemistry and technology*, **23**(2), 197-215.

Brodin, I., Sjöholm, E., Gellerstedt, G. 2010. The behavior of kraft lignin during thermal treatment. *Journal of Analytical and Applied Pyrolysis*, **87**(1), 70-77.

Calvo-Flores, F.G., Dobado, J.A. 2010. Lignin as renewable raw material. *ChemSusChem*, **3**(11), 1227-1235.

Cateto, C.A., Barreiro, M.F., Ottati, C., Lopretti, M., Rodrigues, A.E., Belgacem, M.N. 2014. Lignin-based rigid polyurethane foams with improved biodegradation. *Journal of Cellular Plastics*, **50**(1), 81-95.

Cateto, C.A., Barreiro, M.F., Rodrigues, A.E., Belgacem, M.N. 2009. Optimization study of lignin oxypropylation in view of the preparation of polyurethane rigid foams. *Industrial & Engineering Chemistry Research*, **48**(5), 2583-2589.

Chakar, F.S., Ragauskas, A.J. 2004. Review of current and future softwood kraft lignin process chemistry. *Industrial crops and products*, **20**(2), 131-141.

Chanprateep, S. 2010. Current trends in biodegradable polyhydroxyalkanoates. *Journal of bioscience and bioengineering*, **110**(6), 621-632.

Chen, M.-J., Gunnells, D., Gardner, D.J., Milstein, O., Gersonde, R., Feine, H., Hüttermann, A., Frund, R., Lüdemann, H., Meister, J.J. 1996. Graft copolymers of lignin with 1-ethenylbenzene. 2. Properties. *Macromolecules*, **29**(5), 1389-1398.

Chum, H., Johnson, D., Black, S., Baker, J., Grohmann, K., Sarkanen, K., Wallace, K., Schroeder, H. 1988. Organosolv pretreatment for enzymatic hydrolysis of poplars: I. Enzyme hydrolysis of cellulosic

residues. *Biotechnology and bioengineering*, **31**(7), 643-649.

Chung, Y.-L., Olsson, J.V., Li, R.J., Frank, C.W., Waymouth, R.M., Billington, S.L., Sattely, E.S. 2013. A renewable lignin–lactide copolymer and application in biobased composites. *ACS Sustainable Chemistry & Engineering*, **1**(10), 1231-1238.

Collins, M.N., Nechifor, M., Tanasă, F., Zănoagă, M., McLoughlin, A., Stróżyk, M.A., Culebras, M., Teacă, C.-A. 2019a. Valorization of lignin in polymer and composite systems for advanced engineering applications–a review. *International journal of biological macromolecules*, **131**, 828-849.

Collins, M.N., Nechifor, M., Tanasă, F., Zănoagă, M., McLoughlin, A., Stróżyk, M.A., Culebras, M., Teacă, C.-A. 2019b. Valorization of lignin in polymer and composite systems for advanced engineering applications–a review. *International journal of biological macromolecules*.

Constant, S., Wienk, H.L., Frissen, A.E., de Peinder, P., Boelens, R., Van Es, D.S., Grisel, R.J., Weckhuysen, B.M., Huijgen, W.J., Gosselink, R.J. 2016. New insights into the structure and composition of technical lignins: a comparative characterisation study. *Green Chemistry*, **18**(9), 2651-2665.

Cui, C., Sadeghifar, H., Sen, S., Argyropoulos, D.S. 2013. Toward thermoplastic lignin polymers; part II: thermal & polymer characteristics of kraft lignin & derivatives. *BioResources*, **8**(1), 864-886.

Das, S., Pandey, P., Mohanty, S., Nayak, S.K. 2015. Influence of NCO/OH and transesterified castor oil on the structure and properties of polyurethane: Synthesis and characterization. *Materials Express*, **5**(5), 377-389.

Demuner, I.F., Colodette, J.L., Demuner, A.J., Jardim, C.M. 2019. Biorefinery Review: Wide-Reaching Products Through Kraft Lignin. *BioResources*, **14**(3), 7543-7581.

Ding, Z., Qiu, X., Fang, Z., Yang, D. 2018. Effect of molecular weight on the reactivity and dispersibility of sulfomethylated alkali lignin modified by horseradish peroxidase. *ACS Sustainable Chemistry & Engineering*, **6**(11), 14197-14202.

Domenek, S., Louaifi, A., Guinault, A., Baumberger, S. 2013. Potential of lignins as antioxidant additive in active biodegradable packaging materials. *Journal of Polymers and the Environment*, **21**(3), 692-701.

Du, L., Wang, Z., Li, S., Song, W., Lin, W. 2013. A comparison of monomeric phenols produced from lignin by fast pyrolysis and hydrothermal conversions. *International Journal of Chemical Reactor Engineering*, **11**(1), 135-145.

Duval, A., Lawoko, M. 2014. A review on lignin-based polymeric, micro-and nano-structured materials. *Reactive and Functional Polymers*, **85**, 78-96.

Duval, A., Vilaplana, F., Crestini, C., Lawoko, M. 2016. Solvent screening for the fractionation of industrial kraft lignin. *Holzforschung*, **70**(1), 11-20.

Ederer, J., Janoš, P., Ecorchard, P., Tolasz, J., Štengl, V., Beneš, H., Perchacz, M., Pop-Georgievski, O. 2017. Determination of amino groups on functionalized graphene oxide for polyurethane nanomaterials: XPS quantitation vs. functional speciation. *RSC advances*, **7**(21), 12464-12473.

El Hage, R., Brosse, N., Sannigrahi, P., Ragauskas, A. 2010. Effects of process severity on the chemical structure of Miscanthus ethanol organosolv lignin. *Polymer Degradation and Stability*, **95**(6), 997-1003.

Evtugin, D., Gandini, A. 1996. Polyesters based on oxygen-organosolv lignin. *Acta polymerica*, **47**(8), 344-350.

Evtuguin, D., Andreolety, J., Gandini, A. 1998. Polyurethanes based on oxygen-organosolv lignin. *European polymer journal*, **34**(8), 1163-1169.

Fan, L., Ruan, R., Liu, Y., Wang, Y., Tu, C. 2015. Effects of extraction conditions on the characteristics of ethanol organosolv lignin from bamboo (Phyllostachys pubescens Mazel). *BioResources*, **10**(4), 7998-8013.

Flory, P.J., Rehner Jr, J. 1943. Statistical mechanics of cross-linked polymer networks I. Rubberlike elasticity. *The journal of chemical physics*, **11**(11), 512-520.

Ganewatta, M.S., Lokupitiya, H.N., Tang, C. 2019. Lignin Biopolymers in the Age of Controlled Polymerization. *Polymers*, **11**(7), 1176.

Gao, G., Dallmeyer, J.I., Kadla, J.F. 2012. Synthesis of lignin nanofibers with ionic-responsive shells: water-expandable lignin-based nanofibrous mats. *Biomacromolecules*, **13**(11), 3602-3610.

Garside, M. 2019. Global plastic production 1950-2018. *STATISTA*.

Ghozatloo, A., Mohammadi-Rovshandeh, J., Hashemi, S. 2006. Optimization of pulp properties by dimethyl formamide pulping of rice straw. *Cellulose chemistry and technology*, **40**(8), 659-667.

Gilarranz, M.A., Rodríguez, F., Oliet, M. 2000. Lignin behavior during the autocatalyzed methanol pulping of eucalyptus globulus changes in molecular weight and functionality. *Holzforschung*, **54**(4), 373-380.

Gordobil, O., Delucis, R., Egüés, I., Labidi, J. 2015. Kraft lignin as filler in PLA to improve ductility and thermal properties. *Industrial Crops and Products*, **72**, 46-53.

Gordobil, O., Egüés, I., Llano-Ponte, R., Labidi, J. 2014. Physicochemical properties of PLA lignin blends. *Polymer Degradation and Stability*, **108**, 330-338.

Gosselink, R., Abächerli, A., Semke, H., Malherbe, R., Käuper, P., Nadif, A., Van Dam, J. 2004. Analytical protocols for characterisation of sulphur-free lignin. *Industrial Crops and Products*, **19**(3), 271-281.

Gouveia, J.R., da Costa, C.L., Tavares, L.B., dos Santos, D.J. 2019. Synthesis of lignin-based polyurethanes: a mini-review. *Mini-Reviews in Organic Chemistry*, **16**(4), 345-352.

Goyal, G.C., Lora, J., Pye, E. 1992. Autocatalyzed organosolv pulping of hardwoods: effect of pulping conditions on pulp properties and characteristics of soluble and residual lignin. *Tappi journal*, **75**(2), 110-116.

Gracia-Fernández, C., Gómez-Barreiro, S., López-Beceiro, J., Saavedra, J.T., Naya, S., Artiaga, R. 2010. Comparative study of the dynamic glass transition temperature by DMA and TMDSC. *Polymer Testing*, **29**(8), 1002-1006.

Gruber, P., O'Brien, M. 2002. Polyesters III: applications and commercial products. *Biopolymer*, **4**, 235-249.

Guo, Z.-X., Gandini, A. 1991. Polyesters from lignin—2. The copolyesterification of kraft lignin and polyethylene glycols with dicarboxylic acid chlorides. *European polymer journal*, **27**(11), 1177-1180.

Guo, Z.X., Gandini, A., Pla, F. 1992. Polyesters from lignin. 1. The reaction of kraft lignin with dicarboxylic acid chlorides. *Polymer international*, **27**(1), 17-22.

Han, T., Sophonrat, N., Evangelopoulos, P., Persson, H., Yang, W., Jönsson, P. 2018. Evolution of sulfur during fast pyrolysis of sulfonated Kraft lignin. *Journal of Analytical and Applied Pyrolysis*, **133**, 162-168.

Hatakeyama, T., Hatakeyama, H. 2006. *Thermal properties of green polymers and biocomposites*. Springer Science & Business Media.

Hatakeyama, T., Izuta, Y., Hirose, S., Hatakeyama, H. 2002. Phase transitions of lignin-based polycaprolactones and their polyurethane derivatives. *Polymer*, **43**(4), 1177-1182.

Hilburg, S.L., Elder, A.N., Chung, H., Ferebee, R.L., Bockstaller, M.R., Washburn, N.R. 2014. A universal route towards thermoplastic lignin composites with improved mechanical properties. *Polymer*, **55**(4), 995-1003.

Hosoya, T., Kawamoto, H., Saka, S. 2009. Role of methoxyl group in char formation from lignin-related compounds. *Journal of Analytical and Applied Pyrolysis*, **84**(1), 79-83.

Hu, L., Pan, H., Zhou, Y., Zhang, M. 2011. Methods to improve lignin's reactivity as a phenol substitute and as replacement for other phenolic compounds: A brief review. *BioResources*, **6**(3), 3515-3525.

Ibrahim, M.N.M., Ahmed-Haras, M.R., Sipaut, C.S., Aboul-Enein, H.Y., Mohamed, A.A. 2010. Preparation and characterization of a newly water soluble lignin graft copolymer from oil palm lignocellulosic waste. *Carbohydrate polymers*, **80**(4), 1102-1110.

Ibrahim, M.N.M., Zakaria, N., Sipaut, C.S., Sulaiman, O., Hashim, R. 2011. Chemical and thermal properties of lignins from oil palm biomass as a substitute for phenol in a phenol formaldehyde resin production. *Carbohydrate polymers*, **86**(1), 112-119.

Irvine, G. 1985. The significance of the glass transition of lignin in thermomechanical pulping. *Wood science and technology*, **19**(2), 139-149.

Jang, S.-K., Kim, H.-Y., Jeong, H.-S., Kim, J.-Y., Yeo, H., Choi, I.-G. 2016. Effect of ethanol organosolv pretreatment factors on enzymatic digestibility and ethanol organosolv lignin structure from Liriodendron tulipifera in specific combined severity factors. *Renewable Energy*, **87**, 599-606.

Jeong, H., Park, J., Kim, S., Lee, J., Ahn, N., Roh, H.-g. 2013. Preparation and characterization of thermoplastic polyurethanes using partially acetylated kraft lignin. *Fibers and polymers*, **14**(7), 1082-1093.

Jia, S., Yu, D., Zhu, Y., Wang, Z., Chen, L., Fu, L. 2017. Morphology, crystallization and thermal behaviors of PLA-based composites: wonderful effects of hybrid GO/PEG via dynamic impregnating. *Polymers*, **9**(10), 528.

Jia, Z., Lu, C., Zhou, P., Wang, L. 2015. Preparation and characterization of high boiling solvent lignin-based polyurethane film with lignin as the only hydroxyl group provider. *RSC Advances*, **5**(66), 53949-53955.

Jonoobi, M., Harun, J., Mathew, A.P., Oksman, K. 2010. Mechanical properties of cellulose nanofiber (CNF) reinforced polylactic acid (PLA) prepared by twin screw extrusion. *Composites Science and Technology*, **70**(12), 1742-1747.

Kai, D., Tan, M.J., Chee, P.L., Chua, Y.K., Yap, Y.L., Loh, X.J. 2016. Towards lignin-based functional materials in a sustainable world. *Green Chemistry*, **18**(5), 1175-1200.

Kazzaz, A.E., Feizi, Z.H., Fatehi, P. 2019. Grafting strategies for hydroxy groups of lignin for producing materials. *Green Chemistry*, **21**(21), 5714-5752.

Kelley, S.S., Glasser, W.G., Ward, T.C. 1988a. Engineering plastics from lignin XIV. Characterization of chain-extended hydroxypropyl lignins. *Journal of Wood Chemistry and Technology*, **8**(3), 341-359.

Kelley, S.S., Glasser, W.G., Ward, T.C. 1988b. Engineering plastics from lignin. XV. Polyurethane films from chain-extended hydroxypropyl lignin. *Journal of applied polymer science*, **36**(4), 759-772.

Kim, J.-Y., Hwang, H., Oh, S., Kim, Y.-S., Kim, U.-J., Choi, J.W. 2014. Investigation of structural modification and thermal characteristics of lignin after heat treatment. *International journal of biological macromolecules*, **66**, 57-65.

Koo, B.-W., Min, B.-C., Gwak, K.-S., Lee, S.-M., Choi, J.-W., Yeo, H., Choi, I.-G. 2012. Structural changes in lignin during organosolv pretreatment of Liriodendron tulipifera and the effect on enzymatic hydrolysis. *Biomass and Bioenergy*, **42**, 24-32.

Kumar, A., Tumu, V.R. 2019. Physicochemical properties of the electron beam irradiated bamboo powder and its bio-composites with PLA. *Composites Part B: Engineering*, **175**, 107098.

Kumar, A., Tumu, V.R., Chowdhury, S.R., SVS, R.R. 2019. A green physical approach to compatibilize a bio-based poly (lactic acid)/lignin blend for better mechanical, thermal and degradation properties. *International journal of biological macromolecules*, **121**, 588-600.

Laurichesse, S., Avérous, L. 2014. Chemical modification of lignins: Towards biobased polymers. *Progress in polymer science*, **39**(7), 1266-1290.

Li, J., He, Y., Inoue, Y. 2003. Thermal and mechanical properties of biodegradable blends of poly (L-lactic acid) and lignin. *Polymer International*, **52**(6), 949-955.

Li, L., Yao, X., Li, H., Liu, Z., Ma, W., Liang, X. 2014. Thermal stability of oxygen-containing functional groups on activated carbon surfaces in a thermal oxidative environment. *Journal of Chemical Engineering of Japan*, **47**(1), 21-27.

Li, M., Foster, C., Kelkar, S., Pu, Y., Holmes, D., Ragauskas, A., Saffron, C.M., Hodge, D.B. 2012. Structural characterization of alkaline hydrogen peroxide pretreated grasses exhibiting diverse lignin phenotypes. *Biotechnology for Biofuels*, **5**(1), 1-15.

Li, Y., Luo, X., Hu, S. 2015. Introduction to Bio-Based Polyols and Polyurethanes. in: *Bio-based Polyols and Polyurethanes*, Springer, pp. 1-13.

Li, Y., Ragauskas, A.J. 2012. Kraft lignin-based rigid polyurethane foam. *Journal of Wood Chemistry and Technology*, **32**(3), 210-224.

Li, Y., Sarkanen, S. 2005. Miscible blends of kraft lignin derivatives with low-T g polymers. *Macromolecules*, **38**(6), 2296-2306.

Lin, X., Sui, S., Tan, S., Pittman, C.U., Sun, J., Zhang, Z. 2015. Fast pyrolysis of four lignins from different isolation processes using Py-GC/MS. *Energies*, **8**(6), 5107-5121.

Lisperguer, J., Perez, P., Urizar, S. 2009. Structure and thermal properties of lignins: characterization by infrared spectroscopy and differential scanning calorimetry. *Journal of the Chilean Chemical Society*, **54**(4), 460-463.

Liu, W.-J., Jiang, H., Yu, H.-Q. 2015. Thermochemical conversion of lignin to functional materials: a review and future directions. *Green Chemistry*, **17**(11), 4888-4907.

Lutz, P., Peruch, F. 2012. Graft copolymers and comb-shaped homopolymers.

Ma'ruf, A., Pramudono, B., Aryanti, N. 2017. Lignin isolation process from rice husk by alkaline hydrogen peroxide: Lignin and silica extracted. *AIP Conference Proceedings*. AIP Publishing LLC. pp. 020013.

Marton, J., Marton, T. 1964. Molecular weight of kraft lignin. *Tappi Journal*, **47**(8), 471-476.

McDonough, T.J. 1992. The chemistry of organosolv delignification.

McNaught, A.D., Wilkinson, A. 1997. *Compendium of chemical terminology*. Blackwell Science Oxford.

Mostafa, N., Farag, A.A., Abo-dief, H.M., Tayeb, A.M. 2018. Production of biodegradable plastic from agricultural wastes. *Arabian journal of chemistry*, **11**(4), 546-553.

Mousavioun, P., Doherty, W.O., George, G. 2010. Thermal stability and miscibility of poly (hydroxybutyrate) and soda lignin blends. *Industrial Crops and Products*, **32**(3), 656-661.

Nadji, H., Bruzzese, C., Belgacem, M.N., Benaboura, A., Gandini, A. 2005. Oxypropylation of lignins and preparation of rigid polyurethane foams from the ensuing polyols. *Macromolecular Materials and Engineering*, **290**(10), 1009-1016.

Noreen, A., Zia, K.M., Zuber, M., Tabasum, S., Zahoor, A.F. 2016. Bio-based polyurethane: An efficient and environment friendly coating systems: A review. *Progress in Organic Coatings*, **91**, 25-32.

Norgren, M., Edlund, H., Wågberg, L., Lindström, B., Annergren, G. 2001. Aggregation of kraft lignin derivatives under conditions relevant to the process, part I: phase behaviour. *Colloids and Surfaces A: Physicochemical and Engineering Aspects*, **194**(1-3), 85-96.

Pan, X., Arato, C., Gilkes, N., Gregg, D., Mabee, W., Pye, K., Xiao, Z., Zhang, X., Saddler, J. 2005. Biorefining of softwoods using ethanol organosolv pulping: Preliminary evaluation of process streams for manufacture of fuel-grade ethanol and co-products. *Biotechnology and bioengineering*, **90**(4), 473-481.

Park, S.Y., Kim, J.-Y., Youn, H.J., Choi, J.W. 2018. Fractionation of lignin macromolecules by sequential organic solvents systems and their characterization for further valuable applications. *International journal of biological macromolecules*, **106**, 793-802.

Patt, R., Kordsachia, O., Süttinger, R., Ohtani, Y., Hoesch, J., Ehrler, P., Eichinger, R., Holik, H., Hamm, U., Rohmann, M. 2012. Ullmann's encyclopedia of industrial chemistry, Wiley-VCH, ed. Wiley-VCH Verlag GmbH.

Pedersen, M., Meyer, A.S. 2010. Lignocellulose pretreatment severity–relating pH to biomatrix opening. *New biotechnology*, **27**(6), 739-750.

Pouteau, C., Baumberger, S., Cathala, B., Dole, P. 2004. Lignin–polymer blends: evaluation of compatibility by image analysis. *Comptes rendus biologies*, **327**(9-10), 935-943.

Reimann, A., Mörck, R., Yoshida, H., Hatakeyama, H., Kringstad, K.P. 1990. Kraft lignin in polyurethanes. III. Effects of the molecular weight of PEG on the properties of polyurethanes from a kraft lignin–PEG–MDI system. *Journal of applied polymer science*, **41**(1-2), 39-50.

Ren, W., Pan, X., Wang, G., Cheng, W., Liu, Y. 2016. Dodecylated lignin-g-PLA for effective toughening of PLA. *Green Chemistry*, **18**(18), 5008-5014.

Ren, X. 2003. Biodegradable plastics: a solution or a challenge? *Journal of cleaner Production*, **11**(1), 27-40.

research, G.v. 2020. Lignin Market Size, Share & Trends Analysis Report By Product (Ligno-Sulphonates, Kraft, Organosolv), By Application (Macromolecule, Aromatic), By Region, And Segment Forecasts, 2020 - 2027.

Rials, T.G., Glasser, W.G. 1984. Engineering Plastics from Lignin-IV. Effect of Crosslink Density on Polyurethane Film Properties—Variation in NCO: OH Ratio. *Holzforschung-International Journal of the Biology, Chemistry, Physics and Technology of Wood*, **38**(4), 191-199.

Saba, N., Jawaid, M., Alothman, O.Y., Paridah, M. 2016. A review on dynamic mechanical properties of natural fibre reinforced polymer composites. *Construction and Building Materials*, **106**, 149-159.

Sadeghifar, H., Cui, C., Argyropoulos, D.S. 2012. Toward thermoplastic lignin polymers. Part 1. Selective masking of phenolic hydroxyl groups in kraft lignins via methylation and oxypropylation chemistries. *Industrial & engineering chemistry research*, **51**(51), 16713-16720.

Sadeghifar, H., Wells, T., Le, R.K., Sadeghifar, F., Yuan, J.S., Jonas Ragauskas, A. 2017. Fractionation of organosolv lignin using acetone: water and properties of the obtained fractions. *ACS Sustainable Chemistry & Engineering*, **5**(1), 580-587.

Saito, T., Brown, R.H., Hunt, M.A., Pickel, D.L., Pickel, J.M., Messman, J.M., Baker, F.S., Keller, M., Naskar, A.K. 2012. Turning renewable resources into value-added polymer: development of lignin-based thermoplastic. *Green Chemistry*, **14**(12), 3295-3303.

Saito, T., Perkins, J.H., Jackson, D.C., Trammel, N.E., Hunt, M.A., Naskar, A.K. 2013. Development of lignin-based polyurethane thermoplastics. *Rsc Advances*, **3**(44), 21832-21840.

Sajjan, A.M., Naik, M.L., Kulkarni, A.S., Fazal-E-HabibaRudgi, U., Ashwini, M., Shirnalli, G.G., Sharanappa, A., Kalahal, P.B. 2020. Preparation and characterization of PVA-Ge/PEG-400 biodegradable plastic blend films for Packaging applications. *Chemical Data Collections*, 100338.

Sakakibara, A. 1980. A structural model of softwood lignin. *Wood Science and Technology*, **14**(2), 89-100.

Saïd Azizi Samir, M.A., Alloin, F., Paillet, M., Dufresne, A. 2004. Tangling effect in fibrillated cellulose reinforced nanocomposites.

*Macromolecules*, **37**(11), 4313-4316.

Sannigrahi, P., Ragauskas, A.J., Miller, S.J. 2010. Lignin structural modifications resulting from ethanol organosolv treatment of loblolly pine. *Energy & Fuels*, **24**(1), 683-689.

Saraf, V.P., Glasser, W.G., Wilkes, G.L., McGrath, J.E. 1985. Engineering plastics from lignin. VI. Structure–property relationships of PEG-containing polyurethane networks. *Journal of applied polymer science*, **30**(5), 2207-2224.

Schorr, D., Diouf, P.N., Stevanovic, T. 2014. Evaluation of industrial lignins for biocomposites production. *Industrial Crops and Products*, **52**, 65-73.

Sen, S., Patil, S., Argyropoulos, D.S. 2015. Thermal properties of lignin in copolymers, blends, and composites: a review. *Green Chemistry*, **17**(11), 4862-4887.

Shen, L., Haufe, J., Patel, M.K. 2009. Product overview and market projection of emerging bio-based plastics PRO-BIP 2009. *Report for European polysaccharide network of excellence (EPNOE) and European bioplastics*, **243**.

Shen, M., Song, B., Zeng, G., Zhang, Y., Huang, W., Wen, X., Tang, W. 2020. Are biodegradable plastics a promising solution to solve the global plastic pollution? *Environmental Pollution*, 114469.

Silva, A.M., Kong, X., Hider, R.C. 2009. Determination of the pKa value of the hydroxyl group in the α-hydroxycarboxylates citrate, malate and lactate by 13C NMR: implications for metal coordination in biological systems. *BioMetals*, **22**(5), 771-778.

Spiridon, I., Leluk, K., Resmerita, A.M., Darie, R.N. 2015. Evaluation of PLA–lignin bioplastics properties before and after accelerated weathering. *Composites Part B: Engineering*, **69**, 342-349.

Spiridon, I., Tanase, C.E. 2018. Design, characterization and preliminary biological evaluation of new lignin-PLA biocomposites. *International journal of biological macromolecules*, **114**, 855-863.

Tavares, L., Boas, C., Schleder, G., Nacas, A., Rosa, D., Santos, D. 2016. Bio-based polyurethane prepared from Kraft lignin and modified castor oil. *Express Polymer Letters*, **10**(11).

Thakur, V.K., Thakur, M.K., Raghavan, P., Kessler, M.R. 2014. Progress in green polymer composites from lignin for multifunctional applications: a review. *ACS Sustainable Chemistry & Engineering*, **2**(5), 1072-1092.

Tirtowidjojo, S., Sarkanen, K.V., Pla, F., McCarthy, J.L. 1988. Kinetics of organosolv delignification in batch-and flow-through reactors. *Holzforschung-International Journal of the Biology, Chemistry, Physics and Technology of Wood*, **42**(3), 177-184.

Trzebiatowska, P.J., Echart, A.S., Correas, T.C., Eceiza, A., Datta, J. 2018. The changes of crosslink density of polyurethanes synthesised with using recycled component. Chemical structure and mechanical properties investigations. *Progress in Organic Coatings*, **115**, 41-48.

Upton, B.M., Kasko, A.M. 2016. Strategies for the conversion of lignin to high-value polymeric materials: review and perspective. *Chemical reviews*, **116**(4), 2275-2306.

Vanholme, R., Demedts, B., Morreel, K., Ralph, J., Boerjan, W. 2010. Lignin biosynthesis and structure. *Plant physiology*, **153**(3), 895-905.

Verma, R., Vinoda, K., Papireddy, M., Gowda, A. 2016. Toxic pollutants from plastic waste-a review. *Procedia Environ. Sci*, **35**, 701-708.

Wang, C., Kelley, S.S., Venditti, R.A. 2016. Lignin-based thermoplastic materials. *ChemSusChem*, **9**(8), 770-783.

Wang, J., Yao, K., Korich, A.L., Li, S., Ma, S., Ploehn, H.J., Iovine, P.M., Wang, C., Chu, F., Tang, C. 2011. Combining renewable gum rosin and lignin: Towards hydrophobic polymer composites by controlled polymerization. *Journal of Polymer Science Part A: Polymer Chemistry*, **49**(17), 3728-3738.

Wang, Y.-Y., Wyman, C.E., Cai, C.M., Ragauskas, A.J. 2019. Lignin-based polyurethanes from unmodified kraft lignin fractionated by sequential precipitation. *ACS Applied Polymer Materials*, **1**(7), 1672-1679.

Wayman, M., Lora, J.H. 1980. Simulated autohydrolysis of aspen milled wood lignin in the presence of aromatic additives: Structural modifications. *Journal of Applied Polymer Science*, **25**(10), 2187-2194.

Wei, M., Fan, L., Huang, J., Chen, Y. 2006. Role of Star-Like Hydroxylpropyl Lignin in Soy-Protein Plastics. *Macromolecular Materials and*

*Engineering*, **291**(5), 524-530.

Wen, J.-L., Sun, S.-L., Xue, B.-L., Sun, R.-C. 2013a. Quantitative structures and thermal properties of birch lignins after ionic liquid pretreatment. *Journal of agricultural and food chemistry*, **61**(3), 635-645.

Wen, J.-L., Sun, S.-L., Xue, B.-L., Sun, R.-C. 2013b. Recent advances in characterization of lignin polymer by solution-state nuclear magnetic resonance (NMR) methodology. *Materials*, **6**(1), 359-391.

Wojnowska-Baryła, I., Kulikowska, D., Bernat, K. 2020. Effect of Bio-Based Products on Waste Management. *Sustainability*, **12**(5), 2088.

Yang, J., Ching, Y.C., Chuah, C.H. 2019. Applications of lignocellulosic fibers and lignin in bioplastics: A review. *Polymers*, **11**(5), 751.

Yang, W., Fortunati, E., Dominici, F., Kenny, J., Puglia, D. 2015. Effect of processing conditions and lignin content on thermal, mechanical and degradative behavior of lignin nanoparticles/polylactic (acid) bionanocomposites prepared by melt extrusion and solvent casting. *European Polymer Journal*, **71**, 126-139.

Yáñez-S, M., Matsuhiro, B., Nuñez, C., Pan, S., Hubbell, C.A., Sannigrahi, P., Ragauskas, A.J. 2014. Physicochemical characterization of ethanol organosolv lignin (EOL) from Eucalyptus globulus: Effect of extraction conditions on the molecular structure. *Polymer degradation and stability*, **110**, 184-194.

Yeske, R.A. 1986. Corrosion by kraft pulping liquors.

Yoon, S.-H., Van Heiningen, A. 2008. Kraft pulping and papermaking properties of hot-water pre-extracted loblolly pine in an integrated forest products biorefinery. *Tappi J*, **7**(7), 22-27.

Yoshida, H., Mörck, R., Kringstad, K., Hatakeyama, H. 1987. Kraft lignin in polyurethanes I. Mechanical properties of polyurethanes from a kraft lignin–polyether triol–polymeric MDI system. *Journal of applied polymer science*, **34**(3), 1187-1198.

Yoshida, H., Mörck, R., Kringstad, K.P., Hatakeyama, H. 1990. Kraft lignin in polyurethanes. II. Effects of the molecular weight of kraft lignin on the properties of polyurethanes from a kraft lignin–polyether triol–polymeric MDI system. *Journal of Applied Polymer Science*, **40**(11-

12), 1819-1832.

You, Y.-S., Oh, Y.-S., Kim, U.-S., Choi, S.-W. 2015. National certification marks and standardization trends for biodegradable, oxo-biodegradable and bio based plastics. *Clean technology*, **21**(1), 1-11.

Young, R.J., Lovell, P.A. 2011. *Introduction to polymers*. CRC press.

Zakzeski, J., Bruijnincx, P.C., Jongerius, A.L., Weckhuysen, B.M. 2010. The catalytic valorization of lignin for the production of renewable chemicals. *Chemical reviews*, **110**(6), 3552-3599.

Zhang, K., Pei, Z., Wang, D. 2016a. Organic solvent pretreatment of lignocellulosic biomass for biofuels and biochemicals: a review. *Bioresource technology*, **199**, 21-33.

Zhang, Z., Harrison, M.D., Rackemann, D.W., Doherty, W.O., O'Hara, I.M. 2016b. Organosolv pretreatment of plant biomass for enhanced enzymatic saccharification. *Green chemistry*, **18**(2), 360-381.

Zhao, X., Cheng, K., Liu, D. 2009. Organosolv pretreatment of lignocellulosic biomass for enzymatic hydrolysis. *Applied microbiology and biotechnology*, **82**(5), 815.

Zhao, X., Li, S., Wu, R., Liu, D. 2017. Organosolv fractionating pre-treatment of lignocellulosic biomass for efficient enzymatic saccharification: chemistry, kinetics, and substrate structures. *Biofuels, Bioproducts and Biorefining*, **11**(3), 567-590.

Zhou, Q., Chen, J., Wang, C., Yang, G., Ji, X., Peng, J., Xu, F. 2020. Quantitative structures and thermal properties of Miscanthus× giganteus lignin after alcoholamine-based ionic liquid pretreatment. *Industrial Crops and Products*, **147**, 112232.

# 초 록

## 유기용매 리그닌의 구조적 특성이 리그노-바이오플라스틱의 열적·기계적 특성에 미치는 영향

서울대학교 대학원
산림과학부
환경재료과학전공
최준호

본 연구에서는 유기용매 리그닌의 구조적 특성이 리그노-바이오플라스틱의 열적·기계적 특성에 미치는 영향을 조사하였다. 먼저 에탄올 유기용매 리그닌(EOL)의 구조적 특성에 대한 추출 조건의 영향은 반응표면분석법(RSM)을 이용하여 조사하였다. 설정된 RSM 분석 범위 내에서 추출 조건이 가혹할수록 낮은 분자량, 낮은 다분산도, 높은 방향족 수산기 함량 및 축합된 구조를 가진 EOL이 생산되는 경향을 보였다. 이러한 경향은 추출 조건의 가혹도 지수(CSF)를 도입하여 EOL의 구조와의 명확한 상관관계를 도출함으로써 확인되었다. 또한 다양한 추출 조건에서 파생된 EOL의 구조와 열적 특성 간의 상관관계를 평가하였다. EOL의 열적 특성은 분자량 및 방향족 수산기 인자와 뚜렷한 상관 관계를 보였다. 낮은 분자량, 높은 방향족 수산기 함량 및 축합된 구조를 갖는 EOL은 높은 유리전이온도($T_g$), 낮은 열분해 시작 온도 및

초기 분해 속도를 나타냈다. EOL의 구조와 열적 특성 간의 상관관계 결과를 바탕으로 EOL의 중량 감소율 예측을 위한 회귀 모델(R2 = 0.837)이 제시되었으며, EOL의 분자량이 낮을수록 300 °C에서의 열분해가 느리게 발생할 것으로 예측되었다. 추출 조건의 가혹도가 서로 다른 EOL(LL(#5, 낮은 가혹도 조건에서 추출된 EOL), ML(#16, 중간의 가혹도 조건에서 추출된 EOL), HL(#4, 높은 가혹도 조건에서 추출된 EOL))을 사용하여 제조된 EOL-PLA 바이오플라스틱은 사용된 EOL 종류에 따라 다른 열적·기계적 특성을 나타냈다. EOL-PLA 바이오플라스틱은 순수 PLA에 비해 우수한 열안정성을 나타냈으며, HL를 사용하여 제조한 EOL-PLA 바이오플라스틱은 다른 바이오플라스틱 보다 높은 열분해 시작점과 최대 분해 온도를 나타냈다. EOL-PLA 바이오플라스틱의 인장 강도는 리그닌 함량이 증가함에 따라 감소하는 경향을 나타냈다. 반면 EOL-PLA 바이오플라스틱의 공칭변형률은 EOL에 따라 다른 경향을 보였다.

한편, EOL의 열가소성과 바이오폴리이스터와의 상용성을 개선하기 위해 옥시프로필화를 도입하였다. 옥시프로필화는 구조적 특성이 다른 세 종류의 EOL(LL, ML 및 HL)을 이용하여 EOL의 수산기와 프로필렌 옥사이드(PO)의 다양한 몰비(1:1, 1:2 및 1:5)로 실시했다. 옥시프로필화 과정에서 초기 EOL의 수산기 분포는 프로필 측쇄의 치환도와 중합도에 크게 영향을 미쳤으며, 방향족 수산기 함량이 높은 HL(4.31 mmol/g)은 높은 치환도(0.77)를 보였고, 지방족 수산기 함량이 높은 LL(2.94 mmol/g)은 높은 중합도(11.17)를 나타냈다. 옥시프로필화는 EOL의 열가소성을 향상시켰으며, 구조적 특성과 초기 EOL에 따라

서로 다른 열적 특성을 나타냈다. 특히 옥시프로필화된 LL과 ML은 55−60 °C 범위의 새로운 $T_g$가 생성되었으며, 용융점이 관찰되었다. 또한 개선된 열가소성을 기반으로 EOL과 PLA의 상용성이 옥시프로필화에 의해 향상되었다. 옥시프로필화 LL 및 ML을 이용한 바이오플라스틱에서는 열가소성 및 상용성이 개선되어 초기 EOL을 이용한 바이오플라스틱에 비해 매끄럽고 평평한 표면 구조가 관찰되었다. EOL의 개선된 PLA와의 상용성 및 열가소성은 바이오플라스틱의 인장강도를 PLA와 유사한 수준으로 향상시켰으며 공칭변형률을 PLA보다 높은 수준으로 증가시켰다. 동역학적 열분석 결과, 옥시프로필화 EOL의 첨가는 PLA의 $T_g$를 향상시켜 물리·화학적 특성을 개선하였다.

또한 구조적 특성이 서로 다른 옥시프로필화 리그닌을 이용하여 열적·기계적 특성이 다른 리그노폴리우레탄을 제조하였다. 리그노폴리우레탄은 옥시프로필화 EOL과 헥사메틸렌 디이소시아네이트(HDI)를 이용하여 합성하였으며, 옥시프로필화 EOL의 구조적 특성은 리그노폴리우레탄의 반응성 및 열적·기계적 특성에 영향을 미쳤다. 구조 내 수산기 함량이 높은 옥시프로필화 EOL은 높은 반응 속도를 나타냈다. 리그노폴리우레탄의 초기 열안정성은 각각의 상응하는 옥시프로필화 EOL에 비해 증가하였으며 350 °C 이상의 고온에서 리그노폴리우레탄의 열적 특성은 초기 EOL의 열적 특성에 따라 다르게 나타났다. 또한, 옥시프로필화 EOL의 구조적 특성은 리그노폴리우레탄 필름의 기계적 물성에 큰 영향을 미쳤다. 수산기 함량이 높은 옥시프로필화 EOL은 높은 반응성으로 인해 리그노폴리우레탄의 가교밀도를 증가시켜 높은 인장강도를 야기했다.

결론적으로 EOL의 구조와 물성 간의 상관관계를 바탕으로 옥시프로필화를 통해 EOL의 열가소성을 부여하여 EOL-PLA 바이오플라스틱을 제조하였으며 우레탄 합성을 통해 열경화성을 부여하여 리그노폴리우레탄 필름을 제조하였다. 이때 초기 EOL의 구조적 특성은 리그노-바이오플라스틱의 열적·기계적 특성에 유의미한 영향을 미쳤다.

**주요어: 유기용매 리그닌, 구조적 특성, 열적·기계적 특성, 리그노-바이오플라스틱, 옥시프로필화, 리그노폴리우레탄**

**학 번: 2015-21505**